Earthquake Hazard Associated With Deep Well Injection– A Report to the U.S. Environmental Protection Agency

U.S. GEOLOGICAL SURVEY BULLETIN 1951

Prepared in cooperation with the Environmental Protection Agency

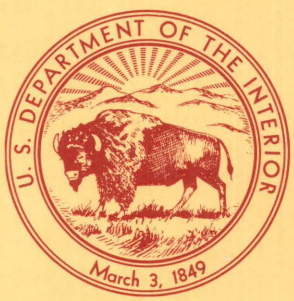

Earthquake Hazard Associated With Deep Well Injection— A Report to the U.S. Environmental Protection Agency

By CRAIG NICHOLSON and ROBERT L. WESSON

Prepared in cooperation with the
Environmental Protection Agency

Under certain circumstances, the increased pore pressure resulting from fluid injection, whether for waste disposal, secondary recovery, geothermal energy, or solution mining, can trigger earthquakes. This report discusses known cases of injection-induced seismicity and how and why earthquakes may be triggered, as well as conditions under which the triggering is most likely to occur. Criteria are established to assist in regulating well operations so as to minimize the seismic hazard associated with deep well fluid injection

U.S. GEOLOGICAL SURVEY BULLETIN 1951

U.S. DEPARTMENT OF THE INTERIOR
MANUEL LUJAN, Jr., Secretary

U.S. GEOLOGICAL SURVEY
Dallas L. Peck, Director

UNITED STATES GOVERNMENT PRINTING OFFICE: 1990

For sale by the
Books and Open-File Reports Section
U.S. Geological Survey
Federal Center, Box 25425
Denver, CO 80225

Library of Congress Cataloging in Publication Data

Nicholson, Craig.
Earthquake hazard associated with deep well injection : a report to the U.S. Environmental Protection Agency / by Craig Nicholson and Robert L. Wesson.
p. cm. — (U.S. Geological Survey bulletin ; 1951)
Includes bibliographical references.
Supt. of Docs. no.: I 19.3: 1951
1. Oil field flooding—Environmental aspects—United States. 2. Injection wells—Environmental aspects—United States. 3. Induced seismicity—United States. I. Wesson, R.L. (Robert L.) II. United States. Environmental Protection Agency. III. Title. IV. Series.
QE75.B9 no. 1951 [TN871.37]*EN(557.3 s—dc29 [622'.33827] 90-3992
CIP

CONTENTS

PLATE

[In pocket]

FIGURES

TABLES

EARTHQUAKE MAGNITUDE SCALE APPROXIMATIONS

Local (M_L)	Body-wave (m_b)	Surface-wave (M_S)	Moment (M)
4.6	4.55	—	4.6
4.8	4.8	—	4.8
5.0	5.0	4.4	5.0
5.2	5.2	4.7	5.2
5.4	5.4	5.0	5.4
5.6	5.55	5.3	5.6
5.8	5.7	5.6	5.8
6.0	5.85	5.9	6.05
6.2	6.0	6.2	6.30
6.4	6.15	6.4	6.55
6.6	6.3	6.75	6.85
6.8	6.5	7.05	7.15
7.0	6.7	7.35	7.45
7.2	6.9	7.65	7.80
7.4	7.1	7.95	8.15

Earthquake Hazard Associated With Deep Well Injection—A Report to the U.S. Environmental Protection Agency

By Craig Nicholson[1] *and* Robert L. Wesson[2]

SUMMARY

Within the United States, injection of fluid into deep wells has triggered documented earthquakes in Colorado, Texas, New York, New Mexico, Nebraska, and Ohio and possibly in Oklahoma, Louisiana, and Mississippi. Investigations of these cases have led to some understanding of the probable physical mechanism of the triggering and of the criteria for predicting whether future earthquakes will be triggered, based on the local state of stress in the Earth's crust, the injection pressure, and the physical and the hydrological properties of the rocks into which the fluid is being injected.

Of the well-documented cases of earthquakes related to fluid injection, most are associated with water-flooding operations for the purpose of secondary recovery of hydrocarbons. This is because secondary recovery operations often entail large arrays of wells injecting fluids at high pressures into small confined reservoirs that have low permeabilities. In contrast, waste-disposal wells typically inject at lower pressures into large porous aquifers that have high permeabilities. This explains, in large part, why, of the many hazardous and nonhazardous waste-disposal wells in the United States, only two have ever been conclusively shown to be associated with triggering significant adjacent seismicity. These are wells located near Ashtabula, Ohio, and near Denver, Colo. In the case near Ashtabula, a series of small, shallow earthquakes was triggered close to the bottom of a 1.8-kilometer (km)-deep well; the largest of these was of magnitude (M) 3.6 and occurred in 1987. In the Denver case, the injection well responsible was located at the Rocky Mountain Arsenal, where fluid was being injected into relatively impermeable crystalline basement rock. This caused the largest known injection-induced earthquakes to date (three M 5–5.5 earthquakes), the largest of which caused an estimated $0.5 million in damages in 1967. Although these induced earthquakes were by no means devastating, they did occasion extensive attention and concern and led, at least in the Denver case, to the cessation of all related injection well operations.

In each of the well-documented examples, convincing arguments that the earthquakes were induced relied upon three principal characteristics of the earthquake activity. First, there was a very close geographic association between the zone of fluid injection and the locations of the earthquakes in the resulting sequence. Second, calculations based on the measured or the inferred state of stress in the Earth's crust and the measured injection pressure indicated that the theoretical threshold for frictional sliding along favorably oriented preexisting fractures likely was exceeded. And, third, a clear disparity was established between any previous natural seismicity and the subsequent earthquakes, with the induced seismicity often being characterized by large numbers of small earthquakes that persisted for as long as elevated pore pressures in the hypocentral region continued to exist.

Earthquakes are generated by slip on faults or fractures. A fault or fracture in close proximity to a high-pressure injection well thus becomes a potential location for induced earthquakes. The conditions for sliding on a fault are characterized by the Mohr-Coulomb failure criterion, which relates the shear stress required for fault slip to the inherent cohesion or shear strength and the coefficient of friction on the fault, the normal stress resolved across the fault, and the pore fluid pressure. This relation, which depends on the orientation of the faults or the fractures relative to that of the existing state of stress, as well as on the effect of any changes in pore pressure resulting from fluid injection, is normally characterized by using the Mohr circle description. In this simple model, as fluid pressure increases, the apparent strength of the fault decreases, thus shifting the Mohr effective stress circle closer towards the failure condition; as a result, the potential for induced earthquakes also increases.

Because the conditions for failure strongly depend on the state of stress in the Earth's crust, measuring the *in situ* stress conditions is important to assess accurately the potential for inducing earthquakes. Several approaches are possible, but the most reliable method is the hydraulic fracture technique in which the pressure required to create

Manuscript approved for publication on June 28, 1990.

[1]Institute for Crustal Studies, University of California, Santa Barbara, CA 93106.

[2]U.S. Geological Survey, Reston, VA 22092.

small fractures in the wellbore is measured precisely. This method is a variation of the standard hydrofracture technique that is used to increase the transmissivity of a reservoir. Although pressures are monitored during commercial hydrofracture operations, few, if any, of these pressure records would constitute an adequate or precise stress measurement. However, because sufficient measurements of stress are now available across much of the United States, a number of regional stress patterns have begun to emerge, and, thus, it is now possible to predict the general orientation and, to some extent, the magnitude of the principal stresses at a given site. Supplemental measurements would be required, however, to provide accurate information relevant to the determination of maximum allowable levels of injection pressure at each specific site of well operations.

The hydrologic properties of the reservoir also have a strong effect on the potential for inducing earthquakes by deep well injection. Transmissivity and storativity control the rate at which pore pressure will increase in the reservoir formation as a result of fluid injection. For a given volume of fluid flow, higher values of transmissivity and storativity allow lower injection pressures required to attain a desired injection rate and, consequently, a lower potential for triggering earthquake activity. Transmissivity and storativity can be estimated from tests made during well completion and can be verified later by actual pressure-time records acquired during well operation. Estimates of the changes in pore pressure as a result of fluid injection into a particular reservoir formation can be predicted by analysis of the pressure history at the wellbore and by using variations of the standard techniques from reservoir engineering or ground-water hydrology.

Unresolved issues relating to the hazard associated with earthquakes induced by deep well injection include a relatively poor understanding of the causes of natural earthquakes in the Central and the Eastern United States and difficulties in quantifying either the spatial or the temporal variations in tectonic stress or in assessing the potential for fault reactivation in general. There is also considerable uncertainty in estimating the maximum size of expected induced earthquakes or in quantifying the significance of small induced earthquakes (should they begin to occur near the bottom of an injection well) relative to the specific level of risk. An additional environmental concern, about which little is understood, is the potential for induced earthquakes to breach the confining layer of a waste-disposal reservoir, which would then permit the possible upward migration of contaminated fluids. This possibility emphasizes the need to monitor an area once adjacent seismicity is detected, to determine accurately the relative position of the earthquakes to the zone of fluid injection, and to assess the type and the extent of the faulting involved.

On the basis of the present understanding of the phenomena of injection-induced earthquakes, several factors are recommended for consideration in the development of regulations and procedures for controlling deep well injection operations. These recommendations are made from a seismological point of view alone and are not intended to supersede or replace alternative considerations made for other purposes. The recommended considerations include the following:

Site Selection

- Reservoirs that are characterized by high transmissivity and storativity and, therefore, are capable of receiving fluid at low injection pressures are less likely to be the site of induced earthquakes.
- An estimate of the tectonic stress based on regional or surface measurements made before drilling could serve as an early warning of potential earthquake problems and unanticipated low formation fracture or breakdown pressures.
- Because faults within the range of influence of an injection well are the potential loci for induced earthquakes, the absence of significant faults reduces the possibility of triggered seismicity. Geologic and geophysical surveys conducted to detect faults that may intersect the reservoir also would help in evaluating the integrity of the confining layer.
- The existence of regional seismicity in the vicinity of a proposed site should be taken as evidence of sufficient levels of tectonic stress and of the presence of potential slip surfaces (faults) necessary for natural and induced earthquakes.

Well Drilling and Completion

- Estimates of the storativity and the transmissivity of the reservoir based on standard measurements of permeability, porosity, and reservoir thickness made at the time of well completion would provide an important means of predicting the buildup of injection pressure required to maintain a given injection rate.
- If it can be accomplished without threatening the confining zone, then a stress measurement that uses the hydraulic fracture technique in or below the reservoir rock is the key environmental parameter for predicting the potential for induced earthquakes and the possibility of low-formation fracture pressures.
- Careful measurement of the initial formation pore pressure at the time of well completion and before injection provides important information on the proximity to failure conditions in the unaltered natural state.
- If anticipated injection pressures approach the levels expected to trigger earthquakes according to the Mohr-Coulomb failure criterion, assuming regional or generic values for the coefficient of friction and the cohesion of faults, then more precise local measurements of these values would reduce, if possible, the

uncertainty in the specific level of injection pressure at which earthquakes would be expected.

Well Operation and Monitoring

- If reliable measurements of the local stress field are available, then it is possible to estimate the maximum injection pressure that can be used without fear of fracturing the formation or inducing earthquakes by allowing slip on a preexisting fault. These estimates can be made by using the Mohr-Coulomb failure criterion.
- Actual pressure-time curves measured at the wellhead can be compared with predicted curves to assure that the reservoir is behaving as assumed. Any increase in apparent transmissivity should be scrutinized as possible evidence for the opening of fractures or the occurrence of faulting.
- If the maximum injection pressure at a site approaches the critical level anticipated to trigger the occurrence of earthquakes, then it would be prudent to monitor the injection operation by using at least one high-sensitivity seismograph. Monitoring should continue as long as significant levels of elevated fluid pressure are maintained in the reservoir.
- The occurrence of any earthquakes near the bottom of an injection well should be reviewed carefully to assess the possibility that potentially damaging earthquakes might be induced and the potential for fracturing or faulting through the containment zone. Installation of additional seismic monitoring stations would then be recommended to locate and analyze any subsequent earthquake activity.

INTRODUCTION

The injection of waste into deep isolated aquifers is being increasingly utilized for the disposal of certain types of hazardous fluid materials (Environmental Protection Agency, 1974, 1985). Other deep well injection operations are carried out routinely for the disposal of nonhazardous waste (for example, excess oil field brine), solution mining, purposes of geothermal energy extraction, the secondary recovery of hydrocarbons, and the underground storage of natural gas intended for later redistribution during peak winter months. Of these different types of well operations, secondary recovery is by far the most common use of deep well fluid injection (Mankin and Moffet, 1987). Although most deep well injection operations have no impact on earthquake activity, it has been shown conclusively that, under some conditions, the increase of fluid pressure in the reservoir associated with deep well injection can trigger or induce earthquakes. The first and best known instance, as well as the largest, of these induced earthquakes occurred during the mid-1960's in association with the waste injection well at the Rocky Mountain Arsenal near Denver, Colo. Since this discovery, additional examples of earthquakes induced by deep well injection have been documented (pl. 1; table 1). It is conceivable, if not likely, that other examples of such induced earthquakes may have gone unnoticed because they were small and no seismograph stations were nearby to record them.

Investigations of several of the earthquakes associated with deep well injection have led to some understanding of the probable physical mechanism for the triggering and of the criteria for predicting whether earthquakes will be triggered that depend on the local state of stress in the Earth's crust, the injection pressure, and the physical and the hydrologic properties of the rocks into which the fluid is being injected. The purpose of this report is to summarize the current state of understanding of this phenomenon, to describe the criteria for predicting whether earthquakes will be triggered by fluid injection, and to indicate from a seismological point of view factors to be considered in developing regulations and operating procedures to minimize the seismic hazard associated with deep well injection.

Although several research issues remain unresolved, considerable information is currently available that may be of use in the development of operating procedures for deep injection wells that will minimize the possibility of problems associated with induced earthquakes. Fortunately, favorable conditions for the siting of a deep injection well, namely the desirability of high permeability and porosity in the injection zone and a site situated away from known fault structures also tend to be conditions for which the occurrence of induced earthquakes is less likely. Thus, implementation of these recommendations probably would have minimal adverse impact on site selection or operational procedures for injection wells located at otherwise favorable sites.

This report also includes four appendixes. Appendix A contains case histories of earthquakes associated with well operations. Appendix B is a brief summary of reservoir-induced seismicity. Appendix C describes the components of the Modified Mercalli Intensity Scale. Appendix D is a glossary.

ACKNOWLEDGMENTS

Preparation of this report was funded by the Office of Drinking Water, U.S. Environmental Protection Agency (EPA). A major portion of this work was completed while the first author held a National Research Council Associateship with the U.S. Geological Survey (USGS) in Reston, Va. Discussions with John Bredehoeft and Evelyn Roeloffs (USGS), Keith Evans and David Simpson (Lamont-Doherty Geological Observatory), and Scott Davis (University of Texas-Austin) are much appreciated. Evelyn Roeloffs per-

Table 1. Acknowledged cases of seismicity associated with well operations

Well site or oil field location	Type	Depth (m)	Injection pressure (bars)	Maximum earthquake magnitude	Year injection began-ended	Year of earthquakes
Ashtabula, Ohio	Waste disposal	1,845	100	3.6	1986–	1987
Cogdell Canyon Reef, Tex.	Secondary recovery	2,071	199	4.6	1956–	1974–79
Dale, N.Y.	Solution mining	426	55	1.0	1971	1971
Rocky Mountain Arsenal, Denver, Colo.	Waste disposal	3,671	76	5.5	1962–66	1962–67
Fenton Hill, N. Mex.	Geothermal/stimulation	2,700	200	<1.0	1979	1979
Flashing Field, Tex.	Gas withdrawal	3,400	?	3.4	1958–	1973?–83
The Geysers, Calif.	Geothermal	3,000	?	4.0	1966–	1975–
Gobles Field, Ontario, Canada	Secondary recovery	884	?	2.8	1969–	1979–84
Imogene Field, Tex.	Gas withdrawal	2,400	?	3.9	1944–	1973?–83
Love County, Okla.	Secondary recovery/stimulation	3,622	277	2.8?	1965–,1979–	1977–79
Matsushiro, Japan	Research	1,800	50	2.8	1970	1970
Northern Panhandle, Tex.	Secondary recovery	2,022	21	3.4	1979–	1983–84
Calhio, Perry, Ohio	Waste disposal	1,810	114	2.7?	1975–	1983–87
Rangely, Colo.	Secondary recovery/research	1,900	83	3.1	1958–	1962–75
Rocky Mountain House, Alberta, Canada.	Gas withdrawal	4,000	?	4.0	1970–	1974–
Sleepy Hollow, Neb.	Secondary recovery	1,150	56	2.9	1966–	1977–84
Snipe Lake, Alberta, Canada	.....do.	?	?	5.1	1963–	1970
Cold Lake, Alberta, Canada	Secondary recovery/waste disposal	?	?	~2.0	?	1984–
Permian basin fields:				4.4		1964–
Dollarhide, Tex.-N. Mex.	Secondary recovery	2,590	138	~3.5	1959–	1964–
Dora Roberts, Tex.	....do.	3,661	431	~3.0	1961–	1964–
Kermit Field, Tex.	....do.	1,829	221	~4.0	1964–	1964–
Keystone I Field, Tex.	....do.	975	103	~3.5	1957–	1964–
Keystone II Field, Tex.	....do.	2,987	176	~3.5	1962–	1964–
Monahans, Tex.	....do.	2,530	207	~3.0	1965–	1964–
Ward-Estes Field, Tex.	....do.	914	117	~3.5	1961–	1964–
Ward-South Field, Tex.	....do.	741	138	~3.0	1960–	1964–
War-Wink South, Tex.	Gas withdrawal	1,853	?	~3.0	1969–	1964–

formed the calculations and provided the originals for figures 12–15. We thank Pradeep Talwani (University of South Carolina), Mary Lou Zoback (USGS), and John Armbruster (Lamont-Doherty Geological Observatory) for copies of their papers, figures, and data in advance of publication and Carl Stover (USGS) for a timely copy of his latest map on U.S. seismicity. James Zollweg (USGS) and James Lawson, Jr. (Oklahoma Geophysical Observatory), provided personal insights into some of the more obscure potentially induced earthquake activity along the Gulf Coast and in Oklahoma, respectively, and Jock Campbell (Oklahoma Geological Survey) and Timothy Baker and Robert McCoy (Oklahoma Corporation Commission) provided additional information on oil and gas activities in their State. For information regarding recent activity in Ohio, we would especially like to thank individuals at the Lamont-Doherty Geological Observatory, the Ohio EPA, the Ohio Geological Survey, Weston Geophysical, and Woodward-Clyde Consultants. We appreciate reviews and comments on the manuscript from John Bredehoeft, Robert Hamilton, William Leith, Evelyn Roeloffs, and Keith Evans.

OVERVIEW OF EARTHQUAKES INDUCED BY DEEP WELL INJECTION

Well-documented examples of seismic activity induced by fluid injection include earthquakes triggered by waste injection near Denver (Healy and others, 1968; Hsieh and Bredehoeft, 1981); secondary recovery of oil in Colorado (Raleigh and others, 1972), southern Nebraska (Rothe and Lui, 1983), West Texas (Davis, 1985), and western Alberta (Milne, 1970) and southwestern Ontario, Canada (Mereu and others, 1986); solution mining for salt in western New York (Fletcher and Sykes, 1977); and fluid stimulation to enhance geothermal energy extraction in New Mexico (Pearson, 1981). In two specific cases—near Rangely, Colo. (Raleigh and others, 1976), and in Matsushiro, Japan (Ohtake, 1974)—experiments to control directly the behavior of large numbers of small earthquakes by manipulation of fluid injection pressure were conducted successfully. Table 1 gives a brief listing of each of the cases in which seismicity was clearly associated with fluid injection or other types of adjacent well activities. A more complete summary is provided in Appendix A.

Other cases of induced seismicity, which were the result of either fluid injection or reservoir impoundment, were reviewed and discussed by Simpson (1986a). Unlike fluid injection, however, induced seismicity associated with dams and reservoirs also is affected by the actual physical weight of the water impounded. By contributing to the local stress regime, this effect of the water load can change the local hydrologic properties of the reservoir rock and thus magnify the resulting changes in pore fluid pressure associated with elevating the local water table (Roeloffs, 1988). A brief discussion of the phenomenon of reservoir-induced seismicity is presented in Appendix B.

Although it is true that earthquakes can be triggered without fluid injection (for example, see the sections on the Wilmington and the Flashing oil fields in Appendix A), most of the earthquakes induced by well activities are associated with water-flooding operations to enhance the secondary recovery of hydrocarbons (table 1). This is not surprising because the conditions for failure are much more favorable in injection operations of this type. Fluid injection for the purpose of secondary recovery typically involves injection at high fluid pressures into confined reservoirs of limited extent and low permeability. Often, the producing field is a structural trap, perhaps defined by fault-controlled boundaries. However, in waste-disposal operations, it is preferable to inject into large porous aquifers having high permeabilities that are away from known fault structures. Furthermore, waste-disposal operations typically involve only one to a few wells at any one location, whereas secondary recovery techniques often involve large arrays that comprise tens of wells over the entire extent of the producing field. These differences between the two types of injection operations make well activities for the purpose of secondary recovery much more conducive to triggering adjacent seismicity.

In each of the well-documented examples of earthquakes triggered by deep well injection, convincing arguments that the earthquakes were induced relied upon three principal characteristics of the earthquake activity. First, there was a very close geographic association between the zone of fluid injection and the locations of the earthquakes in the resulting sequence. Second, calculations based on the measured or the inferred state of stress in the Earth's crust and the measured injection pressure indicated that the theoretical threshold for frictional sliding along favorably oriented preexisting fractures, as indicated by the Mohr-Coulomb failure criterion, was likely exceeded. And, third, a clear disparity was established between any previous natural seismicity and the subsequent earthquakes, the induced seismicity often being characterized by large numbers of small earthquakes occurring within a relatively short time interval.

Many of the sites where earthquakes have occurred operate at injection pressures well above 100 bars ambient (table 1). The exceptions tend to be sites characterized by a close proximity to recognized surface or subsurface faults. In the Rangely and the Sleepy Hollow, Nebr., oil field cases, faults are located within the pressurized reservoir and were identified on the basis of subsurface structure contours. The Attica-Dale, N.Y., and the Matsushiro cases occurred close to prominent fault zones exposed at the surface (the Clarendon-Linden and the Matsushiro fault systems, respectively). In the most prominent case of induced seismicity as the result of waste-disposal operations, the Rocky Mountain Arsenal well near Denver, fluid was inadvertently injected directly into a major subsurface fault structure, which was identified later on the basis of the subsequent induced seismicity (Healy and others, 1968) and the properties of the reservoir into which fluid was being injected, as reflected in the pressure-time record (Hsieh and Bredehoeft, 1981).

The Rocky Mountain Arsenal case is considered to be the classic example of earthquakes induced by deep well injection. Before this episode, the seismic hazard associated with deep well injection had not been appreciated fully. At the Rocky Mountain Arsenal, injection into the 3,700-meter (m)-deep disposal well began in 1962 and was quickly followed by a series of small earthquakes, many of which were felt in the greater Denver area (fig. 1*A*). It was not until 1966, however, that a correlation was noticed between the frequency of earthquakes and the volume of fluid injected (fig. 2). Pumping ceased in late 1966 specifically because of the possible hazard associated with the induced earthquakes; afterward, earthquakes near the bottom of the well stopped. Over the next 2 years (yr), however, earthquakes continued to occur up to 6 km away from the well as the anomalous pressure front, which had been established around the well during injection, continued to migrate outward from the injection point. The largest earthquakes in the sequence (M 5.0–5.5) occurred in 1967 (fig. 1*B*), long after injection had stopped and well away from the point of fluid injection itself.

These results imply that the fluid pressure effects from injection operations can extend well beyond the expected range of actual fluid migration. Indications have shown, however, that the risk posed by triggered earthquakes can be mitigated by careful control of the activity responsible for the induced seismicity. As shown by a number of the cases detailed in Appendix A, seismicity eventually can be stopped either by ceasing the injection or by lowering pumping pressures. The occurrence of the largest earthquakes involved in the Rocky Mountain Arsenal case a year after pumping had ceased, however, indicates that the process, once started, may not be controlled completely or easily.

CONDITIONS FOR EARTHQUAKE GENERATION

The case histories of injection-induced seismicity documented in Appendix A demonstrate that, in sufficiently

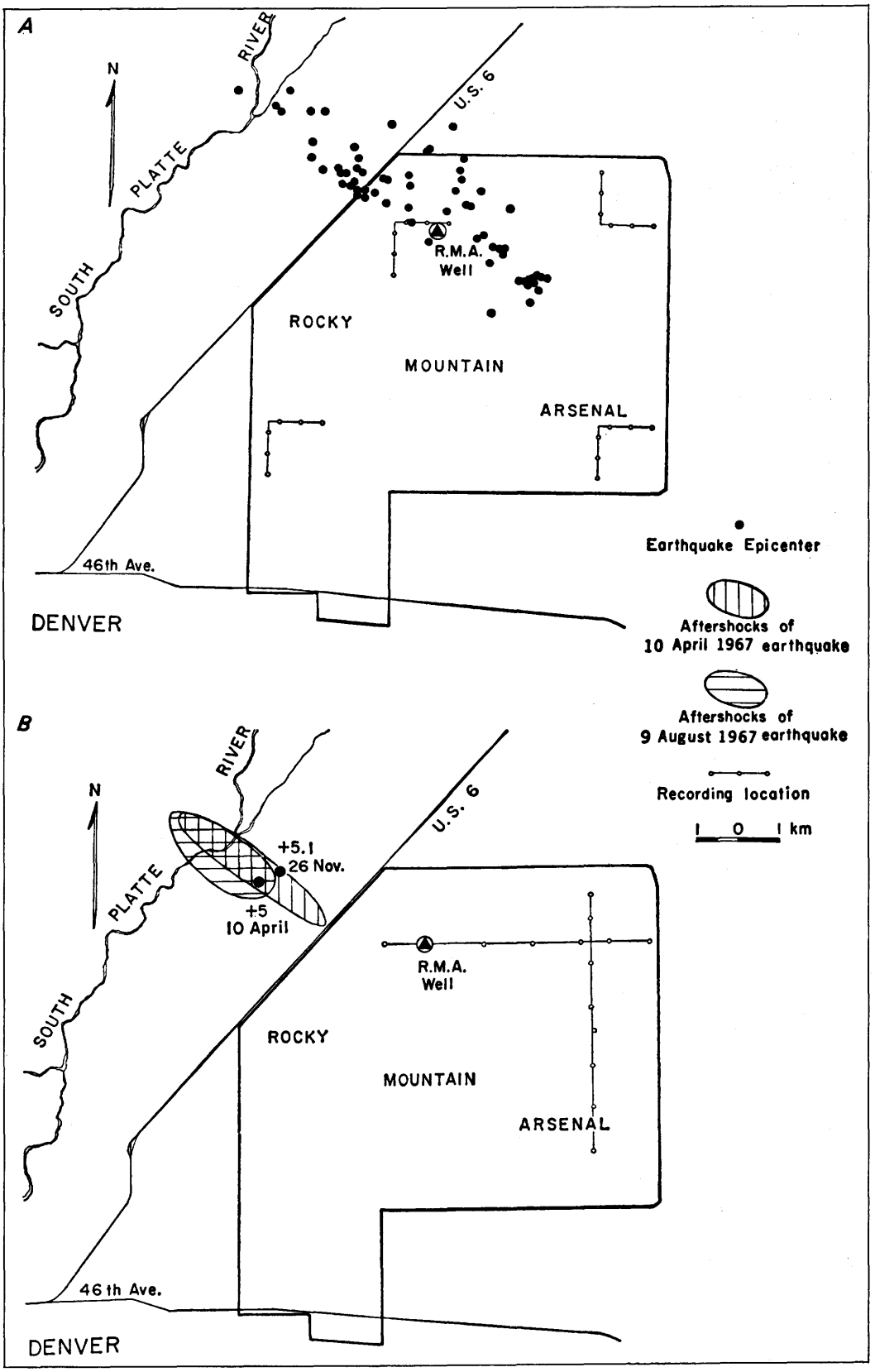

Figure 1. Earthquake activity near the Rocky Mountain Arsenal waste-disposal well, Colorado. *A*, Epicentral distribution of earthquakes during January and February 1966. *B*, Aftershock distributions of the large 1967 earthquakes. Reprinted from Healy and others (1968) and published with permission.

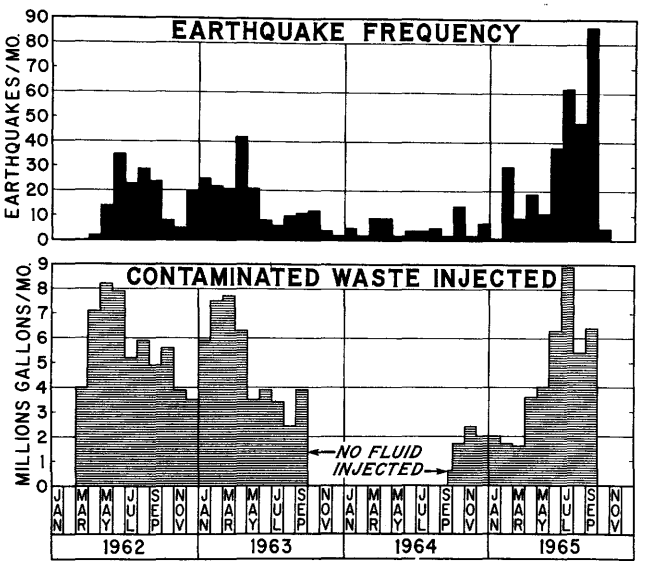

Figure 2. Correlation between earthquake frequency (top) and volume of contaminated waste injected (bottom) at the Rocky Mountain Arsenal well, Colorado. Reprinted from Healy and others (1968) and published with permission.

prestressed regions, elevating formation fluid pressure by several tens of bars can cause a previously quiescent area to become seismically active. However, not all high-pressure injection wells trigger earthquakes. The reasons why depend on the characteristics of the earthquake faulting process, the local hydrologic and geologic properties of the zone of injection, the *in situ* stress field, and the specific conditions for earthquake triggering, many of which have not been understood or appreciated until recently. A fundamental distinction must be recognized, however, between factors that *cause* earthquakes versus mechanisms that may *trigger* earthquakes. Earthquakes result from the sudden release of stored elastic strain energy by frictional sliding along preexisting faults. The underlying causes of earthquakes are, therefore, the forces that are responsible for the accumulation of elastic strain energy in the rock and that raise the existing state of stress to near critical levels. Consequently, the hazard associated with fluid injection is not that it can generate sufficient strain energy for release in earthquakes, but that it may act locally to reduce the effective frictional strength of faults and, thereby, to trigger earthquakes in areas where the state of stress and the accumulated elastic strain energy are already near critical levels as a result of natural geologic and tectonic processes.

Mohr-Coulomb Failure Criterion

Because the shear strength of intact rock is considerably greater than the frictional strength between rock surfaces, slip during an earthquake typically occurs along preexisting faults and will occur when the shear stress (τ) resolved across the fault exceeds the inherent shear strength (τ_0) and the frictional stress on the plane of slip. Quantitatively, this condition is termed the Mohr-Coulomb failure criterion and is expressed by the following linear relation:

$$\tau_{crit} = \tau_0 + \mu\sigma_n,$$

where τ_{crit} is the critical shear stress required to cause slip on a fault, μ is the coefficient of friction, and σ_n is the normal stress acting across the fault (Jaeger and Cook, 1979). For weak fault zones that have little cohesion, τ_0 is nearly zero, and slip will occur when τ is greater than or equal to an amount that is simply the product of μ and the stress normal to the plane of slip; that is, the frictional strength of the fault:

$$\tau_{crit} = \mu\sigma_n.$$

Figure 3 shows values of maximum shear stress (τ) as a function of effective normal stress (σ_n) for a variety of rock types (Byerlee, 1978). For most rock types, the data indicate that μ ranges between 0.6 and 1.0.

When fluid is present in the rocks, the effective σ_n is reduced by an amount equal to the pore pressure, and the shear stress (τ) required to cause sliding is reduced to the following:

$$\tau_{crit} = \mu\,(\sigma_n - p).$$

This reduction in the effective strength of crustal faults is the essential mechanism of induced seismicity; that is, for a constant state of tectonic stress, the effective strength of crustal faults can be reduced below the critical threshold by increasing the fluid pressure contained within the rocks, which leads to a sudden slip and the occurrence of an earthquake.

Description of the State of Stress By Using the Mohr Circle

A simple graphical method for describing the state of stress and how it is altered by the introduction of fluids under pressure is given by the Mohr circle diagram (fig. 4, right; Jaeger and Cook, 1979; Simpson, 1986a). The stresses acting on a given fault plane can be specified with respect to an orthogonal coordinate system and are referred to as the principal stress axes along which stresses are purely compressional. The stress components relative to these principal axes are called the principal stresses and are usually designated σ_1 (maximum), σ_2 (intermediate), and σ_3 (minimum). Shear (τ) and normal (σ_n) stresses along and across fractures of various orientations are linear combinations of the maximum and the minimum compressive stresses (σ_1 and σ_3, respectively) and are defined by the

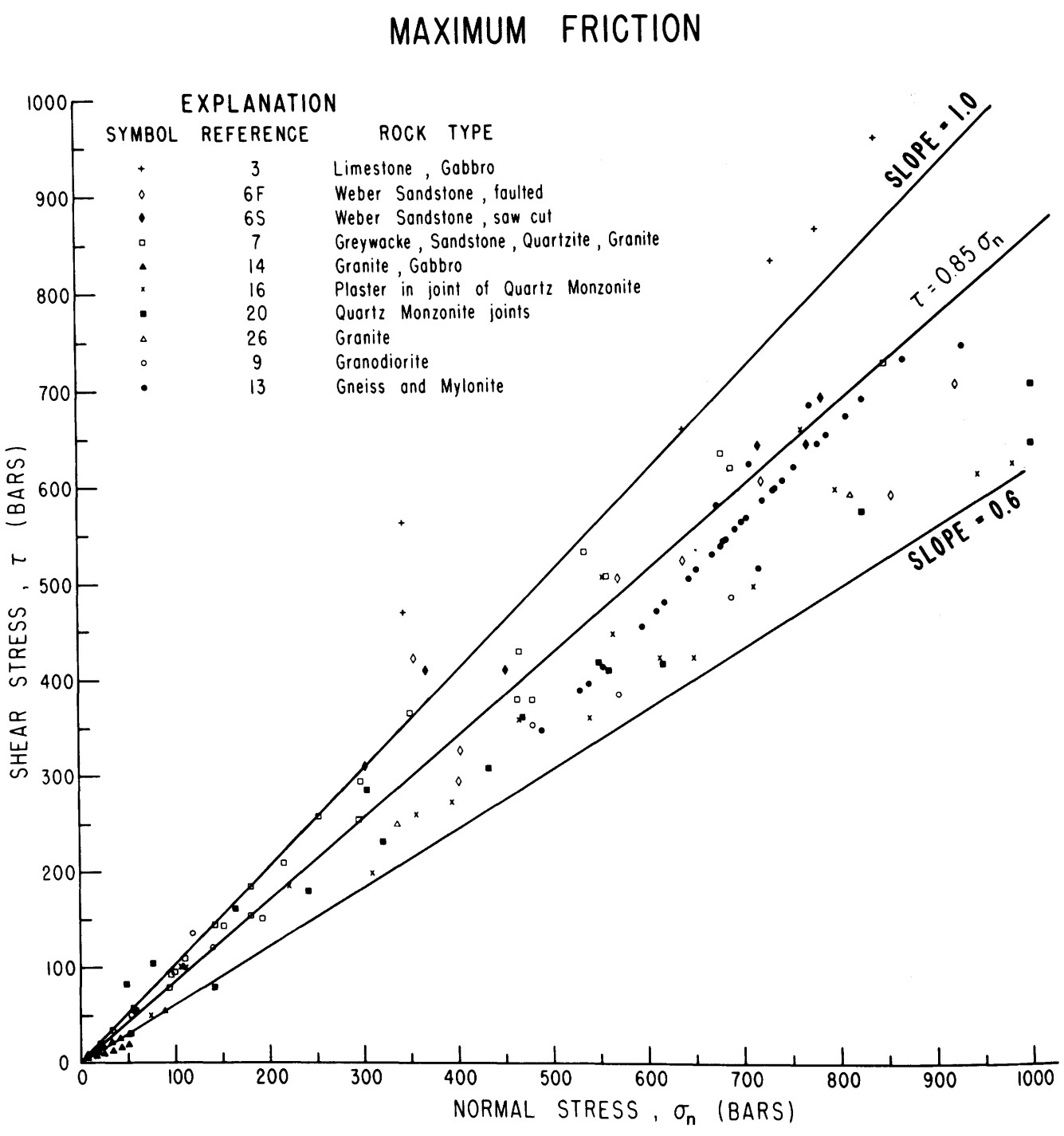

Figure 3. Maximum shear stress as a function of effective normal stress for a variety of rock types. The data suggest that the coefficient of friction ranges between 0.6 and 1.0. τ, shear stress; σ_n, normal stress; and μ, coefficient of friction. Reprinted from Zoback and Healy (1984) and published with permission.

locus of points around the Mohr circle, whose center is the average between σ_1 and σ_3 (fig. 4*B*, right). Thus, for a specific fault plane oriented at angle α with respect to the σ_3 direction (fig. 4*B*, left), τ and σ_n acting along and across that plane will be determined by a specific point on the Mohr circle (identified by angle 2α drawn from the middle, fig. 4*B*, right). Larger stress differences between the maximum and the minimum principal stresses (that is, the deviatoric stress) result in larger Mohr circles and, thus, larger available shear stresses for causing slip along favorably oriented fractures.

The Coulomb failure criterion is represented by a line that has a slope equal to μ and an intercept equal to τ_0 (fig. 4*A*). Relative effective values of σ_1 and σ_3 necessary for

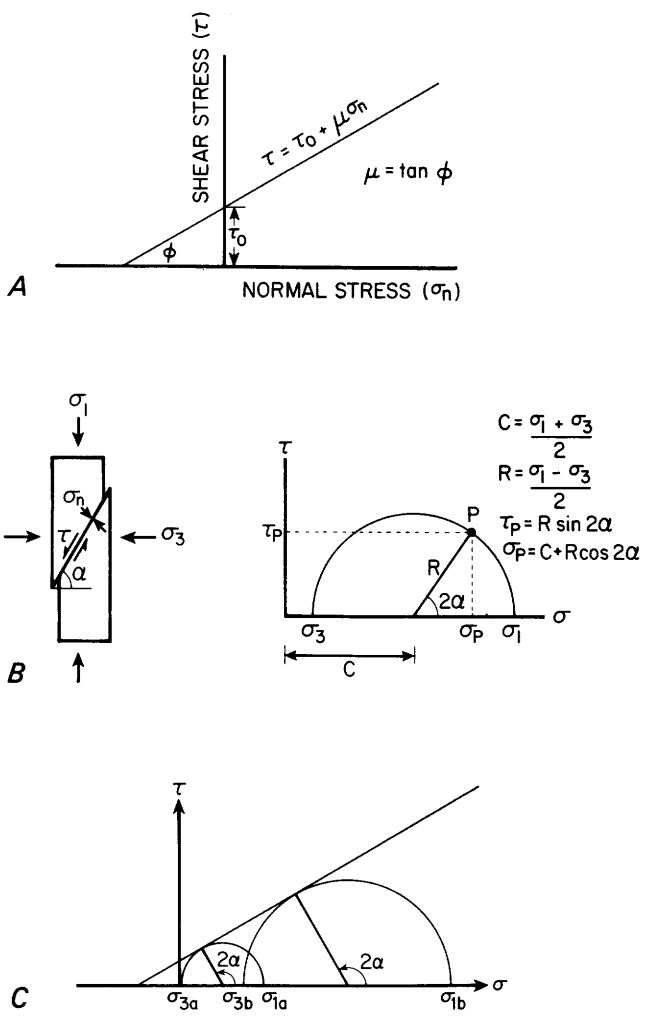

Figure 4. Relations between effective stresses and conditions for failure (slip) on a preexisting fault. *A*, Coulomb's law for failure in dry rock showing the relation between the shear stress (τ) required for failure and the normal stress (σ_n) acting across the plane of slip. Here τ_0 is the cohesion, μ is the coefficient of friction, and ϕ is the angle of internal friction. *B*, The Mohr circle diagram (right), which provides a graphical method by which the maximum (σ_1) and the minimum (σ_3) principal (compressive) stresses can be resolved into shear (τ) and normal (σ_n) components on a plane at angle α to the σ_3 direction (left). The resolved shear (τ_p) and the normal stress (σ_p) define a point (P) given by the radius (R) and center (C) of the Mohr circle. *C*, The Mohr-Coulomb failure criterion. Given any particular state of stress, failure will occur on a plane containing the intermediate stress (σ_2) and oriented at an angle α to σ_3 if the Mohr circle containing points σ_1 and σ_3 intersects the Columb failure curve defined in *A*. Reprinted from Simpson (1986a) and published with permission.

failure thus define circles tangent to this failure envelope (fig. 4*C*). In other words, fault planes whose orientations with respect to a given stress field (σ_1 and σ_3) define values along the Mohr circle that intersect the failure envelope for a given τ_0 and μ will be most likely (most favorably oriented) to slip (fig. 4*C*).

Figure 5 shows how an initial stress state (right Mohr circle) determined at the bottom of a well near Perry, Ohio, is modified by changes in pore pressure (Appendix A). As discussed in the previous section, in the presence of a fluid, compressive stresses are opposed by the hydrostatic fluid pressure. This reduces the effective stress levels by an amount equal to the formation pore pressure and moves the Mohr circle to the left (fig. 5, middle circle). In this example, the state of stress under hydrostatic conditions is close to but does not exceed the failure criterion for a fracture that has no cohesion. Increasing the pore pressure by an amount equal to a nominal injection pressure of 110 bars moves the Mohr circle even farther towards the failure envelope (fig. 5, left circle) and, in fact, for the example shown, indicates that a critical stress level is reached for fractures having τ_0 of as much as 40 bars and μ of 0.6. Fractures that have less cohesion or lower coefficients of friction also would be susceptible to failure.

Conditions for Induced Seismicity

By using the Mohr-Coulomb failure criterion, it is now possible to specify the conditions under which seismicity is most likely to be triggered by fluid injection. First, the existing regional stress field needs to be characterized by high deviatoric stress; that is, the difference between σ_1 and σ_3 is large, which results in large Mohr circles (compare circles in fig. 4*C*). This does not require that the state of stress itself be large, only that large stress differences exist for different fault orientations. In fact, many area identified as close to incipient failure are characterized by relatively low states of stress (σ_{1a} and σ_{3a} in fig. 4*C*). This

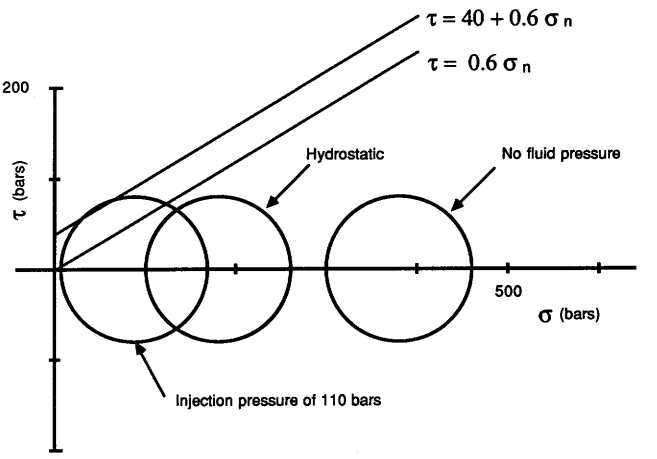

Figure 5. Estimates of shear stress and principal stresses in relation to possible Coulomb failure curves at a nominal depth of 1.8 km near the bottom of an injection well near Perry, Ohio (table 1). τ, shear stress; σ, principal stress; and σ_n, normal stress.

is because low stress states may correspond with low normal stresses acting across potential slip surfaces. Low normal stress implies low frictional strength; thus, faults are weak and easily induced to slip. In the Rocky Mountain Arsenal case, the induced earthquakes occurred in a region of normal faulting that is characterized by a relatively low state of stress and, as a consequence, by a relatively low effective normal stress (but a high shear stress) acting across the fault that slipped (Zoback and Healy, 1984).

Second, preexisting favorably oriented faults or fractures must be available for slip. In general, the shallow part of the Earth's crust is characterized by numerous fractures of different sizes and orientations. However, many of these fractures are small and are capable of generating only small earthquakes of little consequence, and many may not have the proper orientation relative to the existing regional tectonic stress field such that the conditions for failure are met. Thus, for fluid injection to trigger substantial numbers of significant earthquakes, a fault or faults of substantial size must be present that are properly oriented relative to the existing state of stress, characterized by relatively low effective shear strength, and sufficiently close in proximity to well operations to experience a net pore pressure increase. As discussed in in the section "Hydraulic Factors in Earthquake Triggering," the effects of fluid injection dissipate rather quickly as distance from the well increases. This implies that, for typical values of hydrologic properties commonly associated with aquifers of large spatial extent targeted as reservoirs for waste disposal by fluid injection, the pore pressure effect beyond about 10 km is minimal.

Third, injection pressures at which well operations are conducted are relatively high; for example, the Cogdell Canyon Reef oil field in West Texas (table 1), where the largest earthquake known to be associated with secondary recovery operations in the United States was triggered (Davis, 1985), operates at fluid injection pressures of nearly 200 bars above ambient. Other extensive well operations that are in the same tectonic province and, in fact, operate within the same pay zone (the Canyon Reef Formation) are not inducing adjacent seismicity, but these wells typically operate at injection pressures of 100 bars or less. Similarly, the Calhio waste-disposal wells in northeastern Ohio (table 1) may have triggered several small earthquakes in close proximity (<5 km) to the injection site (Nicholson and others, 1988), yet a number of other injection wells that utilize the same basal sandstone layer (the Mount Simon Formation) for the disposal of hazardous and nonhazardous wastes have not done the same. These other wells, however, typically operate at about half the pressure utilized by Calhio. Interestingly, a waste-disposal well located near Ashtabula, Ohio, that became operational in July 1986 and that utilized the same reservoir formation and similar injection pressures to those used by the Calhio wells (Appendix A) triggered a M 3.6 earthquake and a large number of aftershocks in July 1987 (Armbruster and others, 1987).

The hydrologic properties of a reservoir are responsible for how rapidly fluid is accepted and, thus, control the injection pressure required to maintain a constant fluid injection rate (volume of fluid flow into the well). These properties also control how rapidly the pore pressure increase in the reservoir dissipates with distance from the point of fluid injection. Aquifers of large spatial extent, which require low injection pressures for high injection rates, also dissipate the pressure effect most rapidly. This insures that, unless fluid is injected directly into a fault zone (as in the Rocky Mountain Arsenal case), the net pore pressure change from fluid injection will not extend for any appreciable distance from the well. Thus, the distance between a favorably oriented fault or fracture capable of slip and an operating injection well also will become a critical factor in determining the potential for induced seismicity.

Assessing the proximity of favorably oriented preexisting fractures to a potential waste-disposal site in the Central and the Eastern United States is difficult because many of the fault structures responsible for earthquakes in the past and, presumably, the most likely ones responsible for earthquakes in the future are not easily identified. Unlike large historical earthquakes in the Western United States, those that have occurred in the East have yet to produce any primary surface manifestation. This makes identification of active faults or potentially active faults difficult. Reducing the risk of siting an injection well near a major fault may require extensive subsurface geologic mapping to assess the proximity of potential fault structures. Substantial progress has been made, however, in the ability to assess the local state of stress and, thus, to ascertain the degree to which any potential faults or fractures in the vicinity of the well may be close to failure (Evans, 1988).

STATE OF STRESS IN THE EARTH'S CRUST IN THE UNITED STATES

Estimating the state of stress throughout the continental United States has become a very active area of research over the past several years. Its determination is extremely important to a further understanding of regional patterns of crustal deformation and to any accurate assessment of the local seismic hazard. The amount of energy available to be released in an earthquake is determined by the amount of elastic strain energy stored in the rocks of the Earth's crust. The amount of strain energy available for release depends, in turn, on the state of stress. It is the state of stress that determines how close to failure a preexisting fault may be and, as shown in the section "Hydraulic Factors in Earthquake Triggering," how much fluid pressure is required to trigger fault slip or to hydrofracture intact rock. Because of

its importance, the variation in time and space of the magnitude and the direction of the stress field has become the subject of recent intense study. In many cases, the techniques developed to determine the state of stress actually measure secondary effects, such as strain. The greatest difficulty, however, is measuring the necessary parameters at depths where earthquakes actually occur; otherwise, questionable extrapolations must be used from measurements made at shallow depths. In the case of earthquakes induced by fluid injection, the seismicity is likely to be shallow and in close proximity to the well itself. Thus, the advantage in assessing the potential for an existing well to trigger earthquakes is that its presence provides reasonable access to the hypocentral regions where any potential induced events are most likely to occur.

Determining Magnitudes and Orientations of the Local State of Stress

Measurements of the state of stress can be accomplished through a variety of techniques. In general, it is somewhat easier to determine the orientation of the principal stresses than it is to determine their magnitude. Nevertheless, orientations alone are important because the current stress regime may be substantially different from that which existed when major faults in the area were originally produced. This is especially true in the Eastern United States, where most faults are old, seismicity is relatively low, and the identification of active fault structures is more difficult. The orientation of the principal stresses determined from actual *in situ* measurements (fig. 6) can thus aid in identifying those faults that have orientations conducive to slip in the existing tectonic stress field. Orientations and, to some extent, relative magnitudes of the principal stresses can be determined from earthquake focal mechanisms (Michael, 1987), borehole elongations (Gough and Bell, 1981; Plumb and Hickman, 1985), core-induced drilling fractures (Evans, 1979; Plumb and Cox, 1987), and, in some cases, the orientation of young geologic features, such as dikes, volcanic vent alignments, or recent fault offsets (Zoback and Zoback, 1989). Reliable determination of the absolute magnitude of the principal stresses typically requires measurements made by using the hydraulic fracture technique.

Stress Orientation Indicators

Earthquake Focal Mechanism Solutions

Earthquake focal mechanisms are some of the most commonly utilized indicators of principal stress directions (Michael, 1987). Focal mechanism solutions define two alternative planes of slip, as well as two stress axes—one of compression and one of tension (see fig. A1). A discussion of the possible orientations that these particular stress axes may have relative to the principal stress directions is given by McKenzie (1969).

The principal contribution of focal mechanism solutions is that they readily identify the specific type of faulting and the orientation of actual planes of slip (faults) in the local area. By inference, the relative magnitude of the state of stress can then be derived, if one of the three principal stresses (σ_1, σ_2, or σ_3) is assumed to correspond with the vertical stress (S_v) induced by the weight of the overburden. Thus, in areas dominated by normal faulting, S_v corresponds with σ_1, implying that the magnitude of the other two orthogonal stresses (S_H and S_v, which correspond to the maximum and the minimum horizontal compressive streses, respectively) are less than the overburden pressure. In regions of strike-slip faulting, S_v is intermediate, and, in regions of thrust faulting, S_v is less than either S_H or S_h (Anderson, 1951). If the orientation of the principal stresses is known from other data in the same stress province, then focal mechanisms can be used to predict the orientation of available planes of slip and the degree to which such planes are close to the plane of maximum shear.

Wellbore Breakouts

Wellbore breakouts, also known as borehole elongations, are a phenomenon of wellbore deformation induced by inhomogeneous stresses in the crust (fig. 6*C*). When a well is drilled into a medium, the presence of the cavity creates stress concentrations around the borehole wall (Hubbert and Willis, 1957). These stress concentrations are greatest in the section of the wall parallel to the direction of the minimum horizontal compressive stress, S_h. Bell and Gough (1979) interpreted the elongation of the borehole to be the result of spalling of weak material off the wellbore wall caused by localized compressive shear failure in the region where the compressive stress concentration is largest. Subsequent data (Plumb and Hickman, 1985; Plumb and Cox, 1987) has confirmed that wellbore breakouts are indeed the result of stress-induced shear failure under compression and that the orientations of the borehole elongations consistently reflect the orientation of S_h (Zoback and others, 1985). Measurement of the shape of the borehole wall with depth by using standard logging techniques (dipmeter or televiewer) can assess the consistency of the orientations of S_H and S_h as a function of depth, as well as their spatial variation between wells (fig. 6*A*).

Core-Induced Fractures

A recently identified stress orientation indicator, similar in some respects to wellbore breakouts, is the presence of core-induced drilling fractures observed in retrieved bottom-hole cores. These phenomena, also called petal centerline fractures, typically consist of near-vertical or steeply dipping planar fractures observed in the oriented rock cores (fig. 6*C*) and are believed to represent extensional fractures formed in advance of a downcutting drill bit

(Kulander and others, 1977; GangaRao and others, 1979). However, unlike wellbore breakouts, which are compressional features (and, therefore, form parallel to S_h), the orientation of these fractures is thought to parallel the maximum horizontal compressive stress, S_H. Evans (1979) examined oriented cores from 13 natural gas wells in Pennsylvania, Ohio, West Virginia, Kentucky, and Virginia and determined core-induced fracture orientations for hundreds of meters of core in most of the wells. Plumb and Cox (1987) also compiled regional data sets of core-induced fracture orientations (fig. 6*B*). The inferred S_H directions derived from these measurements are generally consistent within wells, between nearby wells, and with adjacent hydraulic fracturing results, borehole elongations, and focal mechanism solutions (fig. 6).

Fault Offsets and Other Young Geologic Features

In the presence of an inhomogeneous stress field, young geologic features, such as dikes or volcanic vent alignments, are most likely to propagate in a direction parallel to S_H. This assumes, however, the absence of any preexisting fabric or other structural features, such as faults, that may preferentially control dike or vent-alignment formation. Fault offset data can be used like focal mechanism solutions to help constrain the orientation and the relative magnitudes of the existing stress field (Angelier, 1979; Michael, 1984), the added advantage being that the actual fault plane is known. The stress orientations derived, however, are valid only for the time period during which fault slip occurred and so are not necessarily valid for the

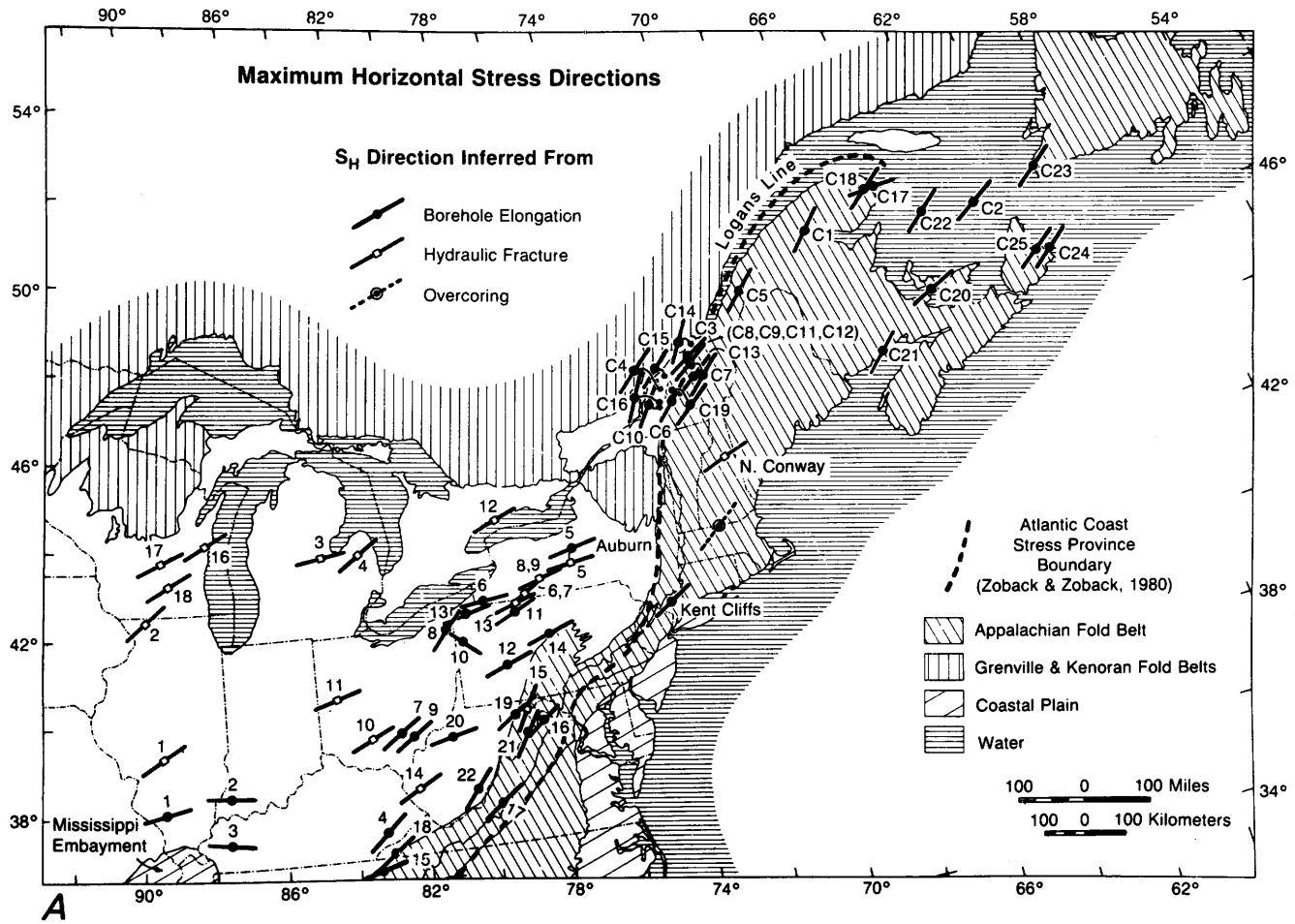

Figure 6. Maximum horizontal stress directions, strikes of core-induced fractures, and the orientation of various stress indicators. *A*, Maximum horizontal stress directions based on borehole measurements—borehole elongation data (dots); hydraulic fracture data (squares); and overcoring measurements (circled dots). *B*, The strikes of centerline fractures observed in Eastern Gas Shales Project (EGSP) cores. East-northeast-trending centerline fractures found throughout the Appalachian Basin correlate with contemporary stress directions shown in *A*. *C*, The relation between orientations of various stress indicators and principal stress directions observed in wells from the Appalachian Basin. Reprinted from Plumb and Cox (1987) and published with permission.

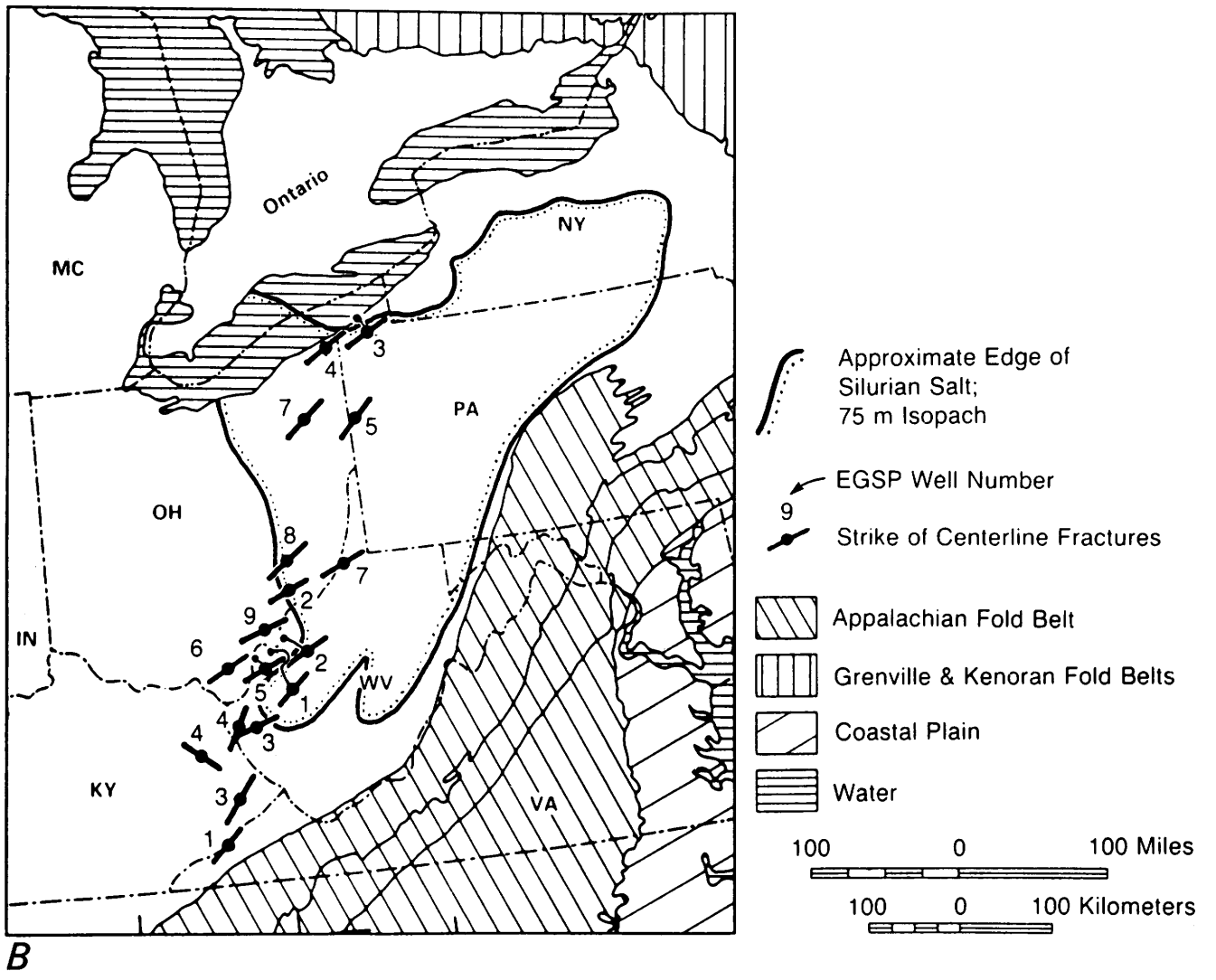

B

Figure 6. Continued.

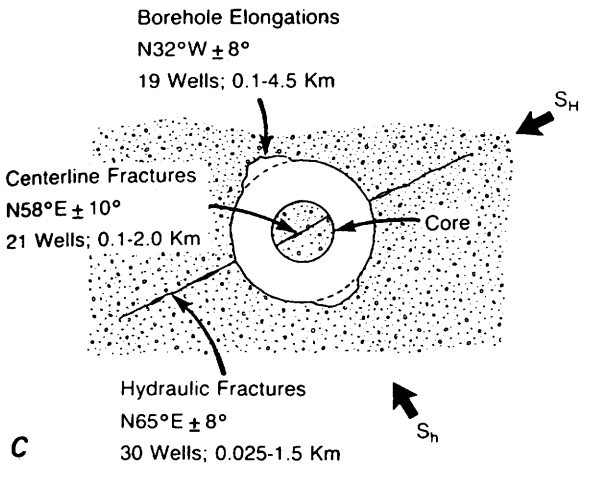

C

Figure 6. Continued.

current tectonic stress field, particularly if the age of faulting is old.

Hydraulic Fracture Stress Measurements in Wells and Types of Pressure-Time Records

The most reliable measurements of the magnitude and the orientation of *in situ* stresses are made by the hydraulic fracture technique (Noorishad and Witherspoon, 1984). The principle involved with this technique is similar to that for core-induced fractures in that failure results from tension rather than from compression. In the hydraulic fracture technique, one principal stress is assumed to be parallel to the borehole and equal in magnitude to the overburden pressure; that is, S_v. If at any point the fluid pressure in the

borehole exceeds the strength of the intact rock and the stress concentration around the wellbore, then a hydraulic fracture is produced (fig. 6*C*). Because the points at which the borehole wall is weakest correspond to a vertical plane perpendicular to S_h, the hydraulic fracture will most likely propagate in that plane. The magnitude of S_h, therefore, can be determined from the pressure acting on the hydraulic fracture immediately after pumping into the well is stopped and the well is shut in. This is called the instantaneous shut-in pressure (ISIP). The magnitude of S_H can then be determined, providing that the assumption of elastic stress concentration around a circular borehole is valid. In some cases, however, the material around the wellbore clearly cannot support the concentration of stresses and fails in compression, resulting in borehole elongation (Bell and Gough, 1983), as discussed above. When this happens, the assumption of elastic behavior near the wellbore is clearly not valid, and S_H cannot be determined in the intervals exhibiting wellbore breakouts.

Basically, the method of hydraulic fracture stress measurement is to pack off an unfractured section of the wellbore and then to increase the fluid pressure in that section until a fracture occurs in the borehole wall. Because the section is isolated (that is, packed off), the pressure is monitored carefully, and, because only a small volume of fluid is used, a small controlled fracture is produced rather than a massive hydraulic fracture, as in the case of well stimulation to enhance circulation (Pearson, 1981). The fluid pressure required to cause the fracture is called the fracture pressure or the breakdown pressure (P_b). After a fracture is produced, fluid pressure in the packed-off section is then cycled repeatedly to determine the pressure required to reopen the fracture (P_{fo}) by pumping small volumes at a constant flow rate and by permitting "flow-backs" to occur following each injection cycle to allow for the drainage of excess fluid pressure. In general, the pressure and flow records produced under these controlled conditions will reflect both of the procedures used during hydraulic fracturing and the *in situ* stress field. Thus, careful analysis of the pressure-time histories recorded during hydrofracturing can be used to estimate the magnitude of the principal stress components. Stress orientation is then determined by using a borehole televiewer or impression packer to ascertain the orientation of the hydraulic fracture created. Figure 7 shows an example of a typical hydraulic fracture pressure-time record from a well drilled to a depth of 185 m in crystalline rock near the San Andreas Fault in central California. In the case of a waste-disposal well, this measurement ideally would be made in the anticipated zone of injection or, if possible, in the basement rock below the waste-disposal aquifer, so as not to interfere with the integrity of the confining layer.

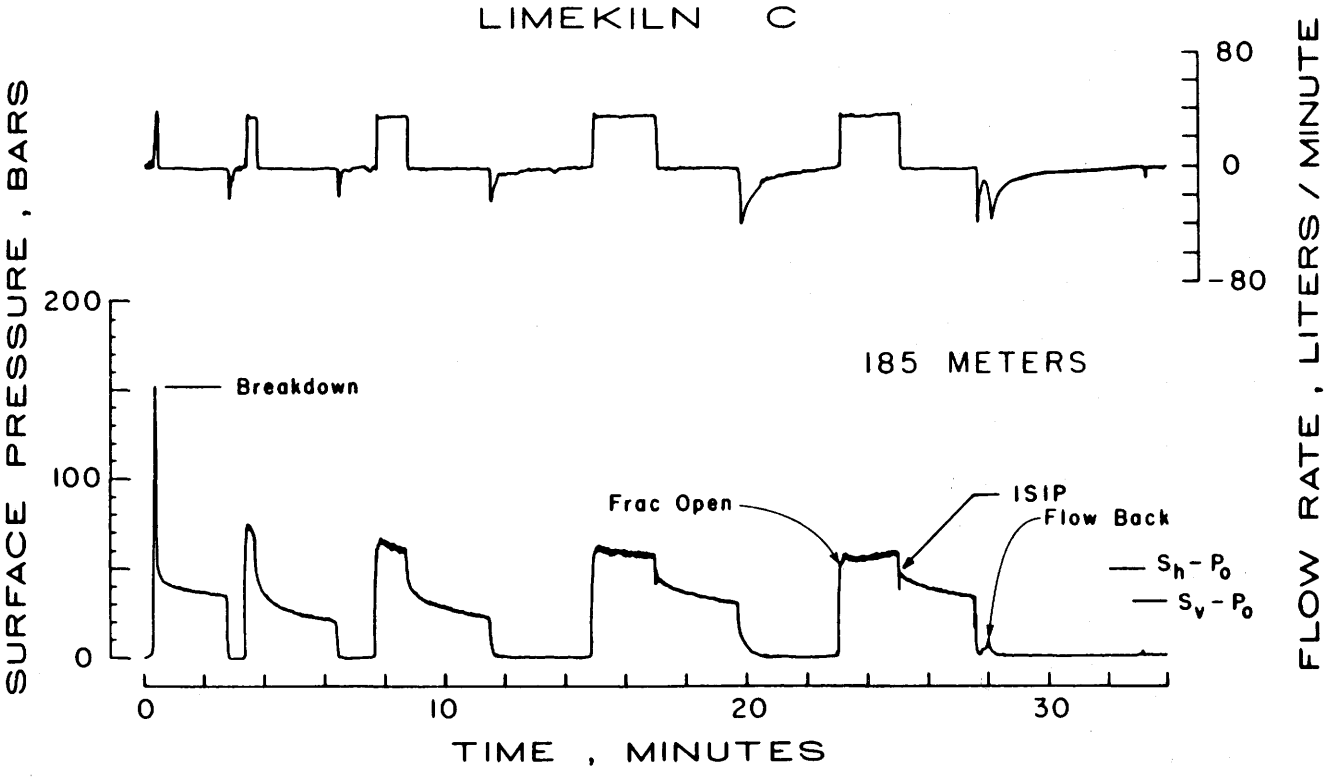

Figure 7. Surface pressure and flow versus time records during a hydraulic fracture stress measurement made at a depth of 185 m in the Limekiln C well, which was drilled 4 km from the San Andreas Fault in central California. The breakdown, fracture opening, and instantaneous shut-in surface pressures (ISIP) are indicated. S_h, minimum horizontal stress; S_v, vertical stress; and P_o, initial pore pressure. Reprinted from Hickman and Zoback (1983) and published with permission.

It should be noted that when the term "fracture pressure" is used in commercial stimulation operations, it rarely corresponds with the value of the "breakdown pressure" referred to in hydraulic fracturing stress measurements. This is because, in commercial stimulation operations, the section of the borehole wall to be fractured often contains preexisting fractures of random orientation that possess various cohesive strengths of unknown quantity. Because commercial stimulation, therefore, typically involves reopening preexisting cracks rather than generating a new fracture of known orientation, "fracture pressure" from commercial hydrofracture operations often represents an unspecified value between the breakdown pressure (P_b) and the fracture-opening pressure (P_{fo}) discussed in the context of hydraulic stress measurement techniques.

From the results of Hubbert and Willis (1957), Haimson and Fairhurst (1967) derived the following equation:

$$P_b = 3S_h - S_H - p + T_0,$$

which relates P_b to S_h and S_H, the initial formation pore pressure (p), and the formation tensile strength (T_0). As mentioned before, S_h can be determined from the ISIP. Determination of the magnitude of S_H requires knowledge of T_0. A good *in situ* measure of T_0 can be inferred from the difference between P_b and P_{fo} (fig. 8*A*). In practice, several successive cycles of fluid injection may be required to measure this quantity accurately (fig. 8*B*). It was then recognized that, if the initial formation p and the ISIP were known, then S_H could be determined directly from P_{fo}:

$$P_{fo} = 3S_h - S_H - p$$

(Bredehoeft and others, 1976). Figure 7 shows how each of the three values (P_b, P_{fo}, and the ISIP) are reflected in the pressure-time history of an actual hydraulic fracture record.

On the basis of the equations above for P_b and P_{fo}, at least three types of pressure-time histories can be identified, depending on the relative values of P_b, P_{fo}, and S_h. Figure 9 shows examples of these three types of pressure records and how each can be distinguished.

Comparison of Fracture Pressure and the Mohr-Coulomb Failure Criterion

The increase in formation pore pressure by fluid injection in a well can induce either a new hydraulic fracture or slip on a preexisting fault. In both cases, the critical pressure necessary for failure is dependent on the *in situ* stress field. Pressure limitations of maximum allowable injection pressures established for various waste-disposal operations typically are set below the estimated value of P_b to prevent an uncontrolled fracture of the confining layer

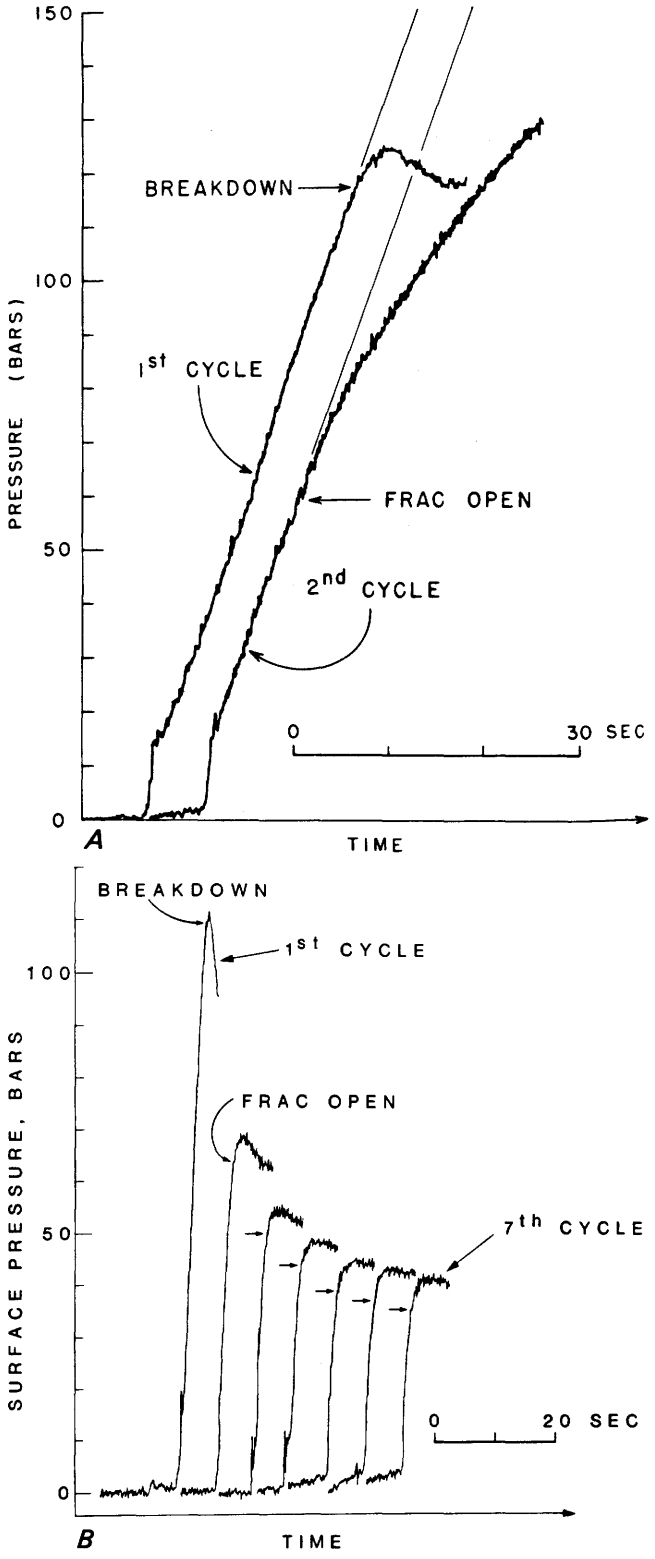

Figure 8. Injection pressure versus time during initial hydraulic fracturing and subsequent cycles of pumping. *A*, Differences between the initial cycle in which a fracture occurs (breakdown) and the subsequent cycles that reopen (fracture-opening pressure) and possibly extend the previously formed crack. *B*, Multiple pumping cycles showing the decrease in fracture-opening pressure with each cycle. Reprinted from Hickman and Zoback (1983) and published with permission.

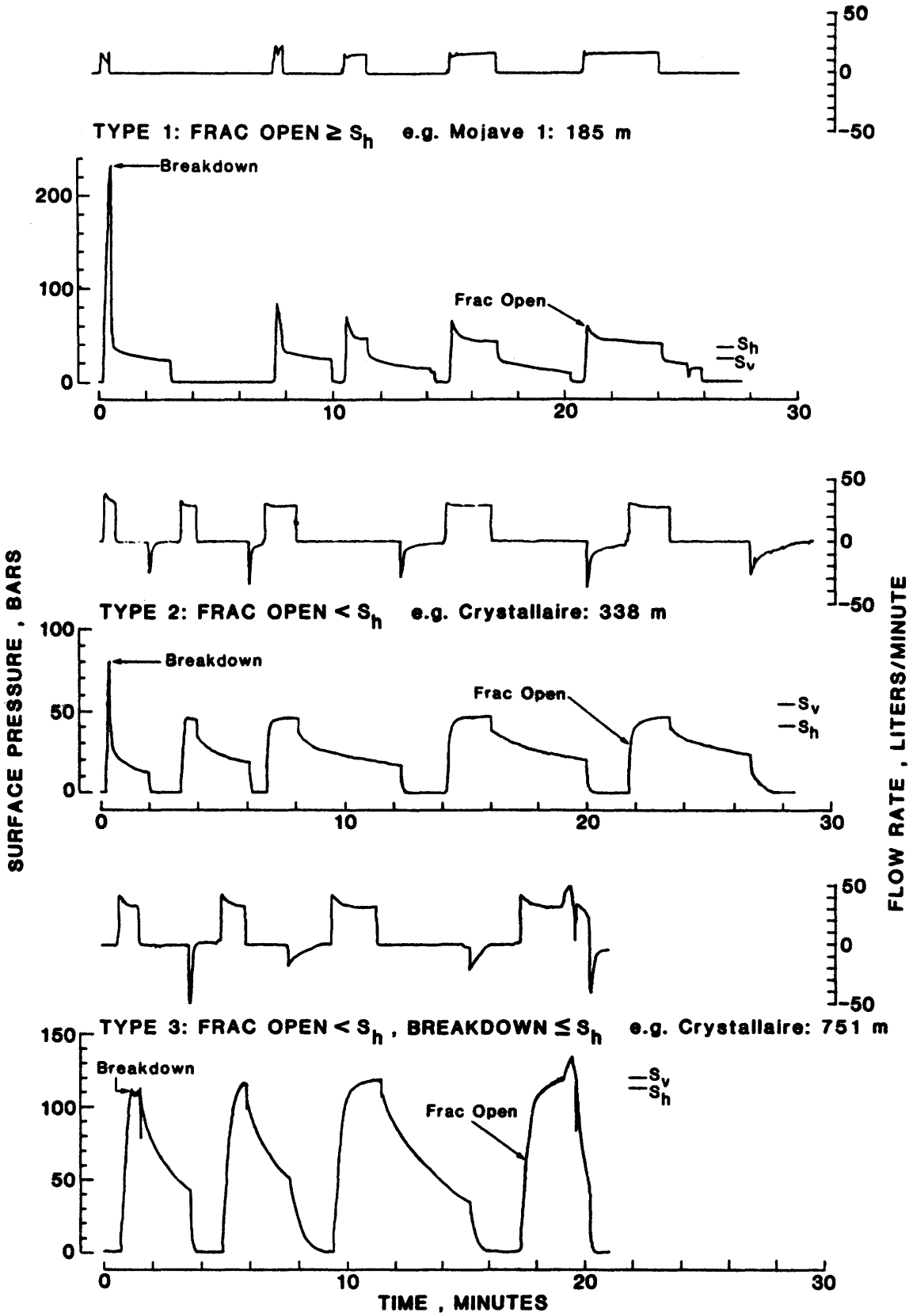

Figure 9. Three different types of hydraulic fracture pressure-time histories taken from two wells drilled near the San Andreas Fault in southern California. The examples are defined by the differences in the magnitudes of the breakdown and fracture opening pressures relative to the minimum horizontal principal stress. The calculated magnitude of the vertical stress is shown for comparison. S_h, minimum horizontal stress; and S_v, vertical stress. Reprinted from Hickman and Zoback (1983) and published with permission.

above the aquifer used for waste disposal and the potential contamination of potable water supplies. Although the concept of P_b is well recognized in the drilling and well-operations industry, its dependence on the regional tectonic stress field, as well as on the tensile strength of the rock, often is not appreciated fully. Thus, before reasonable levels of injection pressure are set, accurate knowledge of the existing state of stress is extremely important.

In terms of the relative magnitudes of fluid pressure needed to induce slip on a preexisting fault versus the fluid pressure necessary to cause a hydraulic fracture, the pressure needed to cause slip is typically much lower; for example, suppose the state of stress can be characterized by a regime in which the vertical stress (S_v) is close to S_H and the stress ratio α of S_h to S_H is 0.65. The breakdown pressure (P_b) required to hydrofracture intact rock is then given by the following equation:

$$P_b = S_v\,(3\alpha - 1) - p + T_0.$$

At a nominal depth of 2 km and for a rock density of 2.6 grams per cubic centimeter, S_v is about 510 bars. If T_0 is taken to be 40 bars and p is near hydrostatic (p = 200 bars), then P_b = 325 bars, or 125 bars above ambient. Fracture-opening pressure (P_{fo}) would be 285 bars, or 85 bars above ambient. However, the critical fluid pressure (P_{crit}) necessary to induce sliding on a favorably oriented preexisting fracture that has no cohesion is equal to the following:

$$P_{crit} = (K\,\sigma_3 - \sigma_1)/(K - 1),$$

where $K = [(\mu^2 + 1)^{1/2} + \mu]^2$ (Jaeger and Cook, 1979). For μ = 0.6 and the stress regime given above, this relation reduces to the following:

$$P_{crit} = S_v\,(3\alpha - 1)/2\ ,$$

which, for the values of α and S_v given above, yields P_{crit} = 242 bars, or only 42 bars above ambient. If the fault exhibits cohesion, then the critical fluid pressure required to induce slip is proportionately greater. Nevertheless, under the conditions assumed above, an increase in fluid pressure of 42 bars above ambient would be sufficient to induce slip on planes having no cohesion that contain σ_2 and are oriented about 30° relative to σ_1; 85 bars above ambient would be sufficient to open preexisting fractures (increase transmissivity) oriented parallel to σ_1; and 125 bars would be sufficient to fracture the intact rock of the borehole wall hydraulically.

Thus, setting maximum injection levels at pressures below that required to fracture the intact borehole wall will *not* guarantee the prevention of induced seismicity if favorably oriented preexisting faults are present near the well. Conducting a controlled hydraulic fracture stress measurement, however, will determine the safe level of fluid injection pressure to prevent an uncontrolled hydrofracture and the proximity to failure of any adjacent potential slip surface.

Summary of Stress Measurements to Date

Compilations of various stress measurements have been made by several investigators (Sbar and Sykes, 1973; Lidener and Halpern, 1978; Zoback and Zoback, 1980, 1989). These summaries suggest that the continental United States can be divided into distinct stress provinces, within which the stress field is fairly uniform in magnitude and in direction. Figures 6 and 10 show some of the most recent compilations of stress orientations within the conterminous United States (Plumb and Cox, 1987; Zoback and Zoback, 1989). Both sets of compilations identify the type of stress indicator used at each site. A more generalized stress map showing average principal stress orientations, the stress regime, and delineating the stress provinces is shown in figure 11. In some cases, the boundary between various provinces is sharp, whereas, in others, it is broad and transitional.

Much of the Central and the Eastern United States, where a large number of waste-disposal wells are concentrated, is characterized by a compressive stress regime (fig. 11). Reverse and strike-slip faulting would be most likely to occur in this part of the country, as the vertical stress (S_v) is less than one or both of the horizontal stresses. Because the maximum principal compressive stress (σ_1) is horizontal and typically oriented northeast to east, planes striking 30° to 45° relative to S_H would be oriented most favorably for slip. For large parts of the Central United States, the magnitudes of the principal stresses indicate that only relatively small increases in pore pressure along such favorably oriented fractures are required to induce slip (Evans, 1988).

HYDROLOGIC FACTORS IN EARTHQUAKE TRIGGERING

In all the well-documented cases of injection-induced seismicity, the increase of pore pressure resulting from the fluid injection is the key perturbation to the natural environment responsible for triggering the earthquakes. A well-developed body of theory and computational techniques exists for the estimation of the temporal and the spatial distribution of the pressure field generated by an injection operation. Relatively straightforward analytic techniques are available for most simple geometries, such as radial flow in a confined horizontal aquifer. Numerical modeling techniques are also available for more complicated geometries. The most complete analyses of the hydrologic factors involved in earthquake triggering were conducted in association with the Rocky Mountain Arsenal and the Rangely earthquake sequences (Raleigh and others,

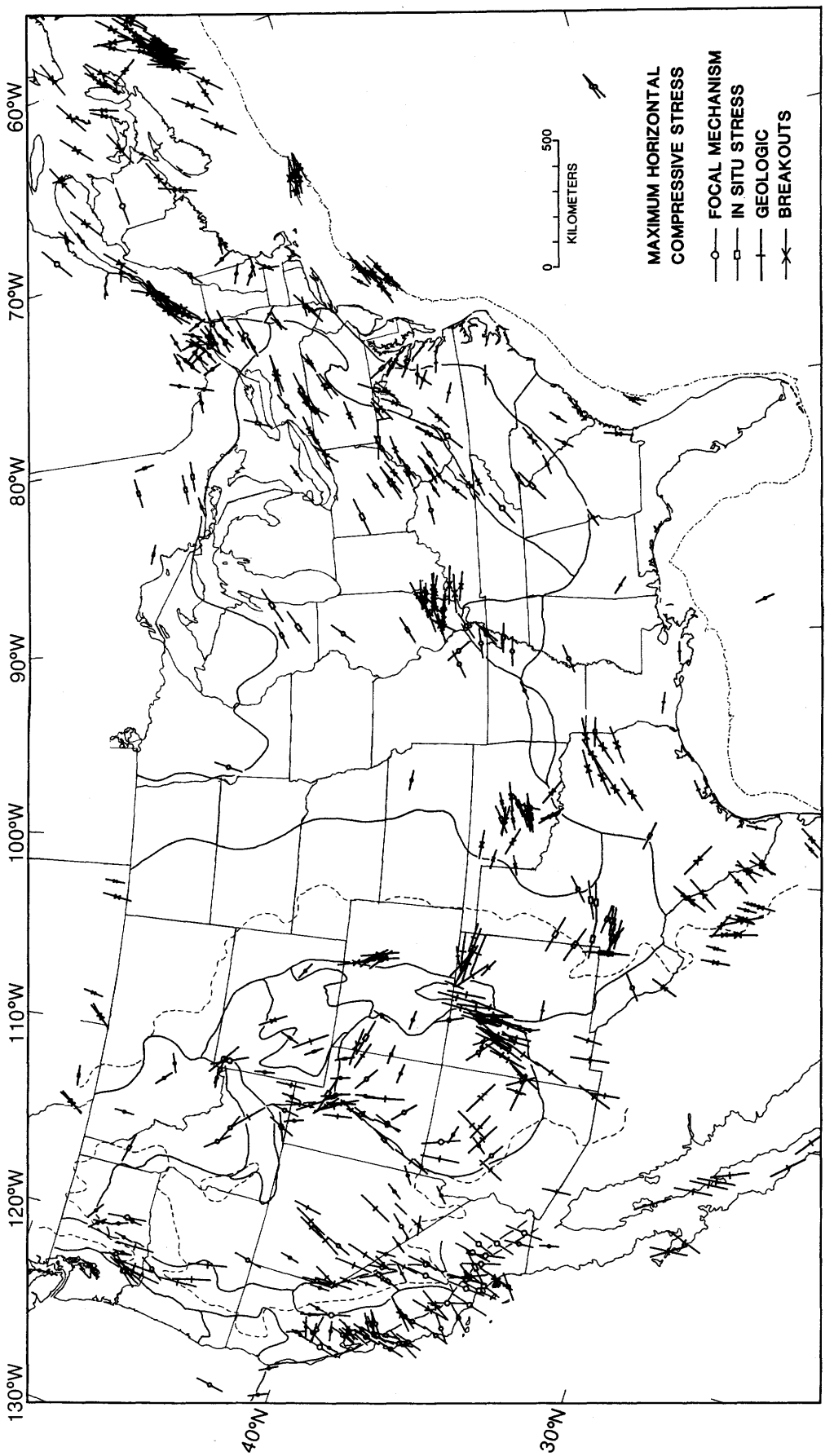
MAXIMUM HORIZONTAL
COMPRESSIVE STRESS
FOCAL MECHANISM
IN SITU STRESS
GEOLOGIC
BREAKOUTS
0
500
KILOMETERS
130°W
120°W
110°W
100°W
90°W
80°W
70°W
60°W
40°N
30°N

1976; Hsieh and Bredehoeft, 1982). In the Rocky Mountain Arsenal case, the pressure field was dominated by a fault or fracture zone of finite width that had high permeability relative to the country rock. Although the reservoir geometry was less complex at Rangely, the pressure field also seemed to be affected by the presence of a zone of high permeability that coincided with a mapped subsurface fault (see fig. A2*A*). For most cases of Class I injection wells (that is, those wells used for the disposal of hazardous waste), sites are chosen to avoid faults where possible, and, in such cases, estimating the development of the pressure field established around the well by fluid injection can rely on using relatively simple methods. However, if, after the completion of the well, evidence comes to light suggesting that a more complex model of reservoir geometry is appropriate, then it would be necessary to reassess the net effect of fluid injection by utilizing more precise and sophisticated techniques for analysis.

Most of the common methods available for calculation of the pressure field from an injection well are adaptations of standard techniques used in ground-water modeling (Davis and DeWiest, 1966; Freeze and Cherry, 1979; Fetter, 1980). However, as mentioned above, changes in the standard techniques are required in the presence of faults, fractures, or other possible pathways for anisotropic fluid flow. In addition, if fluid is being injected into a rock of extremely low permeability, typical of the crystalline basement where most earthquakes occur, then other factors of importance may also come into play. Methods for calculating ground-water flow in such low-permeability environments are discussed by Neuzil (1986).

The critical reservoir characteristics for predicting the pressure field around an injection well are the transmissivity and the storativity of the rocks. The lower the transmissivity is, the more confined the "pressure bulb" around the bottom of the well is and the more likely that high pore fluid pressures will be established, thus increasing the concern for earthquake triggering. Inasmuch as earthquakes occur on faults and these same faults can act as zones of high permeability (high transmissivity), determining the presence of faults or fractures is important for predicting the occurrence of induced seismicity.

In many cases where potentially active faults occur at some distance from the injection well, accurate fluid pressure changes are difficult to anticipate because detailed information about the hydrologic properties of the reservoir away from the injection well are lacking; for instance, supposing waste is injected into a basal sedimentary unit overlying crystalline basement, although much may be known about the zone of injection, little may be known about the hydrologic characteristics of the deeper basement rock, where the potential for earthquakes—owing to the presence of faults and fractures—may be significant. As shown below, some estimate of the average characteristics of the reservoir in the vicinity of a well can be inferred from measurements made during well completion and detailed monitoring of the pressure-time history.

◀ **Figure 10.** Maximum horizontal compressive stress orientations throughout the conterminous United States. Solid lines, physiographic provinces typically exhibiting nearly uniform stress fields. Reprinted from Zoback and Zoback (1989) and published with permission.

Reservoir Properties

For a given reservoir geometry, the fluid pressure field generated by injection is governed by transmissivity and storativity, which are functions of porosity (n), the permeability, and the elastic constants of the aquifer. These parameters can be determined from laboratory tests on well cores, piezometer tests, or pumping tests. Pumping tests have the desirable characteristic that they average over a large *in situ* volume of the aquifer and, therefore, represent the most realistic estimates. The storativity (S), which gives the amount of fluid released per unit column of aquifer for a unit decline in head, can be calculated from the following expression:

$$S = \rho g h\,(\alpha_v + n\beta),$$

where ρ is fluid density, g is the acceleration of gravity, h is the aquifer thickness, α_v is the vertical compressibility of the aquifer, and β is the fluid compressibility. Transmissivity (T) is defined as follows:

$$T = \boldsymbol{K}b,$$

where $\boldsymbol{K}$ is the saturated hydraulic conductivity, and b is the thickness of the aquifer (Freeze and Cherry, 1979). Hydraulic conductivity ($\boldsymbol{K}$) is simply as follows:

$$\boldsymbol{K} = k\rho g/\eta,$$

where k is the specific or intrinsic permeability, and η is the dynamic viscosity of the fluid. The storativity and the transmissivity of the reservoir can be estimated from pumping tests by using curve-matching techniques that apply either the Theis log-log plot or the Jacob semi-log plot methods (Freeze and Cherry, 1979).

Fluid Pressure Changes Resulting From Injection

For purposes of illustration, two types of reservoir models are presented—an infinite isotropic reservoir and an infinite strip reservoir that has infinite length but finite width and thickness; that is, rectangular cross section. These models are simply for the purpose of studying how fluid pressure may propagate horizontally away from an

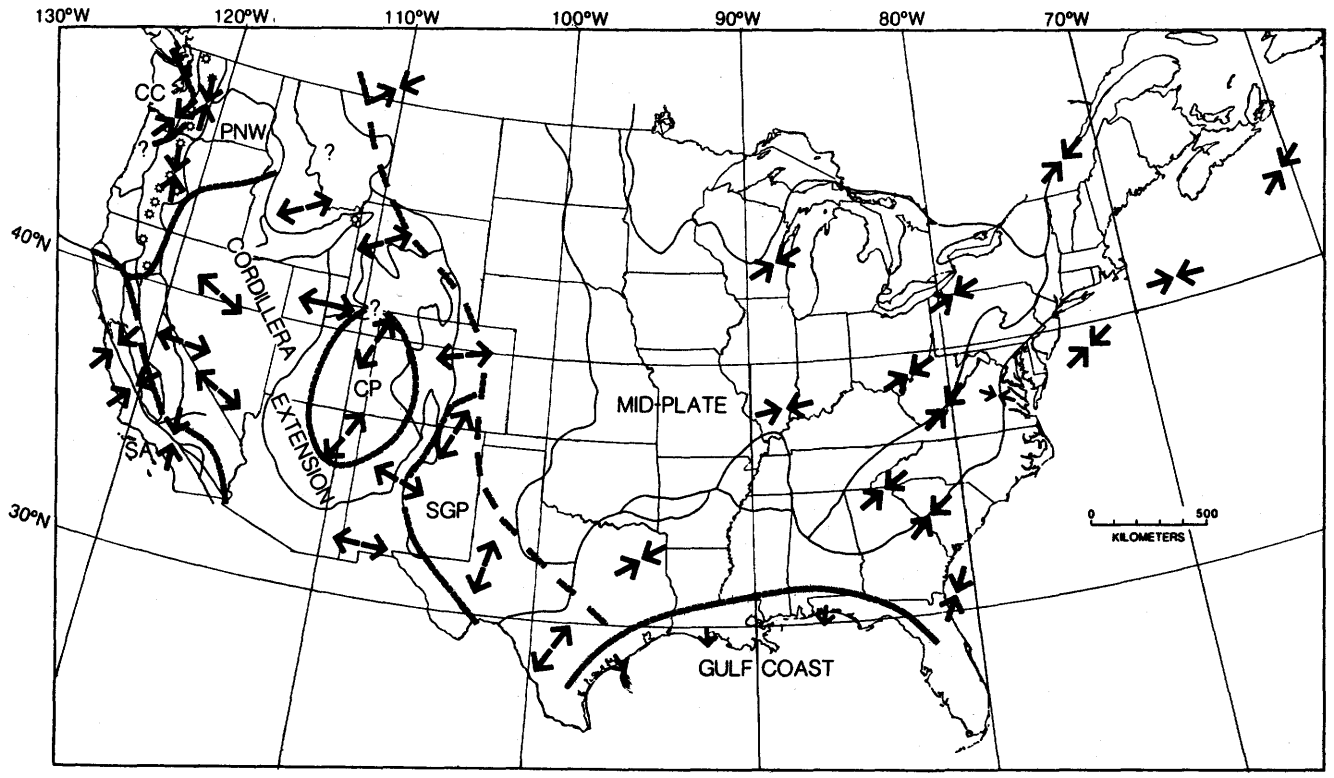

Figure 11. Generalized stress provinces of the conterminous United States. Outward-pointing arrows, areas characterized by extensional deformation (that is, normal faulting); inward-pointing arrows, regions dominated by compressional tectonism (that is, reverse and strike-slip faulting); dashed lines, horizontal stress provinces—CC, Cascade convergent; PNW, Pacific Northwest; SA, San Andreas; CP, Colorado Plateau; and SGP, Southern Great Plains. Reprinted from Zoback and Zoback (1989) and published with permission.

injection well. They do not address the question of how fluid pressure effects might migrate downward from the injection horizon towards potential earthquake-producing structures in the basement.

Infinite Reservoir Model (Radial Flow)

The simplest model for estimating the development of a pressure field around an injection well is radial flow in a single infinite isotropic aquifer of constant thickness. The fluid pressure $p(r,t)$ at distance (r) and time (t) as a result of a constant flow rate (Q) into a reservoir that extends uniformly in all directions is given by the following equation:

$$p(r,t) = \frac{\rho g Q}{4\pi T} \int_u^\infty \frac{e^{-\xi}}{\xi} d\xi ,$$

in which $u = r^2S/4Tt$ (Freeze and Cherry, 1979). Figures 12 and 13 show example calculations for the pressure field around an injection well in Ohio. The values of storativity [5.4×10^{-5} square meters per second (m^2/s)] and transmissivity (4.5×10^{-6} m^2/s) in the radial flow model are rather low compared to those for optimal waste-disposal operations; thus, the pressure at the wellbore required to achieve the desired rate of fluid injection is rather high. Figure 12 shows the pressure change versus time curve at the wellbore for a well that has a radius of 12 cm and assuming a constant injection rate of 6.7×10^6 liters per month (L/mo). Figure 12 also shows how a change in shape of the reservoir can effect the pressure-time history at the wellbore. Thus, whether pressure is rising because of fluid injection or falling because injection has stopped (in this case, after a nominal injection period of 15 yr), the pressure history is characteristic of the reservoir geometry.

In the radial flow model, the pore pressure (p) rises relatively rapidly during the first few years and then continues to rise at an ever-decreasing rate. Once injection has stopped, the decline in pressure at the wellhead is most rapid in the radial flow model. The attenuation of the pressure field with distance away from the well is shown in figure 13. With increasing time, the pressure bulb around the well continues to grow. After 10 yr of injection, the pressure increase at a distance of 5 km from the well is about 15 percent of the value at the wellbore.

Infinite Strip Reservoir Model

If fluid flow is confined to a narrow reservoir of finite width, then the fluid pressure at a given distance from the

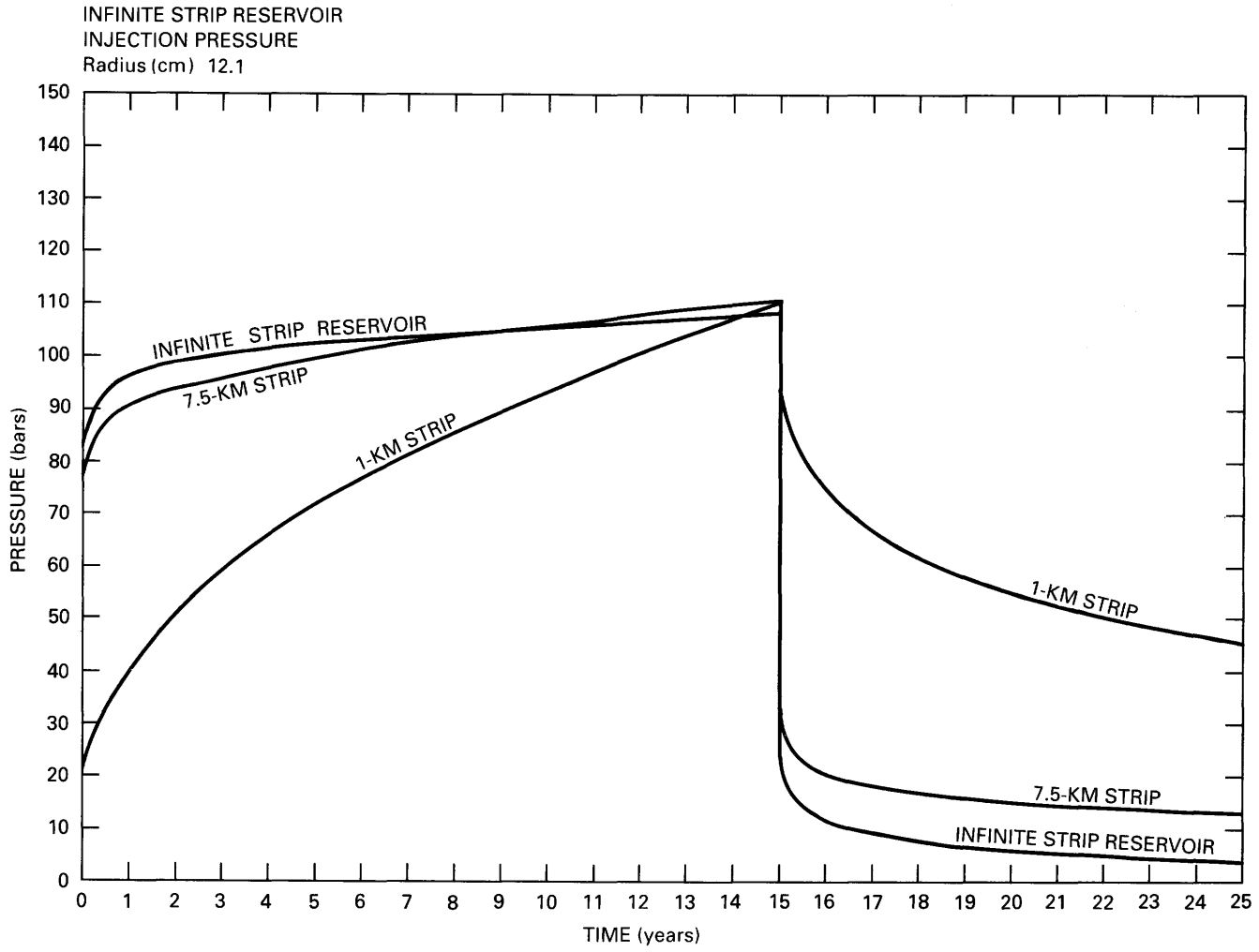

Figure 12. Injection pressure versus time as calculated from the equations in the text for radial flow (infinite width) and finite width (1.0 and 7.5 km) reservoir models. An injection rate of 6.7 million L/mo is used and is assumed to cease after 15 yr. Transmissivities are varied between models to produce approximately 110 bars of wellhead pressure after 15 yr (from Wesson and Nicholson, 1986).

well will be higher than that of the radial flow case. This type of model was used by Hsieh and Bredehoeft (1981) to calculate the pressure distribution around the Rocky Mountain Arsenal well implicated in the 1967 Denver earthquake sequence. Even if no specific evidence suggests that such a similar linear zone of high permeability is characteristic of a particular reservoir geometry, such calculations still may be useful to illustrate how large a pressure buildup is possible at any given distance and to show how the pressure history at the wellbore is diagnostic of the shape of the reservoir into which fluid is being injected.

For injection into the center of a strip of finite width (w) and infinite extent in the x direction, a constant injection rate (Q) produces a pressure given by the following:

$$p(x,y,t) = \frac{\rho g Q}{4\pi T} \sum_{m=-\infty}^{\infty} \int_{u_m}^{\infty} \frac{e^{-\xi}}{\xi} d\xi ,$$

where y is the distance from the center of the strip, and $u_m = [x^2 + (y + mw)^2]S/4Tt$. Figure 12 shows how the pressure at the wellbore will increase with time for reservoirs of infinite length and various widths. Figures 14 and 15 show the attenuation of the pressure field with distance away from the well for the same two models. Two strip models are considered—a width of 1 km and a transmissivity of 2.0×10^{-5} m^2/s and a width of 7.5 km and a transmissivity of 4.5×10^{-6} m^2/s. The transmissivities are selected to make the pressure-time curves comparable to those exhibited by the radial flow case discussed in the previous section. Two points are clear. First, for a constant fluid injection rate, the pressure required at the wellbore initially rises more gradually for either of the two infinite strip reservoir models than for the case of radial flow but continues to rise at a more rapid rate at later time intervals. Second, the narrower the postulated reservoir is, the higher the formation fluid pressure that will be achieved with time

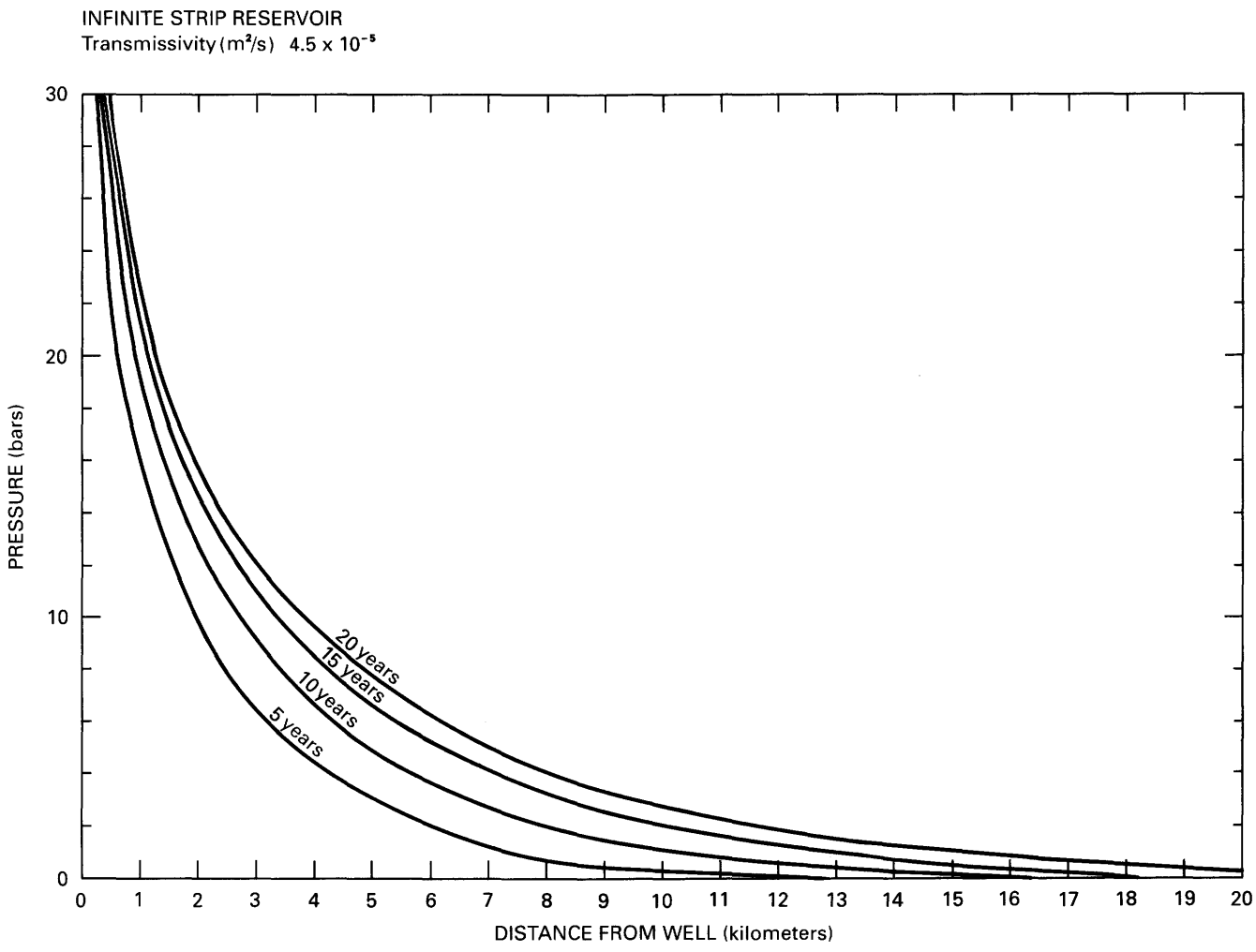

Figure 13. Calculated increased pore pressure versus distance as a result of injection into a confined reservoir of infinite extent (radial flow) and transmissivity of 4.5×10^{-5} m^2/s (from Wesson and Nicholson, 1986). Time intervals are 5, 10, 15, and 20 yr.

at large distances from the wellbore. Moreover, once injection has ceased, the decline in pressure at the wellhead is more gradual for either of the two infinite strip models than for radial flow. Because reservoir geometry has such a significant effect on the pressure-time curves, it is evident that analysis of the history of injection pressure at the wellhead can be used to help discriminate the shape of the reservoir into which fluid is being injected.

UNRESOLVED ISSUES

Although much is known about how earthquakes are induced by deep well injection, full understanding of the earthquake process is far from complete. Many issues remain unresolved and, as such, produce large uncertainties in the confidence with which adequate and appropriate regulations can be formulated. The following problems are considered to be some of the principal unresolved questions that bear directly on the issue of accurate seismic risk assessment.

The Problem of Seismicity in the Central and the Eastern United States

From a seismic hazard point of view, the contiguous United States can be divided along a boundary roughly corresponding to the eastern front of the Rocky Mountains. Most of the earthquakes in the area to the west (pl. 1) are associated with active, well-defined geologic processes. In contrast, the cause of many of the earthquakes in the Central and the Eastern United States is still poorly understood. In the West, the association of earthquakes, particularly large ones ($M \geq 6.5$), with geologic faults is well established. In many cases, these faults are visible at the surface, and, by using geologic techniques, it is possible to demonstrate that displacement has occurred along these faults during the geologically recent past. However, with the exception of

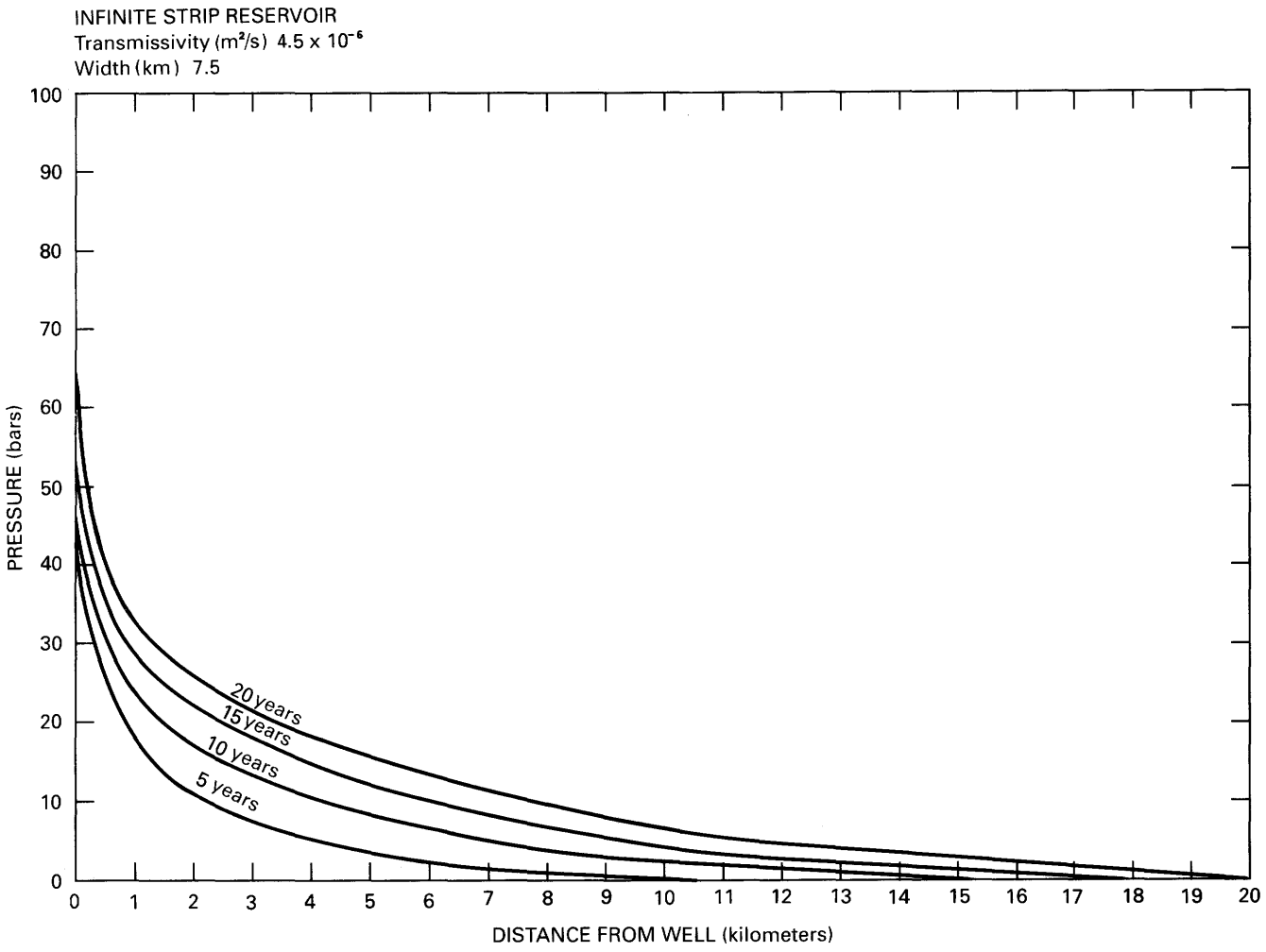

Figure 14. Increased pressure versus distance along the axis of an infinite strip reservoir 7.5 km wide and transmissivity as in figure 13 (from Wesson and Nicholson, 1986). Time intervals are 5, 10, 15, and 20 yr.

evidence for subsurface faulting in the vicinity of the 1811–12 New Madrid, Mo., earthquakes, the relation between faults and earthquakes in the Central and the Eastern United States has been much more elusive. This issue has been clouded even further by the discovery of the Meers Fault in the Wichita Mountains of Oklahoma, along which large, relatively recent movement has occurred (Gilbert, 1985), yet no current or historical seismicity has been associated with it (Lawson, 1985). The Charleston, S.C., earthquake of 1886 provides perhaps the best example of some of the difficulties involved. Despite the continuing occurrence of small earthquakes in the Charleston area, as well as extensive regional and local geologic and geophysical investigations, no commonly agreed upon fault or faults judged to be responsible for the large historic earthquake has yet to be discovered. Consequently, the primary basis for estimating future locations of earthquakes in the Central and the Eastern United States remains the catalog of historic earthquake epicenters.

Magnitudes of Induced Earthquakes

Although it seems extremely unlikely that deep well injection alone could induce a truly large earthquake in the Central or the Eastern United States, no satisfactory method is currently available for estimating the maximum size of earthquake that might be produced. Indeed, no method exists for estimating the increased probability for triggering earthquakes of any magnitude as the result of raising the pore fluid pressure through deep well injection.

Observations indicate that the magnitude of an earthquake increases roughly as the logarithm of the length of fault along which displacement occurs (fig. 16). Slip is also proportional to fault length. Thus, a magnitude 8 earthquake typically involves faulting along hundreds of kilometers of fault and several meters of slip, whereas a magnitude 3 earthquake might involve faulting over a surface that has a dimension of several tens of meters and slip of only a few centimeters. The magnitudes of the largest earthquakes

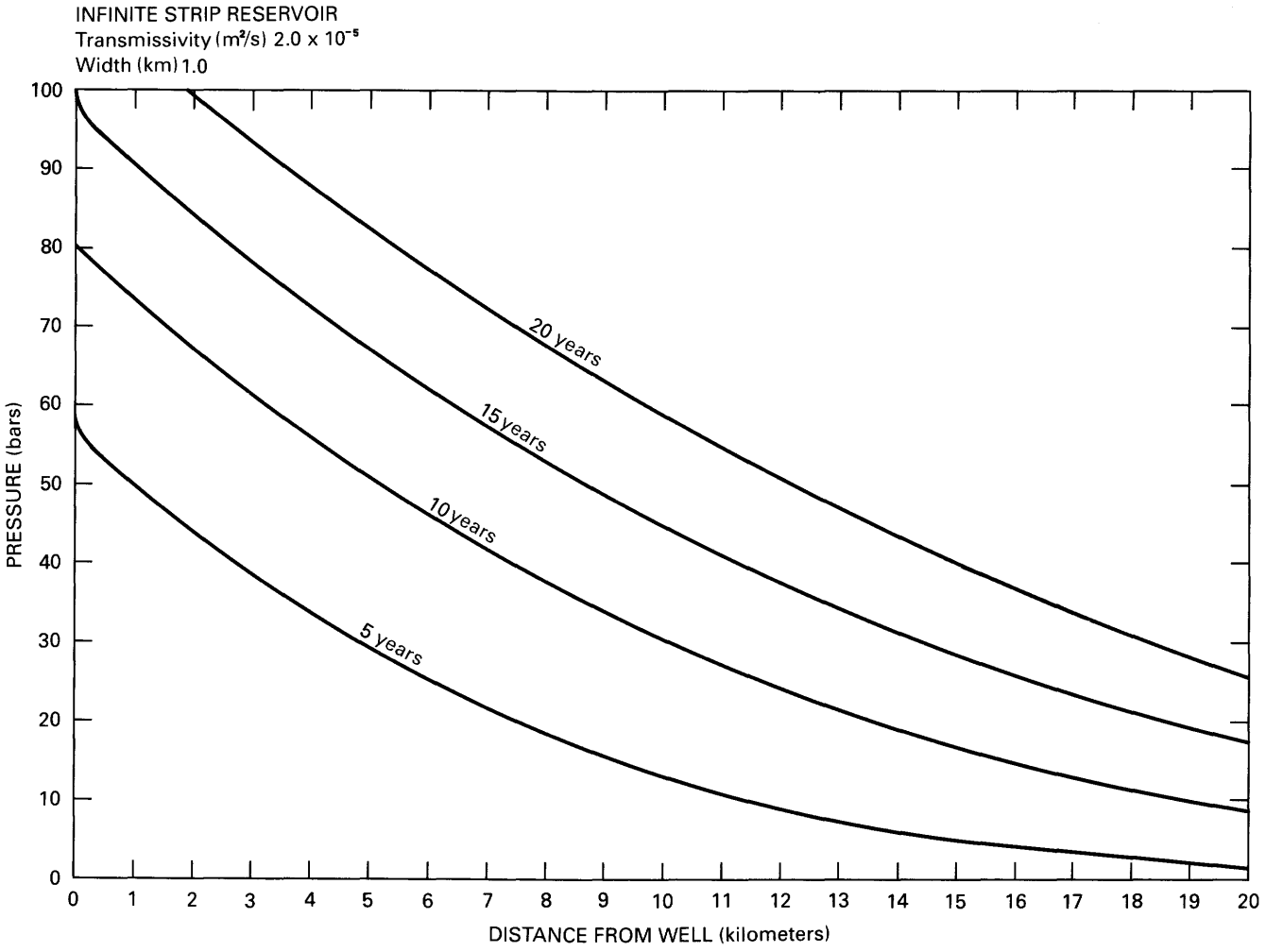

Figure 15. Increased pressure versus distance along the axis of an infinite strip reservoir 1 km wide and transmissivity of 2.0×10^{-5} m^2/s (from Wesson and Nicholson, 1986). Time intervals are 5, 10, 15, and 20 yr.

associated with deep well injection were between 5 and 5.5 (table 1, Rocky Mountain Arsenal in 1967 and Snipe Lake, western Alberta, in 1970). Although none of the induced earthquakes recorded so far would be considered devastating, the potential for damage from such earthquakes could be larger than for those in more tectonically active regions because many of the induced events are shallow and occur in areas of low expected seismic hazard and in regions of low attenuation of seismic waves; for example, the Attica earthquake of 1929 discussed in Appendix A. Earthquakes in the Central and the Eastern United States typically cause damage over much larger areas as compared to earthquakes of the same size in the Western United States. This is primarily the result of the lower attenuation of seismic waves in the East versus the West, but other factors also may be involved.

One of the factors that may affect earthquake damage potential and that seems to distinguish earthquakes in the Central and the Eastern United States from those in the West is a tendency for eastern earthquakes to be associated with relatively small rupture areas for a given magnitude earthquake. If true, then this would imply that eastern earthquakes exhibit more slip per unit fault area than do western earthquakes and would imply that eastern earthquakes reflect higher stress drops. This would be coincident with the thinking that the crust of the Earth beneath the Central and the Eastern United States is older, colder, and, therefore, stronger than that beneath the Western United States. This is also consistent with the idea that large earthquakes east of the Rocky Mountains typically have much longer repeat times than those to the west, allowing faults to heal and regain much of their frictional strength lost during dynamic slip in past earthquakes (fig. 16; Kanamori and Allen, 1986). This apparent difference is important because, if correct, smaller faults in the vicinity of a well located in the Eastern United States could produce larger earthquakes than might be anticipated on the basis of relations derived from more seismically active areas in the West (Thatcher and Hanks, 1973).

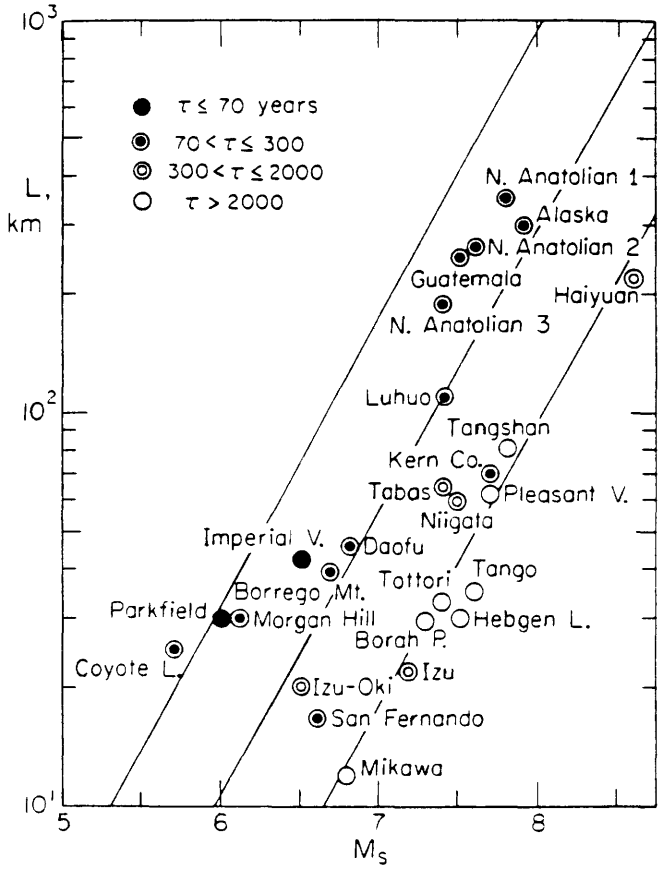

Figure 16. Relation between surface-wave magnitude and fault length. Shown for reference are theoretical lines of constant stress drop (1, 10, and 100 bars, left to right, respectively). Earthquakes that have longer repeat times generally exhibit shorter rupture lengths (L) for the same size earthquake; compare the 1983 M_S 7.3 Borah Peak, Idaho, earthquake with the 1976 M_S 7.5 Guatemala earthquake. M_S, surface-wave magnitude; L, fault length; and τ, repeat times. Reprinted from Kanamori and Allen (1986) and published with permission.

Potential for Reactivation of Old Faults

It is sometimes suggested that earthquakes in the Central and the Eastern United States occur on reactivated, geologically old faults. Currently, the phenomenon of reactivation is poorly understood (Sibson, 1985). Because of the large uncertainties in the inherent shear strength and the time-dependent nature of friction with slip on faults, no criteria exist for predicting whether an old fault might be reactivated, except to determine how close in orientation an existing fault may be relative to preferred planes of slip in the current regional tectonic stress field, as predicted by the Mohr-Coulomb failure criterion.

Importance of Small Induced Earthquakes

It is possible that a deep well injection operation may induce small earthquakes in the immediate vicinity of the bottom of the well, as has been the case in several of the secondary oil recovery and solution mining cases described in Appendix A. If these earthquakes are below the threshold for damage or, perhaps, even below the threshold for noninstrumental detection, then it is not unreasonable to ask whether these earthquakes constitute a risk. Two questions arise—Do these small earthquakes indicate the potential for larger, potentially damaging earthquakes? and do these small earthquakes indicate the possibility of breaching the confining horizon?

In answer to the first question, the occurrence of even small earthquakes indicates that, at least locally, the conditions for seismic slip are satisfied. In the Western United States, the association of small, natural earthquakes with a geologically recognizable fault is taken as sufficient evidence that the entire fault is active and, consequently, that a potentially larger earthquake, controlled by the dimension of the fault, is possible. Unfortunately, our lack of knowledge concerning the size and the distribution of buried faults in the Central and the Eastern United States prevents a similar line of reasoning. Thus, without detail subsurface information, it is not possible to estimate the maximum size of earthquake that could be induced once seismicity is detected near an active injection well.

The second question is more directly pertinent to the containment of hazardous wastes. The occurrence of small earthquakes near the bottom of a deep injection well may indicate faulting or fracturing processes that conceivably could lead to a breach in the overlying confining zone and, therefore, conceivably could permit hazardous materials to migrate upward toward potential drinking water supplies. An important consideration is, therefore, whether the induced seismicity is occurring within the sedimentary section or within the deeper basement rock, and, if so, how close to the confining layer is the zone of seismic activity. Such questions could only be addressed if additional seismic monitoring equipment is installed to locate accurately any subsequent earthquake hypocenters and to resolve the type and extent of faulting involved. However, until such answers are forthcoming, it would seem prudent to regard the occurrence of small earthquakes near the bottom of a deep injection well with concern.

Spatial and Temporal Variability of Tectonic Stress

Although the actual pressure of fluid injection is certainly a critical factor in determining the potential for inducing earthquakes through deep well injection, another key environmental parameter is the state of the preexisting tectonic stress field. If stress conditions on nearby faults have already reached critical levels near failure, then only a small change in pore pressure as a result of fluid injection may prove sufficient to trigger adjacent seismicity. Measurements available to date suggest that the orientations and, possibly, the magnitudes of the principal horizontal stresses are relatively constant, or at least slowly varying,

over wide regions of the country. This suggests that once a particular injection operation has triggered earthquakes, other injection wells in the same tectonic stress province may be equally likely to induce similar seismic activity.

Insufficient measurements exist, however, to indicate how rapidly in time and space the stress field may actually vary. In the Central and the Eastern United States, there is at present little indication that the tectonic stress field changes rapidly with time. In the Western United States, geodetic measurements suggest that small, but significant, stress changes can occur over time scales of months to years (Raleigh and others, 1982). In particular, the occurrence of a major earthquake nearby could dramatically affect the local stress field on a time scale of seconds. Assessing the spatial variation in stress is almost as troublesome; for example, some areas in the Central and the Eastern United States tend to have small earthquakes more frequently than others. Whether this is related to the spatial variation in the tectonic stress field or, alternatively, to the spatial distribution and orientation of potential planes of slip is unknown.

CONSIDERATIONS FOR FORMULATING REGULATIONS AND OPERATIONAL PROCEDURES

In terms of the earthquake hazard associated with deep well injection, the three critical parameters that need to be evaluated are the magnitude of the preexisting tectonic stress, the injection pressure, and the proximity and the characteristics of any faults or fractures that may be affected by pore pressure increases caused by fluid injection operations. The preexisting tectonic stress can be measured at the time of well completion or can be extrapolated from measurements made in adjacent wells within the same geologic province. The injection pressure will be controlled by the desired injection rate and by the hydrologic properties of the receiving reservoir. Although the presence of large faults may be obvious at the surface, the presence of smaller faults within the proposed reservoir formation may be extremely difficult to detect. Thus, the two earthquake-related factors that are most amenable to regulation or control are the site selection (and by inference, the characteristics of the reservoir chosen for injection) and the maximum injection pressure.

The following recommendations are made from the point of view of addressing the potential seismic hazard associated with injection-induced earthquakes. These recommendations are not intended to replace or reduce existing procedures or restrictions established on the basis of environmental concerns or other considerations and, therefore, do not constitute by any means a complete list of all the factors needed to be considered in discussing potential hazards associated with the disposal of hazardous waste by deep well injection.

Site Selection

Reservoir That Has High Transmissivity and Storativity

The potential operator of a waste-injection well desires a reservoir that has high transmissivity and storativity because, for a given volume of fluid to be injected, the higher the transmissivity and the storativity are, the lower the required injection pressure will be. High transmissivity and storativity also are very desirable from the point of view of reducing earthquake hazard because the lower the injection pressure is, the less likely the prospect of inducing or triggering earthquakes becomes.

Stress Estimate

An estimate of the state of stress in the area of the projected reservoir is important at an early stage in the selection of a potential site of deep well injection because, to a large extent, the state of stress controls the formation fracture pressure and the pressure threshold for triggering slip on preexisting faults (the Mohr-Coulomb failure criterion). An estimate of high deviatoric stress in the reservoir region should serve as a warning that the formation fracture pressure (P_b) and the Mohr-Coulomb failure pressure will be low.

The most reliable estimates of the state of stress in the reservoir will be those based upon measurements made in the reservoir rock itself. However, it is likely that a reasonable estimate can be made before drilling from the interpolation of regional stress measurements, particularly from hydrofracturing measurements made in the same reservoir rock at nearby wells. Surface or shallow well measurements also may be of value, although the extrapolation of such measurements to significant depths may be unreliable.

Absence of Faults

The possibility for triggering induced earthquake activity appears to be significantly enhanced if any part of the reservoir affected by the planned injection is cut by a significant fault or fracture. Obviously, the presence of a fault that might present a flow path through the confining zone is also of concern in evaluating the integrity of the reservoir. Moreover, because the effect of the fluid injection pressure typically extends farther from the wellbore than the distance to which any of the injected fluid actually migrates, faults or fractures that are beyond the anticipated migration distance should be considered carefully.

Clearly, it is easier to prove the existence of a fault than to prove the absence of one. Before drilling, the existence of a fault may be inferred from surface geologic mapping, subsurface geologic studies in nearby wells, or geophysical studies, such as gravity, magnetic, or seismic reflection surveys. It should be remembered, however, that should drilling or operation of the well reveal a previously

unknown fault or fracture, then an analysis and reevaluation of the fluid injection operations may be required.

Regional Seismicity

Inasmuch as the occurrence of earthquakes, even relatively small ones, indicates the existence of faults or fractures and the presence of stresses sufficiently high to cause seismic fault slip, a proposal to locate a deep injection well in an area of significant seismicity should be regarded with caution, particularly if there is any indication that some of the earthquakes occur near the depth of the reservoir. Potential well sites located along strike of regional basement structures that exhibit contemporary seismicity or of extrapolated linear trends in earthquake epicenters should also be avoided, if possible.

Well Drilling and Completion

Transmissivity and Storativity

Estimates of the transmissivity and the storativity of the reservoir are critical to the estimate of the maximum injection pressures required over time to accommodate the desired volume and rate of fluid injection. Insofar as possible, estimates of these quantities should be made by *in situ* measurements at the time of well completion and should be supplemented by laboratory measurements as required. Necessary measurements made at the time of well completion include the effective permeability, the average thickness of potential injection zones, and other related measurements, such as the porosity and the elastic constants of the reservoir formation.

Before beginning injection operations, it would be highly desirable for the potential operator to present a calculation of the predicted injection pressure that would be required to accommodate the desired rate of fluid flow and its expected increase over time. This calculation should be based on the inferred values of transmissivity and storativity measured in the borehole and would provide a standard against which any unusual or unanticipated changes in pressure history observed at the well could be evaluated.

Stress Measurement in Reservoir Rock

From the point of view of assessing the potential for inducing earthquakes through deep well injection, the most useful single measurement is a high-quality stress measurement made in the reservoir rock within the injection well itself. Currently, the most reliable and accurate method of making such a measurement is by using the hydraulic fracture technique. In general, the measurements made in association with standard commercial hydraulic fracture operations for well stimulation are not precise enough for this purpose. To make an adequate stress measurement, it is necessary to select an unfractured length of hole by using an impression packer or borehole televiewer; to use a carefully controlled low volume of fluid, which generally requires the use of a specially designed hydrofracture tool (called a double straddle-packer unit); and to monitor the operation by using sensitive fluid pressure equipment. It is also highly desirable to repeat the measurement at several places along the unfractured drill hole to obtain an estimate of the measurement uncertainty.

Given the importance of maintaining the integrity of the confining zone, there may be concern that even the small fractures created by the hydraulic fracture stress measurement technique or the subsequent propagation of those fractures could threaten the integrity of the confining zone. Certainly, if the well is to be stimulated by commercial hydraulic fracturing, then no incremental risk is associated with the fractures generated during the stress measurements. If the well is not to be stimulated, but a stress measurement is still desired, then it should be possible to keep the fractures generated very close to the borehole and nearly limited to the section of the borehole that has been packed off—if the stress measurements are done carefully and at low injection volume. Estimates of the size of the fracture generated by most controlled hydraulic stress measurements, based on borehole televiewer or impression packer results, typically are on the order of 10 m or less (K.F. Evans, Lamont-Doherty Geological Observatory, oral commun., 1987). Such fractures would not represent a significant threat to the integrity of a confining layer that is often chosen (and mandated in the case of hazardous-waste-disposal operations) to have a thickness 10 to 100 times larger. The primary benefit in making these measurements is that the operator and the regulator will have a direct measurement of the formation breakdown and the fracture reopening pressures, as well as a reliable estimate of the zero-cohesion Mohr-Coulomb failure pressure. With these measurements in hand, the operator and the regulator will be in a position to establish relatively safe maximum pressure levels for injection operations, which will minimize the possibility of creating uncontrolled new fractures or of extending or causing seismic failure on preexisting faults.

If it is judged to be undesirable to carry out hydraulic fracturing measurements in the reservoir itself out of concern for the integrity of the confining zone, then it may be possible to obtain meaningful and relevant measurements at depths in the borehole above or below the confining zone. Ideally, such measurements should be carried out at sufficient depth to avoid near-surface effects and possible zones of stress decoupling caused by low-strength sedimentary layers or structures, such as salt beds (fig. 6*B*), between the measurement depth and the reservoir. Strictly from the point of view of the relevance of the stress measurements, the deeper the better.

Pore Pressure Measurement

Because fluid pressures modify the local effective stress fields (and, by supposition, the frictional strength of faults), an important measurement required to understand the state of stress in the reservoir before the beginning of injection is the initial pore pressure (p) in the reservoir formation. This measurement also provides a baseline against which to evaluate, quantify, and monitor the expected increase in formation fluid pressure as a result of the subsequent injection operations.

Faulting Parameters

If there is any indication that the injection pressures will approach the zero-cohesion Mohr-Coulomb failure pressure, then it would be prudent to measure the coefficient of friction (μ) of the reservoir rock and the adjacent basement rock, as well as to estimate, if possible, the cohesion of any adjacent faults or fractures present (or potentially present) in the reservoir or surrounding country rock. These measurements would help provide better, more reliable estimates of the critical stress levels needed for fault slip, as determined by the Mohr-Coulomb failure criterion.

Well Operation and Monitoring

Determination of Maximum Allowable Injection Pressure

From the point of view of earthquake hazard, the key decision facing the operator and the regulator is the establishment of the maximum allowable injection pressure. Without considering the potential for slip on preexisting faults, an absolute upper limit of permissible injection pressure presumably would be the formation fracture (or breakdown) pressure (P_b). It should be emphasized, however, that the standard estimates of a "safe" maximum injection pressure, which are based on some fixed percentage of the so-called normal vertical gradient of formation fracture pressure of about 0.75 to 1.0 pound per square inch per foot may not be conservative at all. This is because the formation fracture pressure critically depends on the local state of stress and, in particular, on the deviatoric stress. The higher this stress is, the lower the formation fracture pressure will be, regardless of the expected values derived from the measured vertical overburden gradient. Strict "rules-of-thumb" that do not take into account the spatial variation in the state of stress will not specify adequately the "safe" upper limit of the formation fracture pressure.

In terms of potential earthquake triggering, however, the lowest possible critical injection pressure is the zero-cohesion Mohr-Coulomb failure pressure. This is the pressure at which frictional sliding would occur on favorably oriented preexisting faults or fractures with no cohesion. If the projected injection pressures are below this threshold, then no earthquake problems should be anticipated. In contrast, if the desired injection pressures are above this threshold, then it is necessary to consider whether any significant faults or fractures exist in close proximity to the point of fluid injection, what their orientation may be, and the magnitude of their possible cohesion. If, as a result of fluid injection, conditions on adjacent faults are allowed to reach the Mohr-Coulomb failure limit, taking into account the appropriate cohesion (τ_0), then earthquake activity should be anticipated.

Comparison of Actual and Predicted Pressure-Time Records

The pattern of fluid injection pressure measured at the wellhead over time and, indeed, the fall of pressure over time during any interruption in injection activities give important information about the average hydrologic characteristics of the reservoir. Comparison of the actual pressure versus time records with those predicted from the measured or the estimated reservoir characteristics (transmissivity, storativity, shape, physical extent) would provide an assessment of whether the initial assumptions, such as radial flow in a confined homogeneous aquifer, were correct or required modification. Obviously, any increase in the apparent transmissivity of the reservoir should be scrutinized as a possible indication that fluid has reached a fracture system. Unexpectedly rapid increases in injection pressure needed to maintain flow rates at constant volume over time may indicate a tighter reservoir formation than anticipated and, thus, a possible need to reduce the desired rate of fluid injection.

Seismic Monitoring

If any question exists about the possibility of inducing earthquakes, particularly if the projected injection pressure is above the zero-cohesion Mohr-Coulomb failure pressure, then it would be prudent to carry out a seismic monitoring program to detect the occurrence of any adjacent earthquake activity. This also would be advisable if the well is situated in an area that has a previously well-defined history of seismic activity or if the well site is in close proximity (less than 20 km) to a known major fault structure. Preferably, this monitoring program should begin as far in advance of the anticipated injection operations as possible to establish a background level of seismicity against which any potentially injection-induced earthquakes might be compared. To be meaningful, instrumentation should be sensitive enough to detect earthquakes in the magnitude 0 to 1 range located near the bottom of the well. Figure 17 is a seismogram of one such microearthquake detected within 3 km of the Calhio, Ohio, injection wells discussed in Appendix A. To obtain this degree of sensitivity in the presence of the high levels of seismic noise often associated with industrial activity in the vicinity of the well itself, it may be necessary to locate the monitoring equipment somewhat off-site or in

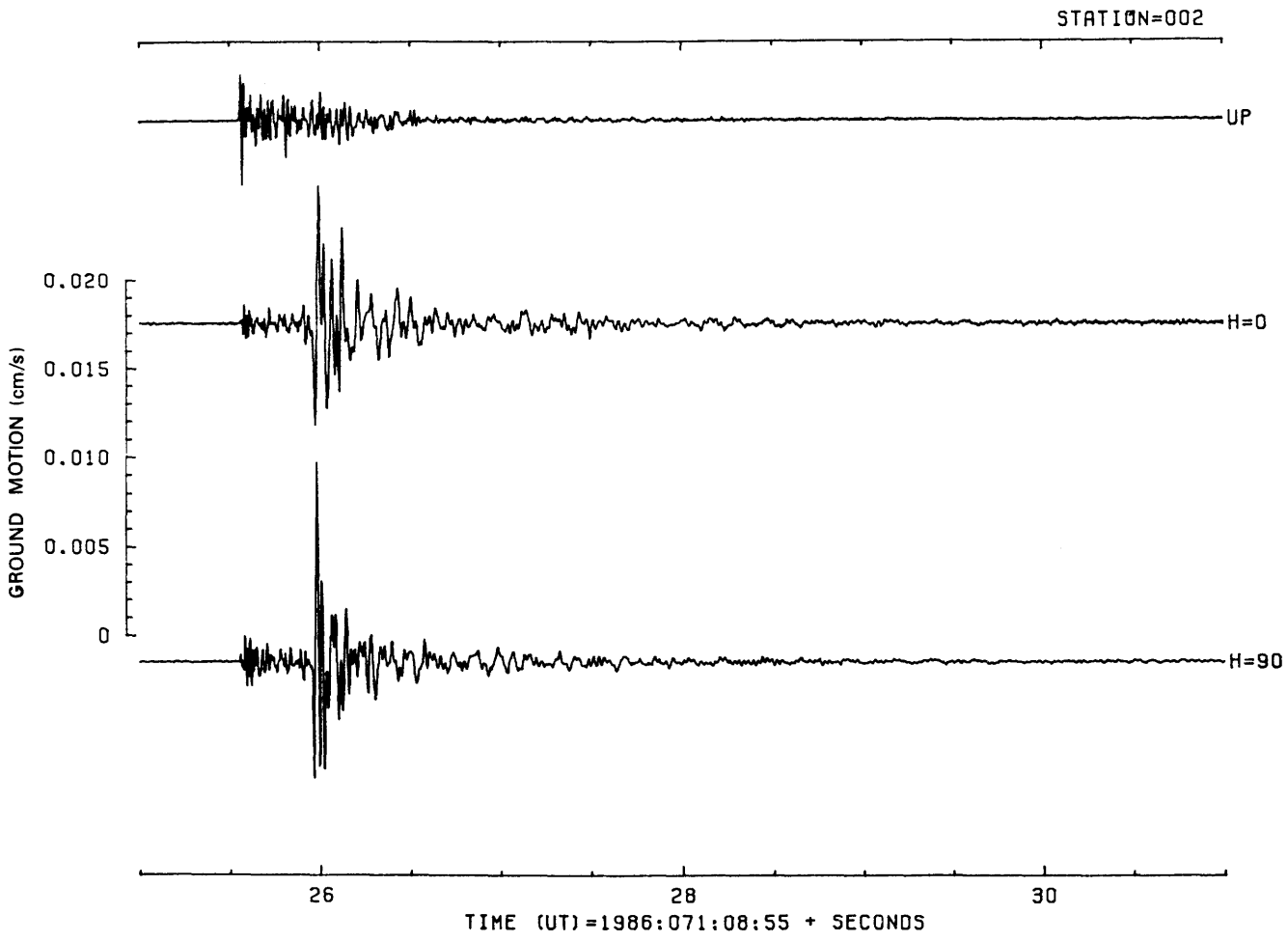

Figure 17. Seismogram of an earthquake that has a magnitude of about 0.5 and that is located at a depth of about 2 km and within less than 3 km of the bottom of an injection well in northeastern Ohio (from Wesson and Nicholson, 1986).

an adjacent borehole. Significant reductions in noise level can be obtained by placing the seismic instrumentation in boreholes at depths as small as a few tens of meters.

Monitoring should continue for as long as it takes to verify that elevated injection pressures are unlikely to trigger significant earthquake activity. This may require several years of observation because of the length of time involved to attain maximum (that is, critical) injection pressure at a constant injection rate and to allow for the diffusion of significant pore fluid effects away from the well. The time interval between initiation of injection and the largest earthquakes at the Rocky Mountain Arsenal site was 5 yr; for the Snipe Lake case (Appendix A), the time lag was 7 yr. Similar time intervals between injection and the largest earthquakes in the triggered sequence have been observed in other cases; however, the time between the initiation of injection and the onset of microearthquake activity is often short; for example, the Rocky Mountain Arsenal, the Attica-Dale, and the Ashtabula cases discussed in Appendix A.

Although one seismic station may be adequate for detecting earthquakes (and, in favorable cases, for estimating the distance of the earthquake to the station), a minimum of three stations would be necessary to determine the locations and focal depths of any earthquakes should they be detected in the vicinity of the well. Thus, once any induced seismicity is detected, it would then be appropriate to supplement an initial monitoring station with additional stations to provide reliable and accurate earthquake locations and focal depths.

Consideration of Small Earthquakes Near the Bottom of a Well

The occurrence of any earthquakes, even as small as magnitude 0, near the bottom of a well should be viewed with concern. Confirmation that earthquakes are indeed triggered by injection operations can often be obtained by comparing the frequency of earthquakes with the cycling of the injection pressure (fig. 2). It should be noted, however, that the pressure changes at the wellbore are damped out

with distance from the well. Therefore, induced or triggered earthquakes at some distance from the borehole should not be expected to correlate as well with the cycling of injection pressure as earthquakes in the immediate vicinity of the bottom of the well. If earthquakes thought to be related to injection operations are detected, then the following questions are appropriate: Is it possible that induced earthquakes might cause damage or injury in the surrounding area? and is it possible that the earthquakes indicate fault displacement that might threaten the integrity of the confining zone? If the answer to either of these questions is "yes," then consideration should be given to reducing the injection pressure. It should be remembered, however, that once the pore pressure in the reservoir or in adjacent rocks is raised above the critical pressure capable of triggering seismic faulting, lowering the pressure at the wellbore may not lead immediately to the cessation of earthquake activity. Seismicity would not be expected to stop until the pressure in the affected region has decayed below the critical value.

BIBLIOGRAPHY

Allen, D.R., 1968, Physical changes of reservoir properties caused by subsidence and repressuring operations: Journal of Petroleum Technology, v. 20, p. 23–29.

Allis, R.G., 1982, Mechanisms of induced seismicity at The Geysers geothermal reservoir, California: Geophysical Research Letters, v. 9, p. 629–632.

Anderson, E.M., 1951, The dynamics of faulting and dyke formation with applications to Britain: London, Oliver and Boyd, 206 p.

Angelier, J., 1979, Determination of the mean principal directions of stresses for a given fault population: Tectonophysics, 56, p. T17–T26.

Armbruster, J.G., Seeber, L., and Evans, K., 1987, The July 1987 Ashtabula earthquake (m_b 3.6) sequence in northeastern Ohio and a deep fluid injection well (abs): Seismological Research Letters, v. 58, no. 4, p. 91.

Bardwell, G.E., 1966, Some statistical features of the relationship between Rocky Mountain Arsenal waste disposal and frequency of earthquakes: Mountain Geologist, v. 3, p 37–42.

Bates, R.L., and Jackson, J.A., eds., [1987], Glossary of geology (3d ed.): American Geological Institute, 788 p.

Bell, J.S., and Gough, D.I., 1979, Northeast-southwest compressive stress in Alberta—Evidence from oil wells: Earth and Planetary Science Letters, v. 45, p. 475–482.

———1983, The use of borehole breakouts in the study of crustal stresses, *in* Hydraulic fracturing stress measurements: Washington, D.C., National Academy Press, p. 201–209.

Brace, W.F., and Kohlstedt, D.L., 1980, Limits on lithospheric stress imposed by laboratory experiments: Journal Geophysical Research, v. 85, p. 6248–6252.

Brace, W.F., and Martin, R.J., III, 1968, A test of the law of effective stress for crystalline rocks of low porosity: International Journal of Rock Mechanics and Mineral Science, v. 5, p. 415–426.

Brazee, R.J., and Cloud, W.K., 1958, United States earthquakes, 1956: U.S. Coast and Geodetic Survey, 78 p.

Bredehoeft, J.D., Wolff, R.G., Keys, W.S., and Shuter, E., 1976, Hydraulic fracturing to determine the regional in-situ stress field, Piceance Basin, Colorado: Geological Society of America Bulletin, v. 87, p. 250–258.

Byerlee, J.D., 1978, Friction of rock: Pure and Applied Geophysics, v. 116, p. 615–626.

Byerlee, J.D., and Brace, W.F., 1972, Fault stability and pore pressure: Bulletin of the Seismological Society of America, v. 62, p. 657–660.

Carder, D.S., 1945, Seismic investigations in the Boulder Dam area, 1940–1944, and the influence of reservoir loading on earthquake activity: Bulletin of the Seismological Society of America, v. 35, p. 175–192.

Carlson, S., 1984, Investigations of recent and historical seismicity in East Texas: Austin, University of Texas, M.S. thesis, 197 p.

Cleveland Electric Illuminating Company, 1982, The Perry Nuclear Power Plant Units I and II—Final safety analysis report: North Perry, Ohio, pagination unavailable.

Clifford, M.J., 1973, Silurian rock salt of Ohio: Ohio Department of Natural Resources, Division of Geological Survey, Report of Investigations 90, 42 p.

———1975, Subsurface liquid-waste injection in Ohio: Ohio Department of Natural Resources, Division of Geological Survey, Information Circular 43, 27 p.

Coffman, J.L., and von Hake, C.A., editors, [1973], Earthquake history of the United States—Through 1970: U.S. Department of Commerce Publication 41–1, 207 p.

Costain, J.K., Bollinger, G.A., and Speer, J.A., 1987, Hydroseismicity—A hypothesis for the role of water in the generation of intraplate seismicity: Earthquake Notes, v. 58, p. 41–64.

Davis, S.D., 1985, Investigations of natural and induced seismicity in the Texas panhandle: Austin, University of Texas, M.S. thesis, 230 p.

Davis, S.D., and Pennington, W.D., 1985, A barrier-asperity model for injection induced deformation in the Cogdell oil field, Kent and Scurry Counties, Texas (abs): Earthquake Notes, v. 55, p. 18.

———1987, Induced seismic deformation in the Cogdell oil field of west Texas: preprint, 20 p.

Davis, S.N., and DeWiest, R.J.M., 1966, Hydrogeology: New York, John Wiley and Sons, 463 p.

Denlinger, R.P., and Bufe, C.G., 1982, Reservoir conditions related to induced seismicity at the Geysers steam reservoir, northern California: Bulletin of the Seismological Society of America, v. 72, p. 1317–1327.

Denlinger, R.P., Isherwood, W.F., and Kovach, R.L., 1981, Geodetic analysis of reservoir depletion at The Geysers steam field in northern California: Journal of Geophysical Research, v. 86, p. 6091–6096.

Dewey, J.W., and Gordon, D.W., 1984, Map showing recomputed hypocenters of earthquakes in the eastern and central United States and adjacent Canada, 1925–1980: U.S. Geological Survey Miscellaneous Field Studies Map MF–1699, scale 1:2,500,00.

Dieterich, J.H., Raleigh, C.B., and Bredehoeft, J.D., 1972, Earthquake triggering by fluid injection at Rangely, Colorado, *in* Percolation through fissured rock: International

Society of Rock Mechanics and International Association of Engineers Symposium Paper T2–B, 12 p.

Docekal, J., 1970, Earthquakes of the stable interior, with emphasis on the mid-continent: Lincoln, University of Nebraska, Ph.D. dissertation, v. 1, 169 p.; v. 2, 232 p.

Dumas, D.B., 1979, Active focus near Snyder, Texas: Bulletin of the Seismological Society of America, v. 64, p. 1295–1299.

Dumas, D.B., Dorman, H.J., and Latham, G.V., 1980, A reevaluation of the August 16, 1931 Texas earthquake: Bulletin of the Seismological Society of America, v. 70, p. 1171–1180.

Dunrud, C.R., and Nevins, B.B., 1981, Solution mining and subsidence in evaporite rocks in the United States: U.S. Geological Survey Miscellaneous Information Map I–1298, scale 1:5,000,000.

Eberhart-Phillips, D., and Oppenheimer, D.H., 1984, Induced seismicity in the Geysers Geothermal Area, California: Journal of Geophysical Research, 89, p. 1191–1207.

Environmental Protection Agency, 1974, Compilation of industrial and municipal injection wells in the United States: U.S. Environmental Protection Agency 520/9–74–020, 700 p.

———1985, Report to Congress on injection of hazardous waste: U.S. Environmental Protection Agency 570/9–85–003, 266 p.

Evans, D.G., and Steeples, D.W., 1987, Microearthquakes near the Sleepy Hollow oil field, southwestern Nebraska: Bulletin of the Seismological Society of America, v. 77, p. 132–140.

Evans, D.M., 1966a, The Denver area earthquakes and the Rocky Mountain Arsenal disposal well: Mountain Geologist, v. 3, p. 23–36.

———1966b, Man-made earthquakes in Denver: Geotimes, v. 10, p. 11–17.

Evans, K.F., 1988, Assessing regional potential for induced seismicity: National Center for Earthquake Engineering Research Technical Report, 30 p.

Evans, M.A., 1979, Fractures in oriented Devonian shale cores from the Appalachian Basin: Morgantown, West Virginia University, M.S. thesis, 278 p.

Fetter, C.W., Jr., 1980, Applied hydrogeology: Columbus, Ohio, Charles E. Merrill Publishing Co., 488 p.

Fletcher, J.B., and Sykes, L.R., 1977, Earthquakes related to hydraulic mining and natural seismic activity in western New York State: Journal of Geophysical Research, v. 82, p. 3767–3780.

Freeze, R.A., and Cherry, J.A., 1979, Groundwater: Englewood Cliffs, N.J., Prentice-Hall, Inc., 604 p.

Frohlich, C., 1982, Seismicity of the central Gulf of Mexico: Geology, v. 10, p. 103–106.

GangaRao, H.V.S., Advani, S.H., Cheng, P., Lee, S.C., and Dean, C.S., 1979, In-situ stress determination based on fracture responses associated with coring operations, *in* U.S. Symposium on Rock Mechanics, 20th, Austin, 1979, Proceedings: p. 683–690.

Gibbs, J.F., Healy, J.H., Raleigh, C.B., and Coakley, J., 1973, Seismicity in the Rangely, Colorado, area—1962–1970: Bulletin of the Seismological Society of America, v. 63, p. 1557–1570, 1973.

Gilbert, M.C., 1985, The Meers fault—Its nomenclature and structural setting (abs): Earthquake Notes, v. 55, p. 1.

Gough, D.I., 1978, Induced seismicity, *in* The assessment and mitigation of earthquake risk: Paris, United Nations Educational, Scientific, and Cultural Organization, p. 91–117.

Gough, D.I., and Bell, J.S., 1981, Stress orientations from oil-well fractures in Alberta and Texas: Canadian Journal of Earth Science, v. 18, p. 638–645.

Grant, U.S., 1954, Subsidence of the Wilmington oil field, California: California Division of Mines Bulletin 170, p. 19–24.

Gupta, H.K., and Rastogi, B.K., 1976, Dams and earthquakes: Amsterdam, Elsevier Scientific Publishing Co., 229 p.

Haimson, B.C., 1972, Earthquake stresses at Rangely, Colorado, *in* Harday, H.R., and Stefanko, R., eds., New horizons in rock mechanics—Earthquakes and other dynamic phenomena: U.S. Symposium on Rock Mechanics, 13th, 1972, Proceedings, p. 680–708.

———1977, Crustal stress in the continental United States as derived from hydrofracturing tests, *in* Heacock, J.C., ed., The Earth's crust: American Geophysical Union Geophysics Monograph Series 20, p. 575–592.

———1978a, Crustal stress in the Michigan Basin: Journal of Geophysical Research, v. 83, p. 5857–5863.

———1978b, The hydrofracturing stress measuring method and recent field results: International Journal of Rock Mechanics, Mineral Science, and Geomechanical Abstracts, v. 15, p. 167–178.

Haimson, B.C., and Doe, T.W., 1983, State of stress, permeability, and fractures in the Precambrian granite of northern Illinois: Journal of Geophysical Research, v. 88, p. 7355–7372.

Haimson, B.C., and Fairhurst, C., 1967, Initiation and extension of hydraulic fractures in rock: Society of Petroleum Engineers Journal, v. 7, p. 310–318.

———1970, In-situ stress determinations at great depth by means of hydraulic fracturing, *in* U.S. Symposium on Rock Mechanics, 11th, New York, 1970, Proceedings: p. 539–584.

Harding, S.T., 1981a, Induced seismicity in the Cogdell Canyon Reef oil field: U.S. Geological Survey Open-File Report 81–167, p. 452–455.

———1981b, Induced seismicity in the Cogdell Canyon Reef oil field: U.S. Geological Survey Open-File Report 81–833, p. 547.

Harding, S.T., Carver, D., Henrissy, R.F., Dart, R.L., and Langer, C.J., 1978, The Scurry County, Texas, earthquake series of 1977–1978—Induced seismicity? (abs): Earthquake Notes, v. 49, p. 14–15.

Hauksson, E., 1987, Seismotectonics of the Newport-Inglewood fault zone in the Los Angeles basin, southern California: Bulletin of the Seismological Society of America, v. 77, p. 539–561.

Healy, J.H., Rubey, W.W., Griggs, D.T., and Raleigh, C.B., 1968, The Denver earthquakes: Science, v. 161, p. 1301–1310.

Herrmann, R.B., 1978, A seismological study of two Attica, New York earthquakes: Bulletin of the Seismological Society of America, v. 68, p. 641–651.

———1986, Earthquake hazard in the central United States: U.S. Geological Survey Open-File Report 86–383, p. 69–70.

Herrmann, R.B., Park, S.-K., and Wang, C.Y., 1981, The Denver earthquakes of 1967–1968: Bulletin of the Seismological Society of America, v. 71, p. 731–745.

Hickman, S.H., Healy, J.H., and Zoback, M.D., 1985, In situ stress, natural fracture distribution, and borehole elongation in the Auburn Geothermal Well, Auburn, New York: Journal of Geophysical Research, v. 90, p. 5497–5512.

Hickman, S.H., and Zoback, M.D., 1983, The interpretation of hydraulic fracture pressure-time data for in-situ stress determination, *in* Hydraulic fracturing stress measurements: Washington, D.C., National Academy Press, p. 44–54.

House, L.S., and McFarland, N., 1985, Locations of microearthquakes induced by hydraulic fracturing at Fenton Hill, New Mexico, in May 1984 (abs): Earthquake Notes, v. 56, p. 12.

Hsieh, P.A., and Bredehoeft, J.S., 1981, A reservoir analysis of the Denver earthquakes—A case of induced seismicity: Journal of Geophysical Research, v. 86, p. 903–920.

Hubbert, M.K., and Rubey, W.W., 1959, Role of fluid pressure in overthrust faulting: Geological Society of America Bulletin, v. 70, p. 115–206.

Hubbert, M.K., and Willis, D.G., 1957, Mechanics of hydraulic fracturing: Transactions of the American Institute of Mining, Metallurgical, and Petroleum Engineers, Society of Petroleum Engineers, v. 210, p. 153–166.

Jaeger, C.J., and Cook, N.G.W., 1979, Fundamentals of rock mechanics: London, Methuen, 593 p.

Johnson, K.S., Luza, K.V., and Roberts, J.F., 1980, Disposal of industrial wastes in Oklahoma: Oklahoma Geological Survey Circular 80, 82 p.

Kanamori, H., and Allen, C.R., 1986, Earthquake repeat times and average stress drop, *in* Das, S., Boatwright J., and Scholz, C.H., eds., Earthquake source mechanics: American Geophysical Union Geophysical Monograph, v. 37, Maurice Ewing v. 6, p. 227–235.

Kapotas, S., and Kanasewich, E.R., 1989, Microseismic activity and stress orientations in Cold Lake oil fields, Alberta (abs): Seismological Research Letters, v. 60, p. 31.

Keller, G.R., Rogers, A.M., Lund, R.J., and Orr, C.D., 1981, A seismicity and seismotectonic study of the Kermit seismic zone, Texas: U.S. Geological Survey Open-File Report 81–37, 383 p.

Keller, G.R., Rogers, A.M., and Orr, C.D., 1987, Seismic activity in the Permian Basin area of West Texas and Southeastern New Mexico, 1975–79: Seismological Research Letters, v. 58, p. 63–70.

Knape, B.K., compiler, 1984, Underground injection operations in Texas—A classification and assessment of underground injection activities: Texas Department of Water Resources Report 291, 120 p.

Kovach, R.L., 1974, Source mechanisms for Wilmington oil field, California, subsidence earthquakes: Bulletin of the Seismological Society of America, v. 64, p. 699–711.

Kulander, B.R., Dean, S.L., and Barton, C.C., 1977, Fractographic logging for determination of pre-core and core-induced fractures—Nicholas Combs well No. 7239, Hazard, Kentucky: U.S. Energy Research and Development Agency, Morgantown Energy Research Center, MERC /CR/3, 44 p.

Lacy, L.L., 1985, Mapping natural and hydraulic fracture orientations with a borehole seismic tool (abs): Earthquake Notes, v. 55, p. 13.

Lawson, J.E., Jr., 1985, Seismicity of the Meers fault (abs): Earthquake Notes, v. 55, p. 2.

Leith, W., and Simpson, D.W., 1986, Seismic domains within the Gissar-Kokshal seismic zone, Soviet Central Asia: Journal of Geophysical Research, v. 91, p. 689–700.

Lidener, E.N., and Halpern, J.A., 1978, In-situ stress in North America—A compilation: International Journal of Rock Mechanics, Mineral Science, and Geomechanical Abstracts, v. 15, p. 183–203.

Lockner, D.A., Okubo, P.G., and Dieterich, J.H., 1982, Containment of stick-slip failures on a simulated fault by pore fluid injection: Journal of Geophysical Research Letters, v. 9, p. 801–804.

Luza, K.V., DuBois, R.L., Lawson, J, E., Jr., Foster, P., and Koff, L., 1978, Seismicity and tectonic relationships of the Nemaha Uplift in Oklahoma: U.S. Nuclear Regulatory Commission NUREG/CR–0050, 67 p.

Luza, K.V., and Lawson, J.E., Jr., 1980, Seismicity and tectonic relationships of the Nemaha Uplift in Oklahoma: U.S. Nuclear Regulatory Commission NUREG/CR–1500, pt. 3, 70 p.

———1983, Seismicity and tectonic relationships of the Nemaha Uplift in Oklahoma: U.S. Nuclear Regulatory Commission NUREG/CR–3109, pt. 5, 115 p.

Majer, E.L., and McEvilly, T.V., 1979, Seismological investigations at The Geysers geothermal field: Geophysics, v. 44, p. 246–269.

Mankin, C.J., and Moffet, T.B., 1987, Should we continue deep-well disposal?: Geotimes, v. 32, no. 9, p. 13–15.

Martin, J.C., 1975, The effect of fluid pressure on effective stresses and induced faulting: Journal of Geophysical Research, v. 80, p. 3783–3785.

Mayuga, M.N., 1970, Geology and development of California's giant Wilmington field, *in* Geology of giant petroleum fields: American Association of Petroleum Geologists Memoir, v. 14, p. 158–184.

McClain, W.C., 1970, On earthquakes induced by underground fluid injection: Oak Ridge National Laboratory Report ORNL–TM–3154, 16 p.

McGarr, A., 1980, Some constraints on levels of shear stress in the crust from observations and theory: Journal of Geophysical Research, v. 85, p. 6231–6238.

McKenzie, D.P., 1969, The relationship between fault plane solutions for earthquakes and the directions of the principal stresses: Bulletin of the Seismological Society of America, v. 59, p. 591–601.

Mereu, R.F., Brunet, J., Morrissey, K., Price, B., and Yapp, A., 1986, A study of the microearthquakes of the Gobles oil field area of southwestern Ontario: Bulletin of the Seismological Society of America, v. 76, p. 1215–1223.

Michael, A.J., 1984, Determination of stress from slip data—Faults and folds: Journal of Geophysical Research, v. 89, p. 11,517–11,576.

———1987, Use of focal mechanisms to determine stress—A control study: Journal of Geophysical Research, v. 92, p. 357–368.

Milne, W.G., 1970, The Snipe Lake, Alberta earthquake of March 6, 1970: Canadian Journal of Earth Science, v. 7, p. 1564–1567.

Milne, W.G., and Berry, M.J., 1976, Induced seismicity in Canada: Engineering Geology, v. 10, p. 219–226.

Munson, R.C., 1970, Relationship of effect of water flooding of the Rangely oil field on seismicity, *in* Adams, W.M., ed., Engineering seismology—The works of man: Geological Society of America Engineering Case Histories, v. 8, p. 39–49.

Musman, S.A., and Schmidt, T., 1986, The relationship of intraplate seismicity to continental scale strains (abs): Eos Transactions American Geophysical Union, v. 67, p. 307.

Nance, J.J., 1989, On shaky ground—America's earthquake alert: New York, Avon Books, 440 p.

Nealon, D.J., 1982, A hydrological simulation of hazardous waste injection in the Mt. Simon, Ohio: Columbus, Ohio State University, M.S. thesis, 279 p.

Neuzil, C.E., 1986, Groundwater flow in low-permeability environments: Water Resource Research, v. 22, p. 1163–1195.

Nicholson, Craig, Roeloffs, E., and Wesson, R.L., 1988, The northeastern Ohio earthquake of January 31, 1986—Was it induced?: Bulletin of the Seismological Society of America, v. 78, p. 188–217.

Noorishad, J., and Witherspoon, P.A., 1984/85, Can injection tests reveal the potential for fault movement?: Pure and Applied Geophysics, v. 2–4, p. 608–618.

Nottis, G.N., 1986, A chronology of events and review of the association of seismicity with well #11 and #12 at the Dale brine field, Dale, New York: Geoscience Services, 19 p.

Nuttli, O.W., and Herrmann, R.B., 1978, State-of-the-art for assessing earthquake hazard in the United States, Report 12—Credible Earthquakes for the Central United States: U.S. Army Engineer Waterways Experimental Station Miscellaneous Paper S–73–1, 99 p.

Nuttli, O.W., and Zollweg, J.E., 1974, The relation between felt area and magnitude for Central United States earthquakes: Bulletin of the Seismological Society of America, v. 64, p. 73–86.

Ohio Environmental Protection Agency, 1985, Ohio UIC permit application for Class I injection well—Perry, Ohio injection well #1: Calhio Chemicals, Inc., 12 p.

Ohio River Valley Water Sanitation Commission, 1976, Evaluation of the Ohio Valley region basal sandstone as a wastewater injection interval: Cincinnati, Ohio, 98 p.

———1976, Registry of wells for use in underground injection of wastewater—1972–1975: Cincinnati, Ohio, 57 p.

Ohtake, M., 1974, Seismic activity induced by water injection at Matsushiro, Japan: Journal of Physics of the Earth, v. 91, 11,463–11,476.

Oppenheimer, D.H., 1986, Extensional tectonics at The Geysers geothermal area, California: Journal of Geophysical Research, v. 91, p. 11,463–11,476.

Orr, C.D., 1984, A seismotectonic study and stress analysis of the Kermit seismic zone: University of Texas at El Paso, PhD. dissertation, 289 p.

Orr, C.D., and Keller, G.R., 1981, Keystone field, Winkler County, Texas—An examination of seismic activity, in-situ stresses, effective stresses, and secondary recovery (abs): Earthquake Notes, v. 52, p. 29–30.

———1985, A study of seismicity and regional stresses in the Delaware Basin-Central Basin Platform region of west Texas and southern New Mexico (abs): Earthquake Notes, v. 55, p. 18.

Pearson, C., 1981, The relationship between microseismicity and high pore pressures during hydraulic stimulation experiments in low permeability granitic rocks: Journal of Geophysical Research, v. 86, p. 7855–7864.

Pennington, W.D., Davis, S.D., Carlson, S.M., DuPree, J., and Ewing, T.E., 1986, The evolution of seismic barriers and asperities caused by the depressuring of fault planes in oil and gas fields of south Texas: Bulletin of the Seismological Society of America, v. 76, p. 939–948.

Plumb, R.A., and Cox, J.W., 1987, Stress directions in eastern North America determined to 4.5 km from borehole elongation measurements: Journal of Geophysical Research, v. 92, p. 4805–4816.

Plumb, R.A., and Hickman, S.H., 1985, Stress-induced borehole elongation—A comparison between the four-arm dipmeter and borehole televiewer in the Auburn geothermal well: Journal of Geophysical Research, v. 90, p. 5513–5521.

Raleigh, C.B., Healy, J.H., and Bredehoeft, J.D., 1972, Faulting and crustal stresses at Rangely, Colorado, *in* Flow and fracture of rocks: American Geophysical Union Geophysics Monograph Series, v. 16, p. 275–284.

———1976, An experiment in earthquake control at Rangely, Colorado: Science, v. 191, p. 1230–1237.

Raleigh, C.B., Sieh, K., Sykes, L.R., and Anderson, D.L., 1982, Forecasting southern California earthquakes: Science, v. 217, p. 1097–1104.

Richter, C.F., 1958, Elementary seismology: San Francisco, W.H. Freeman and Co., 768 p.

Roeloffs, E.A., 1988, Fault stability changes induced beneath a reservoir with cyclic variations in water level: Journal of Geophysical Research, v. 93, p. 2107–2124.

Rogers, A.M., and Malkiel, A., 1979, A study of earthquakes in the Permian Basin of Texas-New Mexico: Bulletin of the Seismological Society of America, v. 69, p. 843–865.

Rondout Associates Inc., 1985, Tectonic framework and seismic source zones of the Eastern United States: Electric Power Research Institute. pagination unavailable.

Rothe, G.H., and Lui, C.-Y., 1983, Possibility of induced seismicity in the vicinity of the Sleepy Hollow oil field, southwestern Nebraska: Bulletin of the Seismological Society of America, v. 73, p. 1357–1367.

Sanford, A.D., Sanford, S., Caravella, F., Merritt, L., Sheldon, J., and Ward, R., 1978, Seismic studies of the Los Medanos area in southeastern New Mexico: New Mexico Institute of Mining Technology, Geophysics Open-File Report 20, 39 p.

Sanford, A.D., and others, 1980, Seismicity in the area of the Waste Isolation Pilot Plant (WIPP): Sandia Laboratories Report SAND 80–7096, 36 p.

Sanford, A.D., and Toppozada, T.R., 1974, Seismicity of proposed radioactive waste disposal site in southeastern New Mexico: New Mexico Bureau Mines and Mineral Resources Circular 143, 15 p.

Sbar, M.L., and Sykes, L.R., 1973, Contemporary compressive stress and seismicity in eastern North America—An example of intraplate tectonics: Geological Society of America Bulletin, v. 84, p. 1861–1882.

Seeber, L., Armbruster, J.G., and Evans, K., 1988, Recent historical seismicity in northeastern Ohio reactivating Pre-

cambrian faults and the role of deep fluid injection (abs): Geological Society of America Abstracts with Programs, v. 20, p. 387.

Segall, P., 1985, Stress and subsidence resulting from subsurface fluid withdrawal in the epicentral region of the 1983 Coalinga earthquake: Journal of Geophysical Research, v. 90, p. 6801–6816.

Shurbet, D.H., 1969, Increased seismicity in Texas: Texas Journal of Science, v. 21, p. 37–41.

Sibson, R.H., 1985, A note on fault reactivation: Journal of Structural Geology, v. 7, p. 751–754.

Simpson, D.W., 1976, Seismicity changes associated with reservoir impounding: Engineering Geology, v. 10, p. 371–385.

———1986a, Triggered earthquakes: Annual Reviews of Earth and Planetary Science, v. 14, p. 21–42.

———1986b, Reservoir-induced earthquakes and the hydraulic properties of the shallow crust (abs): Eos Transactions of the American Geophysical Union, v. 67, p. 242.

Simpson, D.W., and Leith, W., 1985, The 1976 and 1984 Gazli, U.S.S.R, earthquakes—Were they induced?: Bulletin of the Seismological Society of America, v. 75, p. 1465–1468.

Simpson, D.W., and Negmatullaev, S.Kh., 1981, Induced seismicity at the Nurek reservoir, Tadjikistan, U.S.S.R.: Bulletin of the Seismological Society of America, v. 71, p. 1561–1586.

Snow, D.T., 1982, Hydrogeology of induced seismicity and tectonism—Case histories of Kariba and Koyna: Geological Society of America Special Paper, v. 189, p. 3117–3360.

Steeples, D.W., 1985, Induced seismicity in the Sleepy Hollow oil field, Red Willow County, Nebraska: U.S. Geological Survey Open-File Report 85–464, p. 429–432.

Stevenson, D.A., 1985, Geopressured-geothermal well development and seismic activity in Gulf Coast Louisiana (abs): Earthquake Notes, v. 55, p. 18.

Stover, C.W., 1986, Seismicity map of the conterminous United States and adjacent areas—1974–1984: U.S. Geological Survey Geophysics Investigation Map GP–984, scale 1:5,000,000.

Stover, C.W., Reagor, B.G., and Algermissen, S.T., 1979, Seismicity map of the state of Ohio: U.S. Geological Survey Miscellaneous Field Studies Map MF–1142, scale 1:5,000,000.

Talebi, S., and Cornet, F.-H., 1987, Analysis of the microseismicity induced by a fluid injection in a granitic rock mass: Geophysical Research Letters, v. 14, p. 227–230.

Talwani, P., and Acree, S., 1985, Pore pressure diffusion and the mechanism of reservoir-induced seismicity: Pure and Applied Geophysics, v. 122, p. 947–965.

———1986, Deep well injection at the Calhio Wells and the Leroy, Ohio earthquake of January 31, 1986—A report to the Cleveland Electric Illuminating Co.: 92 p.

———1988, Did deep well injection induce the Leroy, Ohio, earthquake of January 31, 1986? (abs): Geological Society of America Abstracts with Programs, v. 20, p. 391.

Teng, T.L., Real, C.R., and Henyey, T.L., 1973, Microearthquakes and water flooding in Los Angeles: Bulletin of the Seismological Society of America, v. 63, p. 859–875.

Terashima, T., 1981, Survey on induced seismicity at Mishraq area in Iraq: Journal Physics of the Earth, v. 29, p. 371–375.

Texas Railroad Commission, 1971, A survey of secondary recovery and pressure maintenance operations in Texas to 1970: Bulletin 70, 650 p.

———1985, A survey of secondary recovery and pressure maintenance operations in Texas to 1984: Bulletin 84, 710 p.

Thatcher, W., and Hanks, T.C., 1973, Source parameters of southern California earthquakes: Journal of Geophysical Research, v. 78, p. 8547–8576.

van Poollen, H.K., and Hoover, D.B., 1970, Waste disposal and earthquakes at the Rocky Mountain Arsenal, Derby, Colorado: Journal Petroleum Technology, v. 22, p. 983–993.

Voss, J.A., and Herrmann, R.B., 1980, A surface wave study of the June 16, 1978 Texas earthquake: Earthquake Notes, v. 51, p. 3–14.

Walker, W.R., and Cox, W.E., 1976, Deep well injection of industrial wastes—Government controls and legal constraints: Virginia Water Resources Research Center, 163 p.

Waller, R.M., Turk, J.T., and Dingman, R.J., 1978, Potential effects of deep-well waste disposal in Western New York: U.S. Geological Survey Professional Paper 1053, 39 p.

Warner, D.L., 1972, Survey of industrial waste injection wells: U.S. Geological Survey, 3 v., pagination unavailable.

Warner, D.L., and Lehr, J.H., 1981, Subsurface wastewater injection: Berkeley, Premier Press, 344 p.

Wesson, R.L., and Nicholson, Craig, editors, 1986, Studies of the January 31, 1986 northeastern Ohio earthquake—A Report to the U.S. Nuclear Regulatory Commission: U.S. Geological Survey Open-File Report 86–331, 109 p.

Weston Geophysical Corporation, 1986, Investigations of confirmatory seismological and geological issues—Northeastern Ohio earthquake of January 31, 1986—A Report to the Cleveland Electric Illuminating Co.: 233 p.

Wetmiller, R.J., 1985, Earthquakes near Rocky Mountain House, Alberta and their relationship to gas production facilities (abs): Earthquake Notes, v. 55, p 18.

———1986, Earthquakes near Rocky Mountain House, Alberta, and their relationship to gas production facilities: Canadian Journal of Earth Science, v. 23, p. 172–181.

Witherspoon, P.A., and Gale, J.A., 1977, Mechanical and hydraulic properties of rocks related to induced seismicity: Engineering Geology, v. 11, p. 23–25.

Wong, I.G., Humphrey, J.R., Silva, W., Gahr, D.A., and Huizingh, J., 1985, A case of microseismicity induced by solution mining, southeastern Utah (abs): Earthquake Notes, v. 55, p. 18.

Yerkes, R.F., and Castle, R.D., 1976, Seismicity and faulting attributed to fluid extraction: Engineering Geology, v. 10, p. 151–167.

Ziony, J.J., 1985, Evaluating earthquake hazards in the Los Angeles region—An earth-science perspective: U.S. Geological Survey Professional Paper 1360, 505 p.

Zoback, M.D., and Healy, J.H., 1984, Friction, faulting and "in situ" stress: Annales Geophysicae, v. 2, p. 689–698.

Zoback, M.D., and Hickman, S., 1982, In situ study of the physical mechanisms controlling induced seismicity at Monticello Reservoir, South Carolina: Journal of Geophysical Research, v. 87, p. 6959–6974.

Zoback, M.D, Moos, D., and Mastin, L., 1985, Well bore breakouts and in situ stress: Journal of Geophysical Research, v. 90, p. 5523–5530.

Zoback, M.D., and Zoback, M.L., 1981, State of stress and intraplate earthquakes in the United States: Science, v. 213, p. 96–104.

Zoback, M.L., and Zoback, M.D., 1980, State of stress in the conterminous United States: Journal of Geophysical Research, v. 85, p. 6113–6156.

———1989, Tectonic stress field of the continental United States, *in* Pakiser, L., and Mooney, W., eds., Geophysical framework of the continental United States: Geological Society of America Memoir 172, p. 523–539.

APPENDIXES A–D

APPENDIX A—CASE HISTORIES OF EARTHQUAKES ASSOCIATED WITH WELL OPERATIONS

Rocky Mountain Arsenal, Colorado

The first well-documented case of injection-induced seismicity occurred at the Rocky Mountain Arsenal near Denver in 1966–67. The injection of 17 to 21 million L/mo of hazardous waste into a 3,671-m-deep disposal well was quickly followed by many felt earthquakes (fig. A1*A*) in a region where the last felt earthquake occurred in 1882 (Healy and others, 1968). Comparisons between the onset of seismicity and well operations and between earthquake frequency and average injection rate showed a convincing correlation (fig. 2; Evans, 1966a). Although injection ceased in February 1966, earthquakes triggered by the increased fluid pressure established around the wells continued for several years (fig. A1*C*). In 1967, three large earthquakes—each with a magnitude of greater than 5—occurred, causing minor structural damage in and around the greater Denver area.

In terms of their relative spatial distribution, a study of event locations indicated that the induced earthquakes began initially near the bottom of the injection well, then migrated out along a northwesterly trend for a distance of about 6 to 7 km (fig. A1*A*). After the earthquake sequence had been in progress for 5 yr (1½ yr after injection had stopped), earthquakes primarily occurred, not near the base of the well, but within the previously defined linear zone at a distance of 4 to 6 km from the well and at depths of 4 to 7 km. The largest earthquakes in the sequence (M 5–5.5) occurred in April, August, and November 1967 (fig. A1*B*), after which activity began to decline.

A total of 620 million liters (L) of fluid were injected at average rates of 478 L/min before well operations ceased. Maximum top-hole pressure (THP) reached 72 bars, which corresponded to an estimated bottom-hole pressure (BHP) of 415 bars (Evans, 1966a). Hsieh and Bredehoeft (1981) demonstrated that the records of pressure falloff at the disposal well were consistent with injection into a long narrow reservoir, a conclusion supported by the elongate shape of the seismogenic zone. No hydraulic stress measurements were ever made near the Rocky Mountain Arsenal. From the pressure at which the volume rate of fluid injection increased rapidly, Healy and others (1968) inferred a least compressive stress of 362 bars at the bottom of the disposal well and estimated a maximum compressive stress to be at least the overburden pressure of 830 bars. This assumption proved valid when it was demonstrated that the three largest earthquakes exhibited predominantly normal faulting along nodal planes that were parallel to the trend of earthquake epicenters (fig. A1*B*; Herrmann and others, 1981). Formation pore pressure before injection was estimated to be 269 bars. From these calculations and by using the Mohr-Coulomb failure criterion, a fluid pressure increase of 32 bars was determined to be sufficient to trigger seismic activity along favorably oriented preexisting fractures (Hsieh and Bredehoeft, 1981; Zoback and Healy, 1984). The observation that the earthquake locations were confined to those parts of the reservoir where the pressure buildup from fluid injection exceeded the critical threshold, as predicted by the Mohr-Coulomb failure criterion, strongly supports the conclusion that the earthquake activity was related to injection well operations and was consistent with fluid pressures within the reservoir initiating failure along favorably oriented fractures that had cohesive strengths of as much as 82 to 100 bars. The continuation of seismicity over time and the outward migration of earthquakes from the well were explained by the outward propagation of the critical levels of fluid pressure, even after the injection had stopped.

Rangely, Colorado

Water flooding for the secondary recovery of oil near Rangely began in 1958. Wells drilled to the producing horizon extended to depths of about 2 km. As of June 1970, 9,700 million L of water had been injected at a THP of about 83 bars; this represented a net increase of 2,300 million L after accounting for petroleum withdrawal (Gibbs and others, 1973). Following the installation of seismic monitoring equipment in 1962, earthquakes were found to be occurring within the oil field. In 1969, a dense network of stations was installed to determine accurate earthquake hypocenters and fault plane orientations. Seismic activity was found to be concentrated in a narrow zone, about 4 km long and 1.5 km wide, which crossed the boundary of the field to the southeast (fig. A2*A*; Raleigh and others, 1972). Hypocenters tended to cluster in two groups—one located at depths of 2 to 2.5 km near the wells and within the injection zone, and the other at depths of 3 to 5 km about 1 to 2 km from the wells. The maximum magnitude of the earthquakes generated was 3.1.

Hydraulic fracture data obtained at the bottom of one of the wells (fig. A2, top) indicated values for the maximum compressive stress (σ_1) of 552 bars, the intermediate principal stress (σ_2) oriented vertically and equal to 427 bars, and the least compressive stress (σ_3) of 314 bars. By using the Mohr-Coulomb failure criterion, Raleigh and others (1972) combined these hydraulic stress measurements with the locations and the fault orientations of the earthquakes, as well as laboratory-determined properties of the rock at depth to calculate that a pore pressure of about 260 bars (or 90 bars above the original formation fluid pressure of 170 bars) would have been sufficient to induce slip. This value was consistent with the formation fluid pressure of 275 bars measured in the oil field at the time that

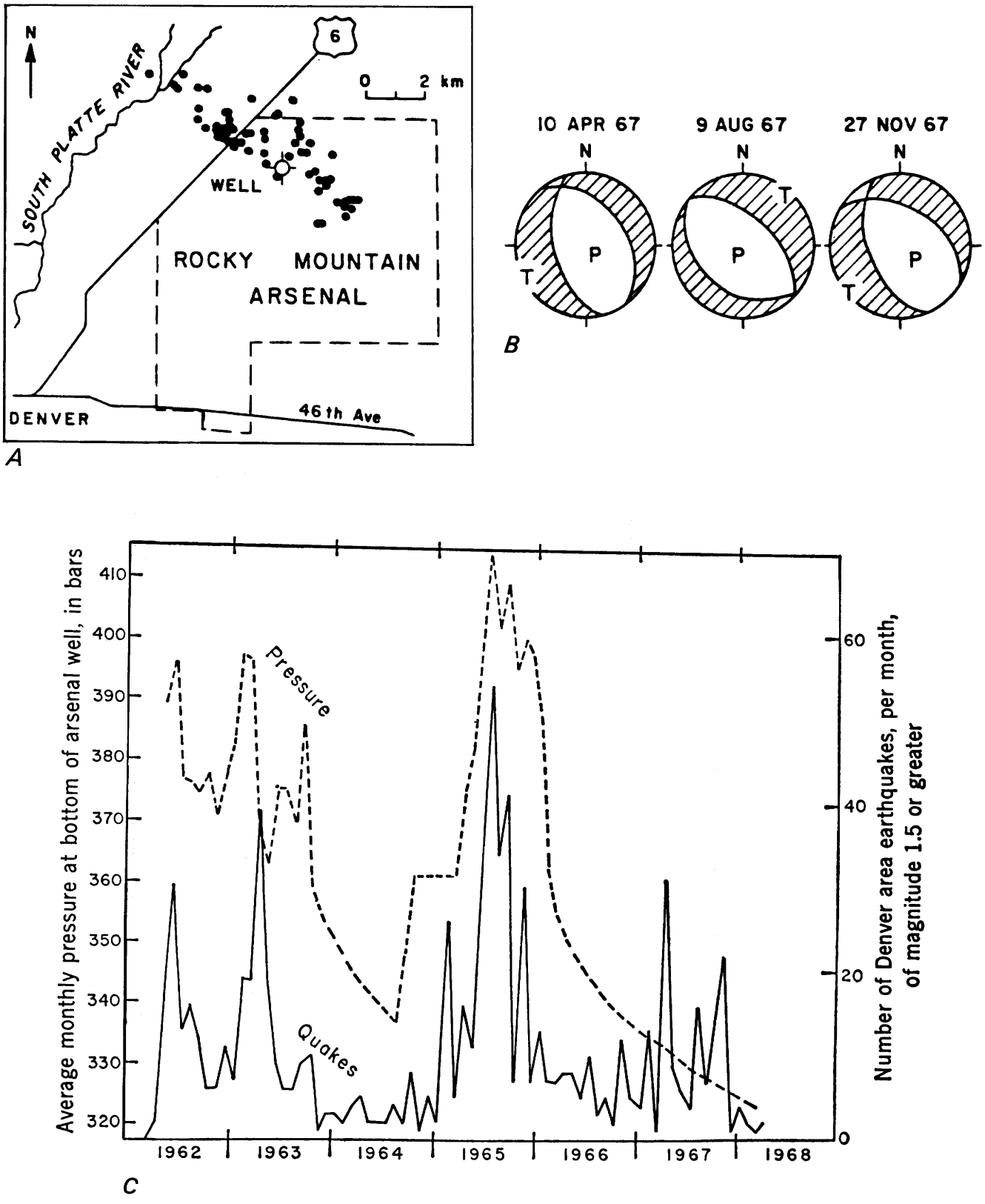

Figure A1. Earthquakes associated with the Rocky Mountain Arsenal well near Denver, Colo. *A*, Locations of earthquakes. Solid circle, location. *B*, Surface-wave focal mechanism solutions of the three largest Denver earthquakes. *C*, Numbers of earthquakes per month and average monthly injection pressure at the bottom of the well. *A*, reprinted from Healy and others (1968) and published with permission. *B* and *C*, reprinted from Zoback and Healy (1984) and published with permission.

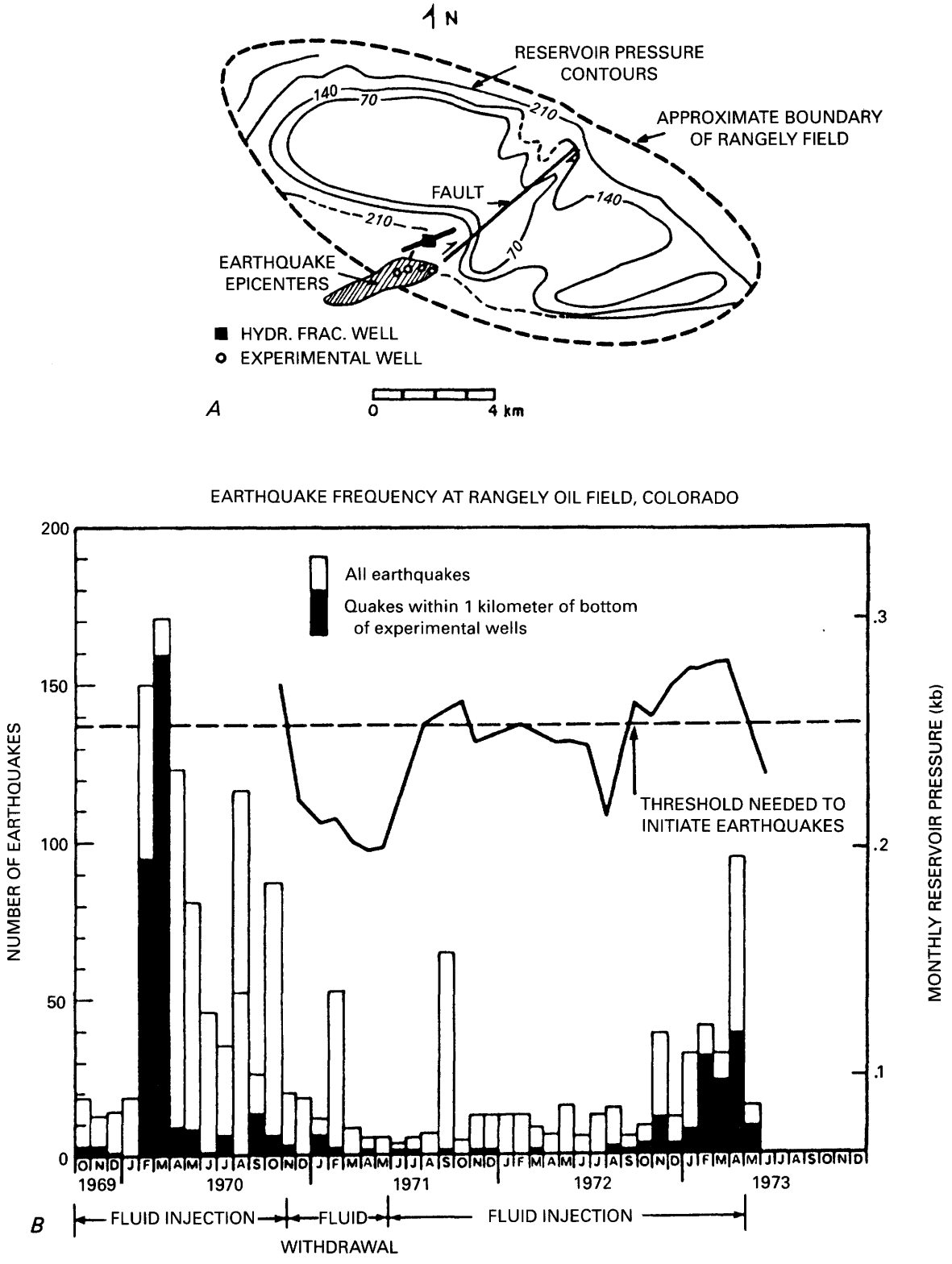

Figure A2. Seismicity and fluid injection, Rangely oil field, Colorado. *A*, Field geometry. Heavy dashed lines, approximate field boundary; light solid lines (dashed where inferred), reservoir pressure contours; hachured region, seismicity; solid square, location of the well used for hydrofracture stress measurements; and short line crossing the solid square, direction of the maximum horizontal compressive stress (S_H). *B*, Seismicity correlated with monthly reservoir pressure (heavy solid line). Reprinted from Raleigh and others (1976) and published with permission.

the induced seismicity began and corresponded to the critical pore pressure below and above which earthquake activity could be turned off and on when the injection pressure was varied intentionally in a later controlled experiment (fig. A2*B*; Raleigh and others, 1976). This experiment in earthquake control established the validity of the Mohr-Coulomb failure model in predicting the critical threshold of stress and pore pressure necessary for earthquake occurrence. Each time the fluid pressure in the part of the field where earthquakes had appeared previously exceeded the predicted threshold, more earthquakes began to occur (fig. A2*B*). Earthquake activity declined whenever the fluid pressure fell below the threshold.

Attica-Dale, New York

Solution mining for salt in the Attica-Dale area (fig. A3) triggered a marked increase in microearthquake activity in 1971. As many as 80 earthquakes per day were concentrated within 1 km of a 426-m-deep injection well (fig. A4; Fletcher and Sykes, 1977) in an area where the previous record of activity was less than 1 event per month. All these earthquakes were small and had estimated magnitudes of between -1.0 and 1.0. THP at the injection well typically operated between 52 and 55 bars, or only a few bars less than that calculated to induce sliding on preexisting fractures that have no cohesion, based on the Mohr-Coulomb failure criterion and analysis of hydrofracture stress measurements conducted about 100 km from the activity. Seismicity continued in the Dale brine field for as long as elevated pore pressure was maintained (fig. A5). The low level of background activity before high-pressure injection began, the dramatic increase in activity following injection, and the rapid cessation of activity following a decrease in injection pressure below about 50 bars (fig. A6) strongly suggest that this seismicity was induced by injection activities.

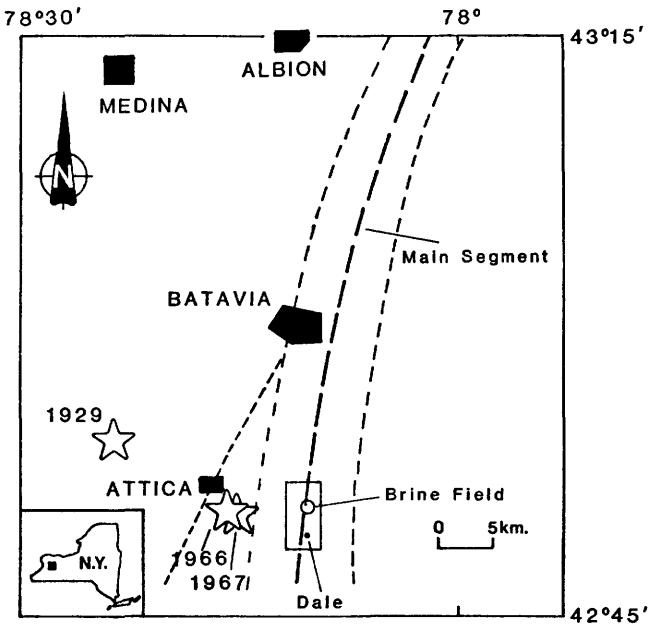

Figure A3. Location of the Dale brine field, western New York. Circle, field; heavy dashed line, Clarendon-Linden Fault; lighter dashed line, lesser secondary faults; stars, epicenters of large historical earthquakes near Attica in 1929, 1966, and 1967; and box, approximate area shown in figure A4 (from Nottis, 1986).

Texas Oil Fields

Permian Basin, West Texas and Southeastern New Mexico

Cases of induced seismicity associated with fluid injection operations for the secondary recovery of oil and gas have been suggested for several areas in Texas (pl. 1). One of the earliest reports alludes to an increase in seismicity associated with petroleum production and water-flooding operations in the Permian basin of West Texas near Kermit (Shurbet, 1969). A marked increase in earthquakes above magnitude 3 was observed to correlate with a dramatic increase in the number of injection wells operating at pressures greater than 70 bars. This increase in seismicity was of particular interest because of its proximity to a radioactive-waste-disposal site in southeastern New Mexico (fig. A7*A*; Rogers and Malkiel, 1979). About 20 earthquakes (the largest of which was about M 4.4) were recorded between November 1964 and December 1976. Twelve stations were subsequently installed to monitor this seismicity and to determine whether, in fact, the earthquakes were directly related to oil field activities. Between December 12, 1975, and June 26, 1977, 406 earthquakes were detected, most of which were at depths of less than 5.0 km and nearly all in areas that had active water-flooding operations (fig. A7*B*). Continued monitoring through September 1979 by the local network identified several pronounced clusters of seismic activity. The largest and most active area coincides with the War-Wink South oil and gas field located in the Delaware Basin region of Ward County, West Texas (Keller and others, 1981; Keller and others, 1987). Much of this seismicity is shallow and exhibits predominantly normal faulting (Keller and others, 1987), which is consistent with subsidence as a result of gas withdrawal. Other areas of activity include earthquakes in 1976 and 1977 associated with the Dollarhide oil field that extends into southeastern New Mexico, as well as more-recent seismicity located on the Central Basin Platform in the vicinity of the Keystone oil field (Orr, 1984; Orr and Keller, 1985). Nine of the local water-flooding projects that typically operated at injection pressures of greater than 100 bars are listed in table A1 (Texas Railroad Commission, 1971, 1985). These wells range in depth from 800 to 3,700 m. Measurements of *in situ* stress determined from hydrofracturing indicated a maximum regional compressive stress

Table A1. Characteristics of well operations and reservoir properties associated with possible induced seismicity

[Depth, bottom of well; thickness, of reservoir; k, permeability; THP, top hole pressure; BHP, bottom hole pressure; p_0, initial formation pore pressure; S_h, minimum horizontal compressive stress; S_H, maximum horizontal compressive stress; S_v, vertical stress; Max mag, maximum magnitude; ***, not applicable (injection not performed)]

Well site or oil field location	Depth (m)	Thickness (m)	k (mD)	Porosity (percent)	THP (bars)	BHP (bars)	p_0 (bars)	S_h (bars)	S_H (bars)	S_v (bars)	Max mag	Year of earthquakes
Ashtabula, Ohio	1,845	46	0.6	10	100	284	191	320	>460	460	3.6	1987
Catoosa, Okla.											4.7?	1956, 1960
Cogdell Canyon Reef, Tex.	2,071	43	18–30	7	199	406	215			476	4.6	1974–79
Dale, N.Y.	426	16			55	98		76	>109	109	1.0	1929?, 1966?, 1971
Rocky Mountain Arsenal, Denver, Colo.	3,671		0.03	2	76	415	269	362	<830	830	5.5	1962–67
East Texas, Tex.	1,113	3	200	23	103	214	70			256	4.3	1957, 1985
Fenton Hill, N. Mex.	2,700		.01		200	493	265	405	<635	635	<1.0	1979
Flashing Field, Tex.	3,400	50	13	15	***	71	352			768	3.4	1973–83
The Geysers, Calif.	3,000		<.05	3			<35	245	785	785	4.0	1975–
Gobles Field, Ontario, Canada	884	9			***		45			225	2.8	1979–84
Hunt Field, Miss.											3.6	1976–78
Imogene Field, Tex.	2,400	33	14	17	***	146	246			542	3.9	1973–84
Lake Charles, La.	1,411	49			93	234			<325	325	3.8	1983–
Love County, Okla.	3,622	427			277	632		538	~833	833	2.8?	1977?–, 1979
Matsushiro, Japan	1,800				50	230				460	2.8	1970
Northern Panhandle, Tex.	2,022	21	50	15	21	223	145			465	3.4	1983–84
Calhio, Perry, Ohio	1,810	88	6	8	114	294	200	320	>460	460	2.7?	1983–87
Rangely, Colo.	1,900	350	1	12	83	275	170	314	552	427	3.1	1962–75
Rocky Mountain House, Alberta, Canada.	4,000				***			>1,020	>1,020	1,020	4.0	1974–80
Sleepy Hollow, Nebr.	1,150	100	26		56	171	115		<265	265	2.9	1977–84
Snipe Lake, Alberta, Canada											5.1	1970
Permian basin fields:											4.4	1964–79
Dollarhide, Tex.-N. Mex.	2,590	59	17	14	138	397	179			596	~3.5	1964–79
Dora Roberts, Tex.	3,661	38	1	7	431	797	324			842	~3.0	1964–79
Kermit Field, Tex.	1,829	5	1	15	221	404	198			421	~4.0	1964–79
Keystone I Field, Tex.	975	11	21	20	103	200	90			224	~3.5	1964–79
Keystone II Field, Tex.	2,987	101	7	3	176	475	204			687	~3.5	1964–79
Monahans, Tex.	2,530	12	6	4	207	460	131			582	~3.0	1964–79
Ward-Estes Field, Tex.	914	11	35	16	117	208	103			210	~3.5	1964–79
Ward-South Field, Tex.	741	5	30	21	138	212	76			170	~3.0	1964–79
War-Wink South, Tex.	1,853	2.5	17	18	***					426	~3.0	1964–79

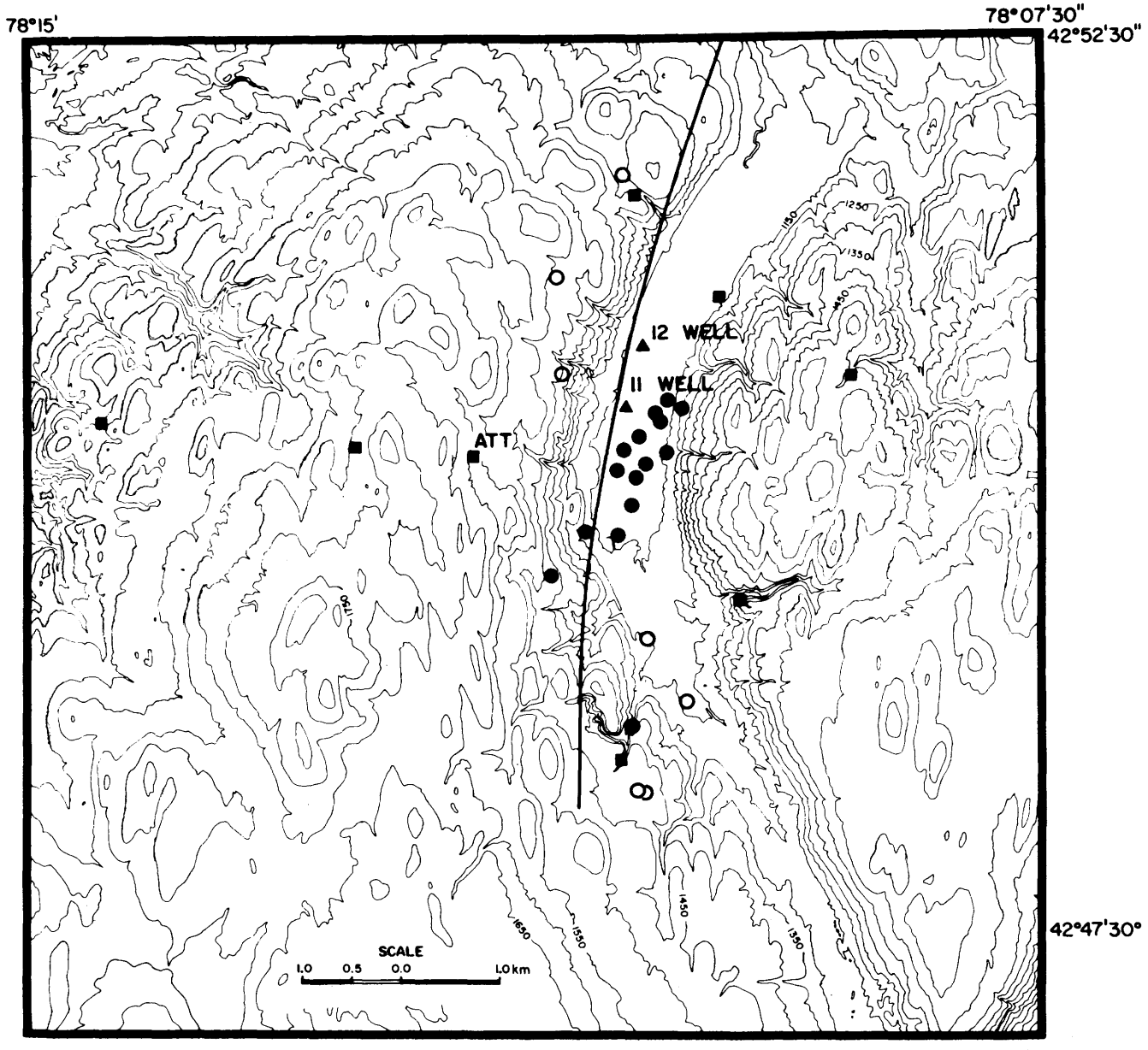

Figure A4. Epicenters of well located earthquakes near the Dale brine field, New York. Solid circles, well located earthquakes; squares, monitoring stations; triangles, injection wells; open circles, epicenters that have poor resolution; and solid line, Clarendon-Linden Fault. *A*, October 1971. *B*, November 1971. Reprinted from Fletcher and Sykes (1977) and published with permission.

of 150 bars and a minimum compressive stress of 85 bars at depths of about 485 m.

Cogdell Canyon Reef Oil Field, West Texas

The largest earthquake to occur in known association with an oil field injection operation within the United States was a magnitude 4.6 to 4.7 event near Snyder in June 1978. This earthquake, which was part of a sequence of events that apparently had been active since 1974 (Davis, 1985), was located in the Cogdell Canyon Reef oil field of West Texas (fig. A8). Initial formation pressure at the time of discovery (1949) amounted to 215 bars BHP. By 1956, pressure in the field had dropped to 79 bars BHP, which necessitated a water-flooding and pressure-maintenance program. A dramatic increase in the numbers of injection wells, volumes of fluid pumped, and effective pressures took place in the early 1970's, shortly after which the first felt earthquake was experienced (Harding, 1981a). Surface injection pressures ranged as low as 45 to 95 bars, but

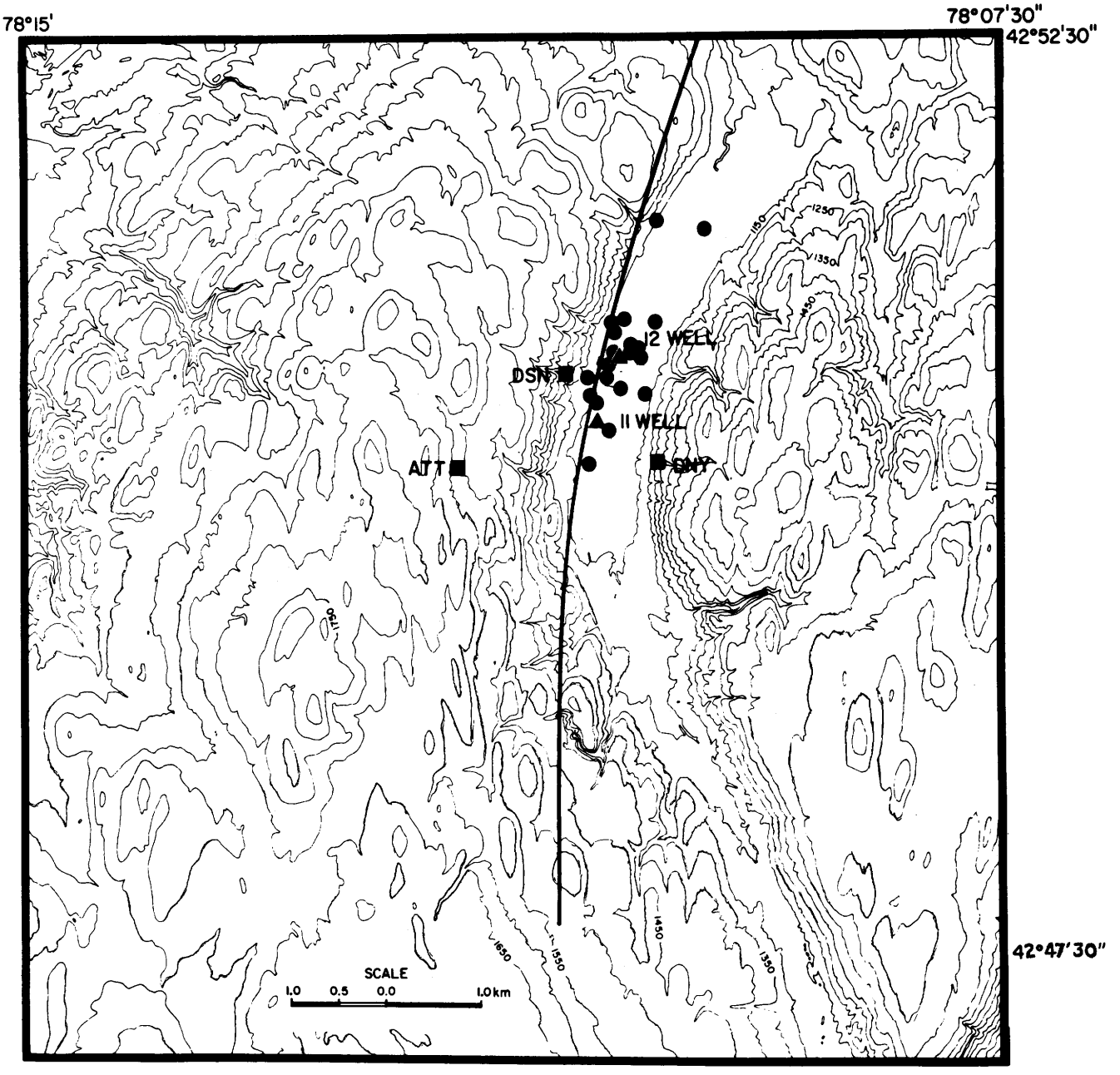

B

Figure A4. Continued.

typically operated between 186 to 217 bars THP. By using the Mohr-Coulomb failure criterion, these higher values of injection pressure were determined to be sufficient to induce slip on favorably oriented fractures (Davis, 1985). Because injection pressure in the field remained fairly constant, there is little correlation between the injection pressure and the episodic nature of the earthquake activity. There is some correlation, however, between volumes of fluid injected and the rate of local earthquake occurrence (fig. A9). The data were interpreted to suggest that large (felt) earthquakes were preceded by a reduction in field permeability (which corresponded to a drop in volume of water accepted by the reservoir at constant pressure) followed by an increase in permeability after each of the major earthquake sequences (Harding, 1981a).

Because of the proximity of the earthquakes to oil field operations, a small local network of stations was operated from February 1979 through August 1981 (fig. A8; Harding, 1981a). As of 1985, a total of about 30 earthquakes had been spatially associated with the Cogdell

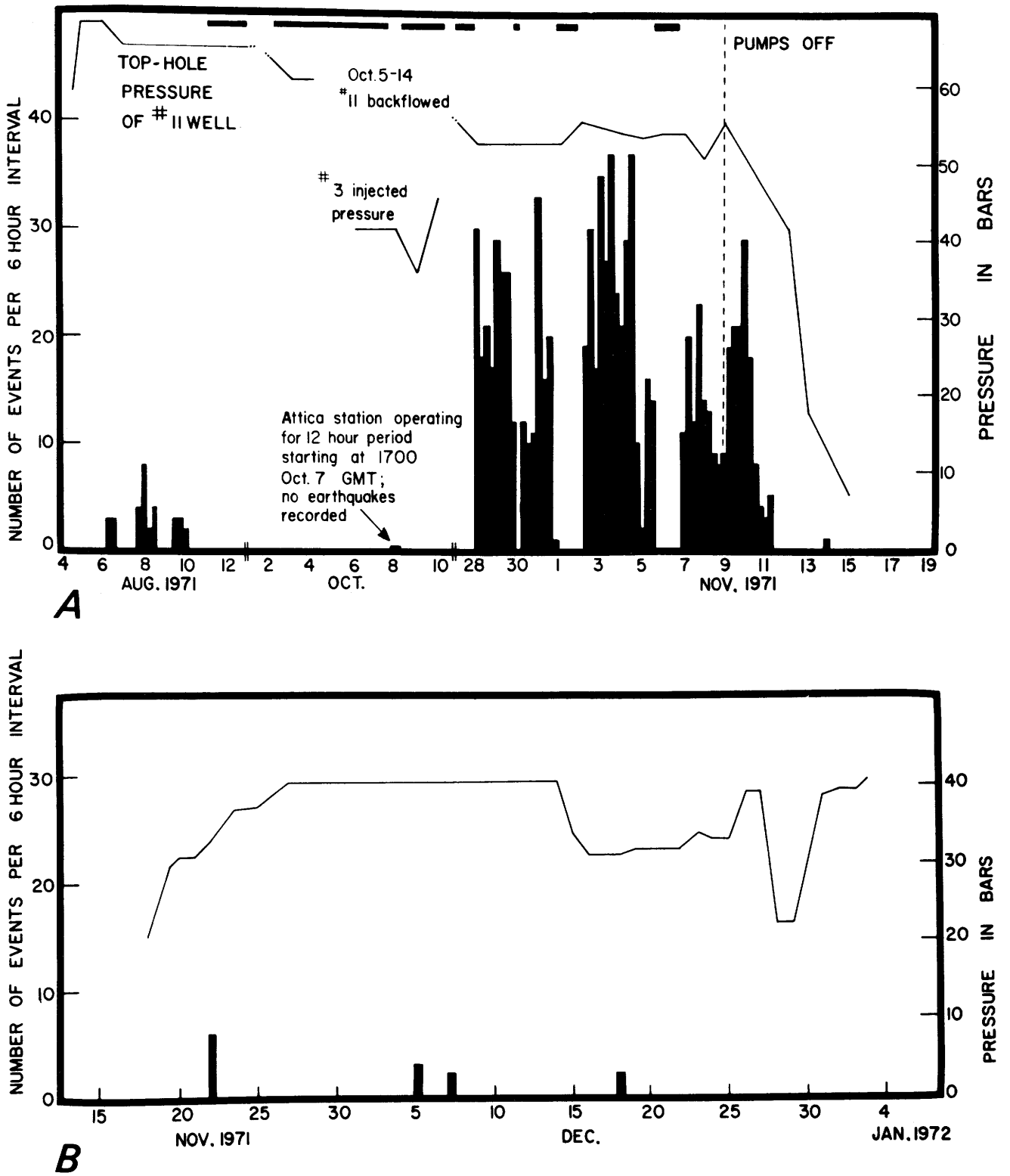

Figure A5. Number of earthquakes and pumping pressures (light solid lines) with time in the Dale brine field, New York. *A*, From August 4 to November 19, 1971, when top-hole injection pressures in well 11 typically exceeded 50 bars. Note the abrupt cessation of activity after pumping was shut down on November 9. *B*, Similar to *A* but from November 15, 1971, to January 4, 1972, when the maximum injection pressure did not exceed about 40 bars. Reprinted from Fletcher and Sykes (1977) and published with permission.

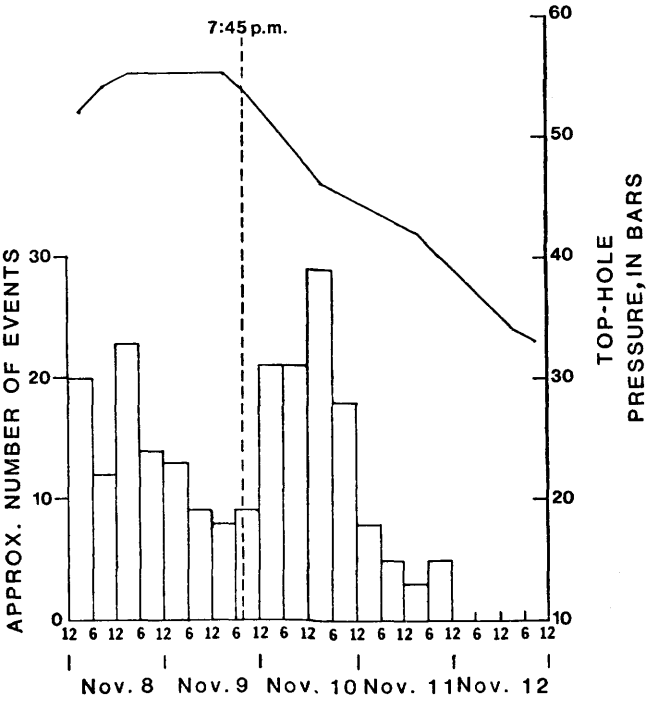

Figure A6. Enhanced section of figure A5 for well 11 of the Dale brine field, New York, showing the rapid decrease in seismicity after pumping ceased at 7:45 p.m. on November 9, 1971, and well pressure (solid line) subsequently declined below about 50 bars (from Nottis, 1986).

Canyon Reef oil field (fig. A8); most of the events occurred between April 1977 and August 1979. Many of the wells that penetrate to the Canyon Reef Formation operate at depths of between 2,070 and 2,265 m. These well depths coincide with the shallow focal depths (on the order of 3 km or less) of the earthquakes located within the oil field (Harding, 1981b) and are nearly the same as the focal depth (3 km) determined for the June 1978 event (Voss and Herrmann, 1980).

Atascosa County, South Texas

Seismic activity also has been identified with the *withdrawal* of oil and gas from two fields in south Texas (pl. 1; Pennington and others, 1986). Production from the Imogene oil and gas field began in 1944; the depth of the producing horizon is 2.4 km. Initial fluid pressure in the field was approximately 246 bars and was reduced to 146 bars by 1973. In the Flashing gas field, production began in 1958 at a depth of 3.4 km. Initial pore pressure in the producing formation was 352 bars but was reduced to only 71 bars (or 20 percent of the original value) by 1983. The rapid withdrawal of fluid and gas apparently resulted in subsidence and differential compaction of the producing horizon in both fields, which is similar to the situation in the War-Wink gas field. Seismic activity began in 1973; the largest earthquake (M 3.9) occurred in the Imogene field in March 1984. In both cases, the sizes and the number of earthquakes increased over time, which is consistent with a model for the evolution of the hydrologic characteristics of the field whereby the strength of the rock increases as fluid pressure decreases. The earthquakes are believed to be generated as formation pore pressure is reduced to the point that further fluid extraction and subsequent subsidence results in strain accumulation in the newly strengthened rock. If the strains are large enough, then the amount of energy accumulated in the rock is apparently sufficient to cause earthquakes as large as magnitude 3 to 4 (Pennington and others, 1986).

The Geysers, California

In a case similar to Atascosa County, Tex., a large number of small earthquakes ($M_L \leq 4$) have been triggered by the reduction in steam pressure caused by energy production in The Geysers geothermal area near Clear Lake in northwestern California (fig. A10; Oppenheimer, 1986). The Geysers is the site of a vapor-dominated steam field where, by the early 1980's, 150 wells had been drilled to depths of between 0.8 and 3.0 km. Earthquake activity has increased in The Geysers area by nearly a factor of two over seismicity levels before production; about 10 microearthquakes that have magnitudes of greater than 0.5 typically occur each day. Evidence that the increased seismicity was induced relied upon the spatial and the temporal distribution of the microearthquakes in the vicinity of the producing steam wells. During the period from 1975 to 1981, earthquakes were found to occur in previously aseismic areas within months following the initiation of steam extraction from newly developed regions of the reservoir. Seismic activity also correlated with energy production or rate of steam extraction (fig. A11). Earthquake hypocenters were found to extend from 0 to 6.5 km in depth, but earthquakes that had focal depths of less than 3.5 km were typically located within a few hundred meters laterally from the sites of active steam wells (Eberhart-Phillips and Oppenheimer, 1984). Although some of the extracted steam is condensed and reinjected, the reduction in effective normal stress caused by increased pore pressure is not considered to be the likely mechanism to explain the induced seismicity. Steam pressure in the field actually has declined by about 1 bar/yr since 1966 as a result of cooling, and the number of earthquakes did not correlate with volumes of steam condensate injected into the wells. The two possible mechanisms thought to be responsible for the increased seismicity are the increased shear stresses that are a result of volumetric thermal contraction caused by reservoir cooling (Denlinger and others, 1981) and by reservoir subsidence arising from large fluid mass withdrawal (Majer and McEvilly,

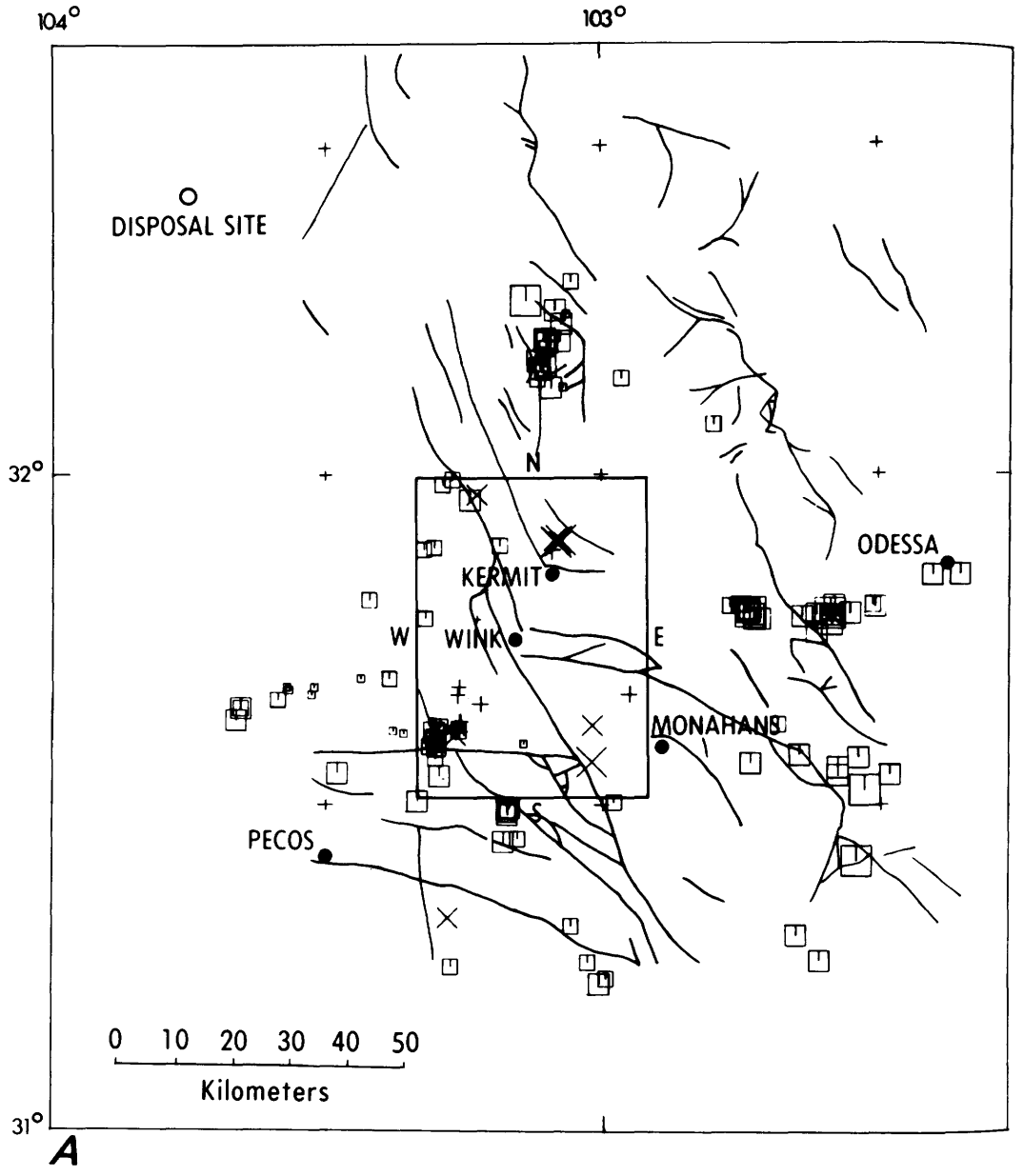

Figure A7. Earthquakes located in the Central Basin Platform of the Permian Basin, West Texas, from January 1976 to July 1977. *A*, Earthquake epicenters and known pre-Permian basement faults shown with solid lines; radioactive-waste-disposal site in New Mexico is shown by the open circle. *B*, Epicenters and outlines of oil fields; labeled fields are sites of active water-flooding operations during the same time period. *A* and *B*, Size of symbol indicates magnitude—X, 3.0 to 4.0; x, 2.0 to 3.0; +,1.0 to 2.0; +, ≤1.0; square sizes indicate less reliable earthquake epicenters in the same magnitude ranges. Reprinted from Rogers and Malkiel (1979) and published with permission.

1979) or, alternatively, the conversion of continuous aseismic slip into seismic slip (that is, earthquakes) by an increase in the coefficient of friction following the deposition of exsolved solids (probably silica) onto slipping fracture surfaces (Allis, 1982).

Fenton Hill, New Mexico

Several hundred microearthquakes were generated during a massive hydraulic fracturing experiment conducted at Fenton Hill (pl. 1) in March 1979 (Pearson, 1981). The

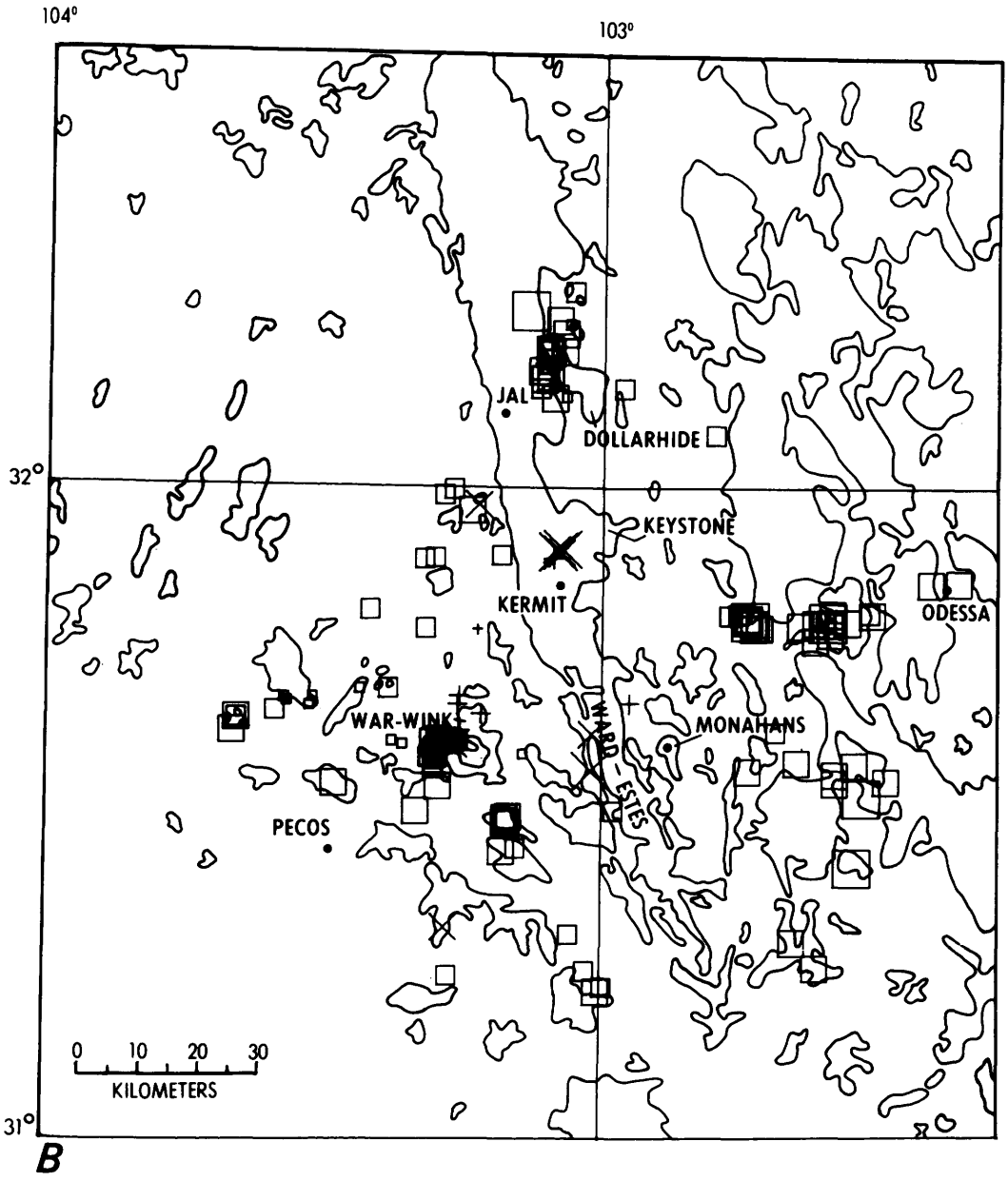

Figure A7. Continued.

purpose of the experiment was to stimulate a fracture in a deep (2,930-m) injection well that would propagate so as to intersect an adjacent production well to be used in a hot-dry rock geothermal energy project. Hydraulic stimulation involved nearly 460,000 L of water injected over a 5½-hr period. Maximum THP was held constant at 200 bars. During the experiment, activity averaged 3 to 4 microearthquakes per minute. Formation pore pressure before injection was measured at about 265 bars. Maximum and minimum effective horizontal stresses were found to be 370 and 140 bars, respectively. By using the Mohr-Coulomb failure criterion, Pearson (1981) determined that only 30 bars of increased pore pressure was sufficient to initiate slip on favorably oriented preexisting joints. Most of the small earthquakes appeared to be localized to within 30 m of the expanding hydraulic fracture. Unfortunately, the stimulated fracture failed to intersect the desired production well. In a subsequent attempt, 7.6 million L of water was injected at a depth of 3,400 m at a rate of 1,600 L/min, which triggered an additional 850 microearthquakes in the vicinity of the well (House and McFarland, 1985).

Sleepy Hollow Oil Field, Nebraska

After the installation of sensitive monitoring equipment in Nebraska in 1977, a concentration of seismic

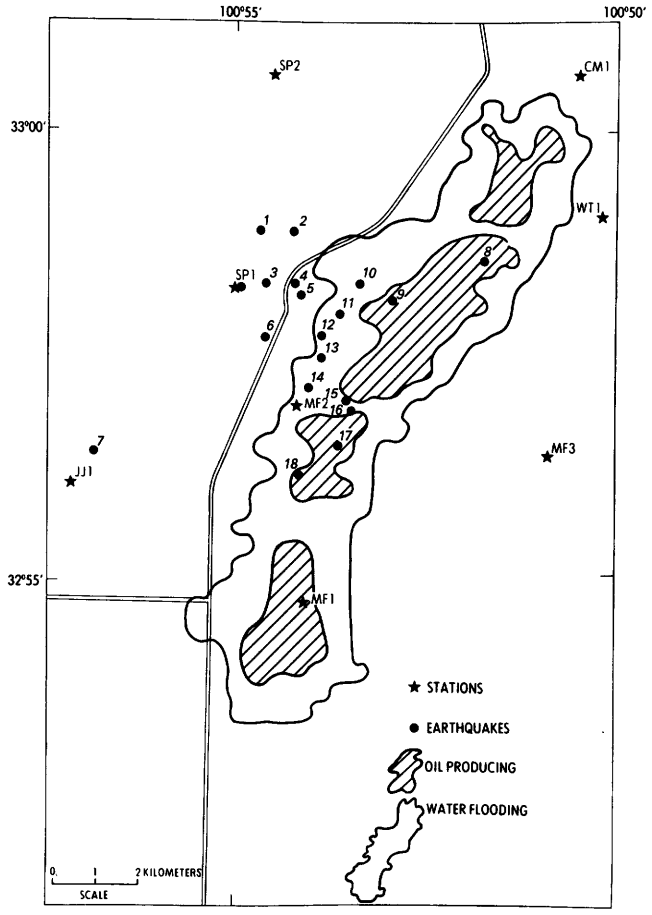

Figure A8. Epicenters of well located earthquakes in the Cogdell Canyon Reef oil field near Snyder, Tex. Also shown are the locations of network stations and the extent of water flooding and oil production (from Harding, 1981a).

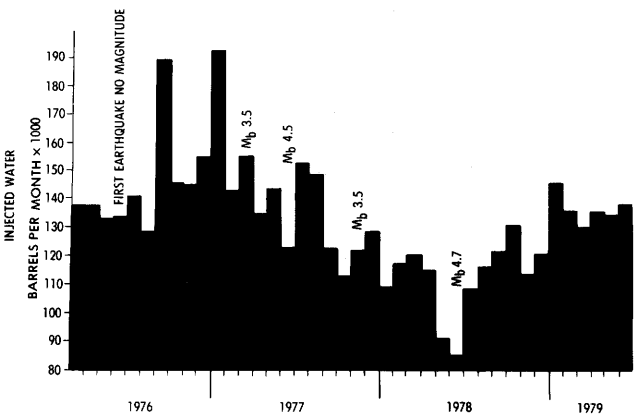

Figure A9. Cumulative monthly volume (barrels) of water injected in the Cogdell Canyon Reef oil field, Texas, and times of reported felt earthquakes (from Harding, 1981a). M_b, body-wave magnitude.

activity was identified near the Kansas-Nebraska border (pl. 1). From March 1979 to March 1980, subsequent investigations using portable instruments (fig. A12*A*) detected 31 earthquakes in close proximity to the most productive oil field in the State—the Sleepy Hollow (Evans and Steeples, 1987). Water flooding to enhance recovery had been in operation since 1966. As shown in figure A13*A*, water injection typically operated at 52 bars THP within the Lansing Group (depths of 1,050–1,130 m) and 22 bars within the Sleepy Hollow sandstone (Reagan) formation (1,150–1,170 m depth), which corresponded to 172 and 142 bars BHP, respectively. Most of the well located earthquakes occurred within the confines of the producing field and at depths of less than 2 km (Rothe and Lui, 1983) in an area where well-defined subsurface faults (fig. A13*B*) were present, based on structure contour maps. Maximum magnitude of the induced seismicity was 2.9. In a later monitoring program, an additional 250 microearthquakes were detected within the active field between April 1982 and June 1984 (fig. A12*B*; Evans and Steeples, 1987), when the average THP in the field reached as high as 56 bars.

Southwestern Ontario, Canada

Oil and gas production from the Gobles oil field, which is located in southwestern Ontario about 55 km east-northeast of London (fig. A14*A*) began in 1960 (Mereu and others, 1986); the producing horizon is 884 m deep. Because formation fluid pressure was lower than expected, water-flooding operations to enhance recovery began in 1969. Historically, this area of southwestern Ontario has had a very low level of seismic activity. In December 1979, a M 2.8 earthquake was detected in the vicinity of the oil field. From July 1980 through August 1984, a portable network of stations recorded 478 earthquakes within and around the producing area (fig. A14*B*). All the locatable events were shallow and exhibited travel-times consistent with hypocenters at a focal depth coincident with the producing horizon. No spatial correlation with specific wells was identifiable, however, and, although earthquake activity varied considerably in time, fluctuations in activity rate did not correlate with injection pressure, which, for the most part, remained nearly constant. This area is located just west of the Dale brine field in western New York and just north of injection-induced seismicity in northeastern Ohio (see section "Recent Seismicity and Injection Operations—Northeastern Ohio").

Matsushiro, Japan

Besides the Rangely oil field experiment, one of the few attempts to specifically manipulate earthquake behavior by fluid injection occurred near Matsushiro, Japan. In 1970, 2.9 million L of water was injected at a depth of 1,800 m,

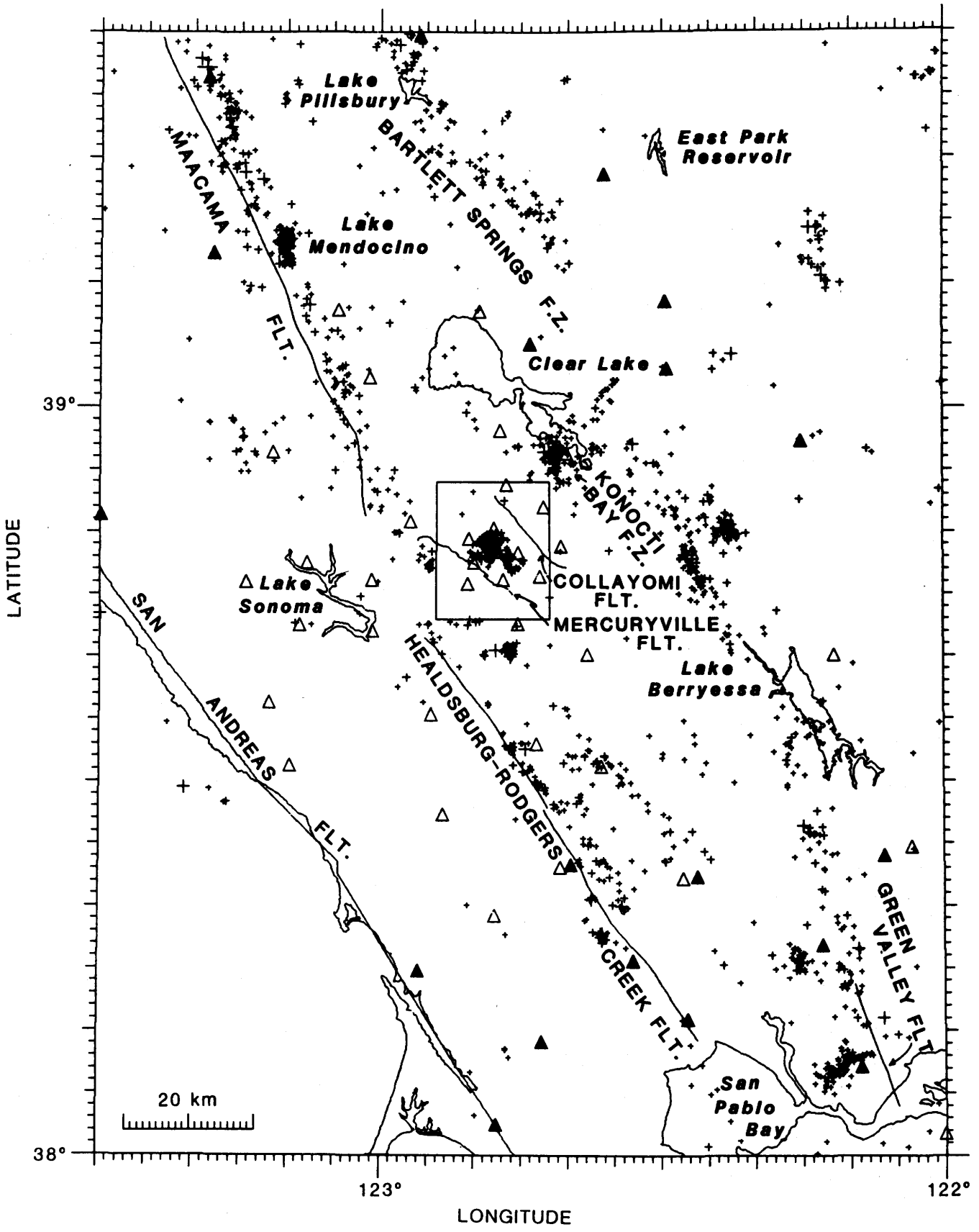

Figure A10. The Geysers geothermal area, California, and surrounding region. Epicenters outside the box represent well located earthquakes from January 1976 through December 1984. Seismicity inside the box is from the period January 1984 through October 1985. Open box, geothermal area; +, $M_L \geq 1.5$ epicenters; open triangles, locations of CALNET stations; and solid triangles, locations of stations used for locations of regional seismicity. Reprinted from Oppenheimer (1986) and published with permission.

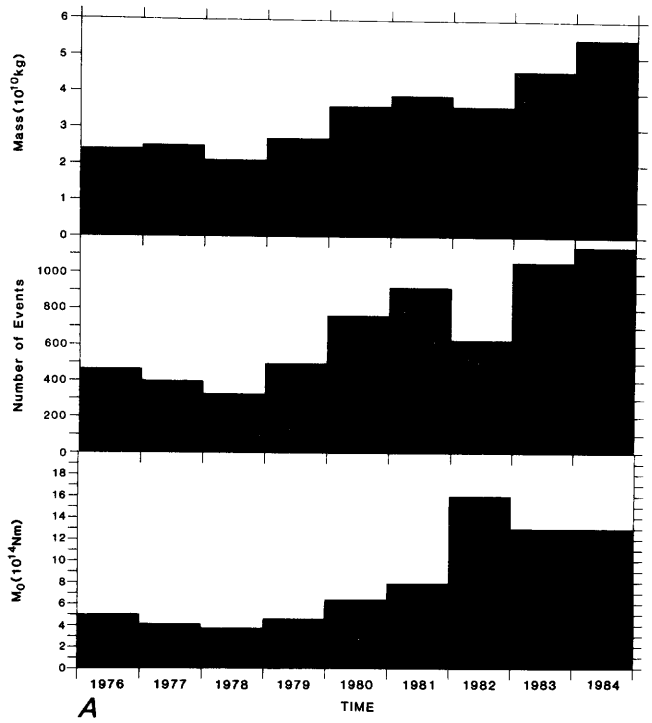

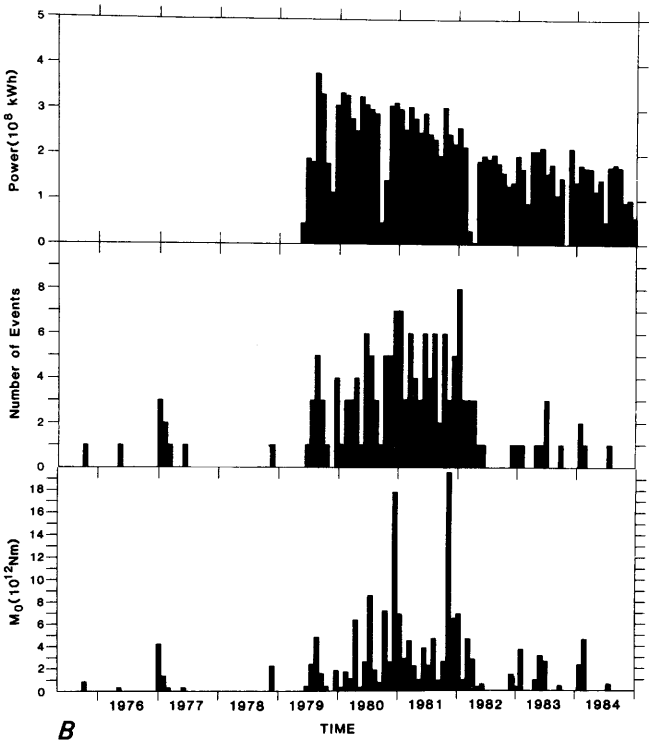

Figure A11. Water withdrawn and power generated as compared with the rates of seismicity at The Geysers geothermal field, California. *A*, Yearly net mass of water withdrawn. *B*, Monthly power generated. Both are compared with numbers and moments of earthquakes. Reprinted from Oppenheimer (1986) and published with permission.

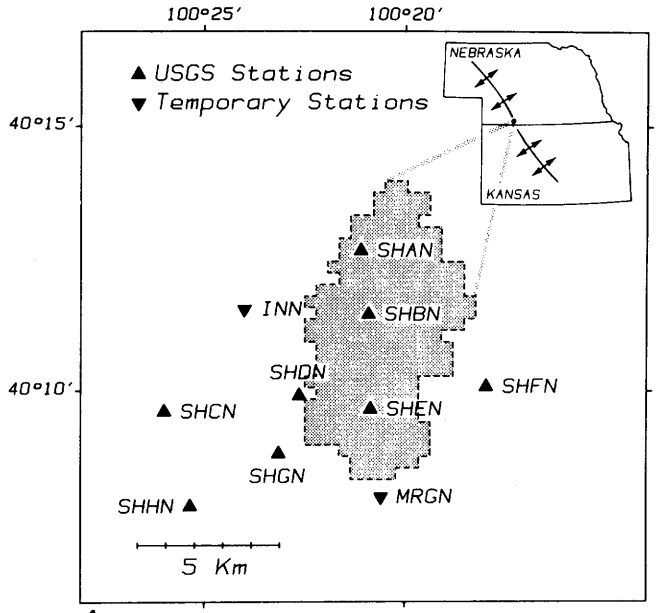

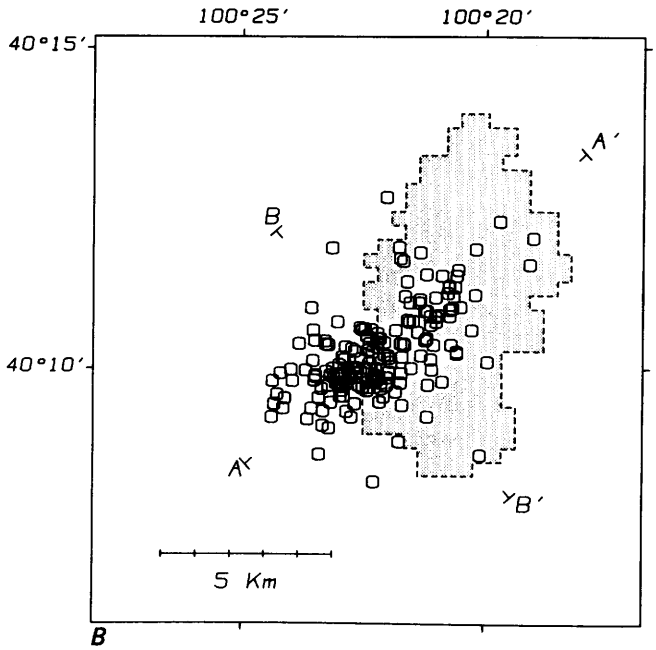

Figure A12. Seismic monitoring stations and earthquake epicenters, Sleepy Hollow oil field, Nebraska. *A*, Seismic monitoring stations. Shaded region, producing area of the field; and triangles, stations. *B*, Earthquake epicenters in the vicinity of the field between April 1982 and June 1984. Reprinted from Evans and Steeples (1987) and published with permission.

THP's of 14 to 50 bars, and injection rates of 120 to 300 L/min (Ohtake, 1974). During the 2 months (mo) of the experiment, several hundred small earthquakes were triggered within 4 km of the well and at depths of 1.5 to 7.5 km. A delay of 5 to 9 days (d) was observed between the onset of the increased seismicity and the increased injection pressure. Activity was significantly greater during injection than either before or after the experiment. Much of the induced seismicity was localized along the northeast-dipping Matsushiro fault zone, whereas most of the background seismicity was scattered in the hanging wall (Ohtake, 1974). No attempts were made to determine the *in situ* state of stress or the critical threshold for failure as indicated by the Mohr-Coulomb failure criterion, but the observed time delay for the onset of seismicity and the subsequent migration in depth of the earthquakes were consistent with inferred values of permeability and the time required for pore pressure effects to migrate to the area where the earthquakes were observed.

Less Well Documented or Possible Cases

Western Alberta, Canada

On March 8, 1970, a M 5.1 earthquake occurred near Snipe Lake (fig. A15; Milne, 1970). No significant earthquakes had previously occurred in the area, and, on the basis of the limited felt area and preliminary determinations of focal depth (<9 km), the 1970 event appeared to have been relatively shallow (Milne and Berry, 1976). At the time of the earthquake, 646 oil and gas wells were in operation within 80 km of Snipe Lake. Production began in 1954, and water injection to maintain field pressure had been in effect in 56 wells since 1963. Although little else is known about this event, this earthquake is considered to be the first and largest known Canadian example of an earthquake induced by fluid injection in a producing oil field because it occurred within an oil-producing area where fluid injection was actively taking place (Milne and Berry, 1976).

Confirmation that well activities in western Alberta are triggering earthquakes was documented near Rocky Mountain House (fig. A15; Wetmiller, 1985, 1986), where a microearthquake survey was conducted in 1980. In 23 d of operation, a seven-station network detected 146 earthquakes, of which 67 events were locatable. The largest earthquake recorded was a magnitude 3.4. All the locatable earthquakes occurred in a very small source area (fig. A16*A*) that was about 4 km long by 4 km wide by 1 km thick at a depth of 4 km. This source region coincides with the base of the Paleozoic section and is the site of the Strachan D-3A gas field, which is a Devonian-aged limestone-reef sour gas reservoir and western Alberta's major producer of natural gas. Production began in the field in the early 1970's, and a marked increase in seismicity, including earthquakes as large as M 4.0, began in 1974 (fig.

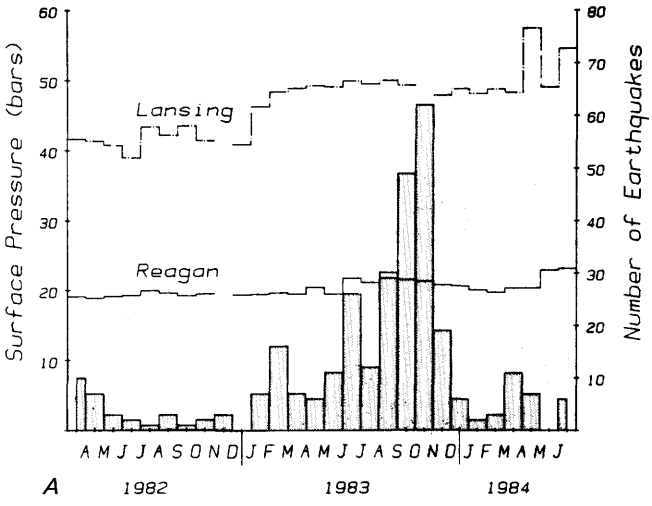

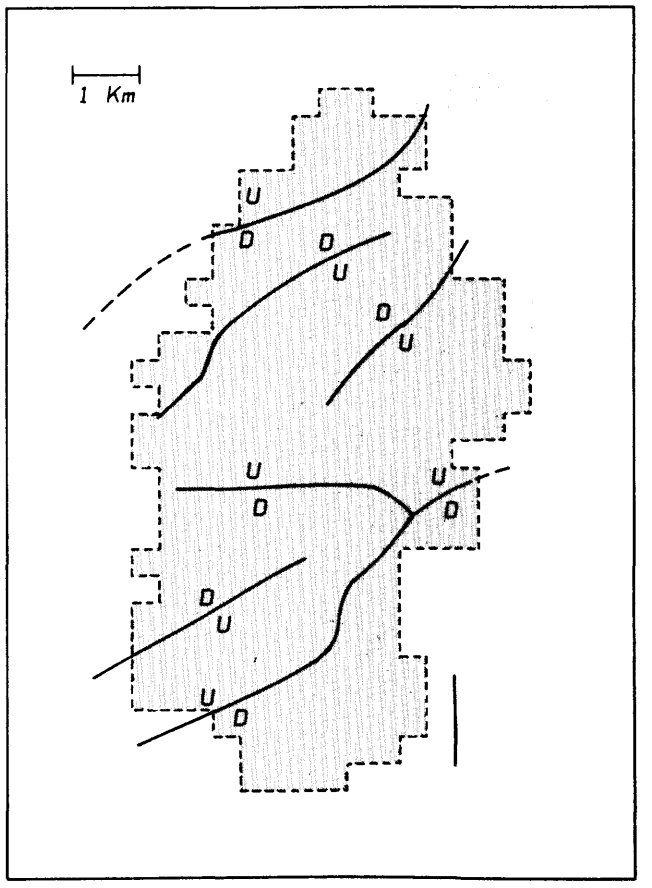

Figure A13. Formation fluid pressures and mapped faults, Sleepy Hollow oil field, Nebraska. *A*, Average monthly pressures within the two formation reservoirs used for injection and the number of earthquakes per month. Ten injection wells were added in May and June 1983. *B*, Mapped faults in the Precambrian basement in the vicinity of the field (shaded area). Reprinted from Rothe and Lui (1983) and published with permission.

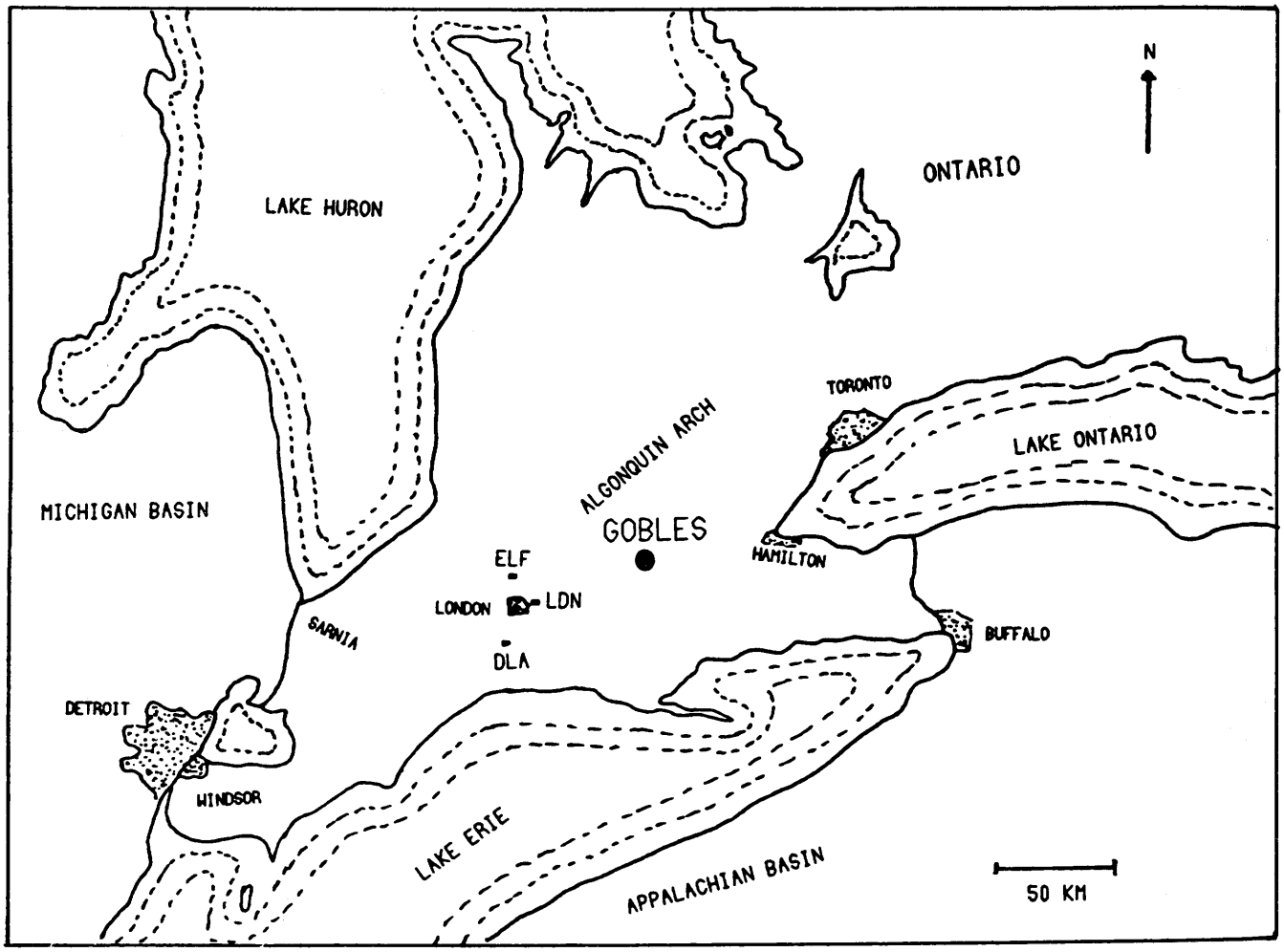

Figure A14. Location and earthquake epicenters, Gobles oil field, southwestern Ontario, Canada. Seismic stations of the University of Western Ontario permanent seismic array are shown. *A*, Location of the field (solid circle). *B*, Earthquake epicenters in the vicinity of the field relative to location of local monitoring stations (solid squares). Reprinted from Mereu and others (1986) and published with permission.

A16*B*; Wetmiller, 1986). The timing and the spatial correspondence of the microearthquake activity directly in or below the actual zone of production strongly suggests that the local seismicity is being triggered by gas production. The predominant thrust-faulting focal mechanisms exhibited by the earthquakes, however, indicate that the seismicity may be related to crustal unloading, which is similar to the situation of possible induced earthquakes near the Gazli gas field in Soviet Uzbekistan (Simpson and Leith, 1985), rather than to other cases of shallow normal-faulting events associated with subsidence of petroleum fields without secondary fluid injection (Yerkes and Castle, 1976; Pennington and others, 1986).

Since 1984, a six-station seismic network has been operating in the Cold Lake area of Alberta (Kapotas and Kanasewich, 1989), where heavy oil is being extracted by using an *in situ* process of steam injection. Local microearthquake activity ranges from 20 to more than 100 events per year. The induced tremors are mostly less than M 2 and, on the basis of geomorphological characteristics of the bedrock topography, appear to follow a major inferred subsurface fault structure through the area of heavy-oil production. Within the network, induced earthquakes occur at shallow focal depths consistent with formation levels of steam injection and oil extraction. Southeast of the array, earthquakes are also detected in association with fluid injection operations to dispose of excess oil field brine (Kapotas and Kanasewich, 1989).

Historical Seismicity and Solution Salt Mining

Western New York

The identification of recent induced seismic activity with the Dale brine field (Fletcher and Sykes, 1977) and

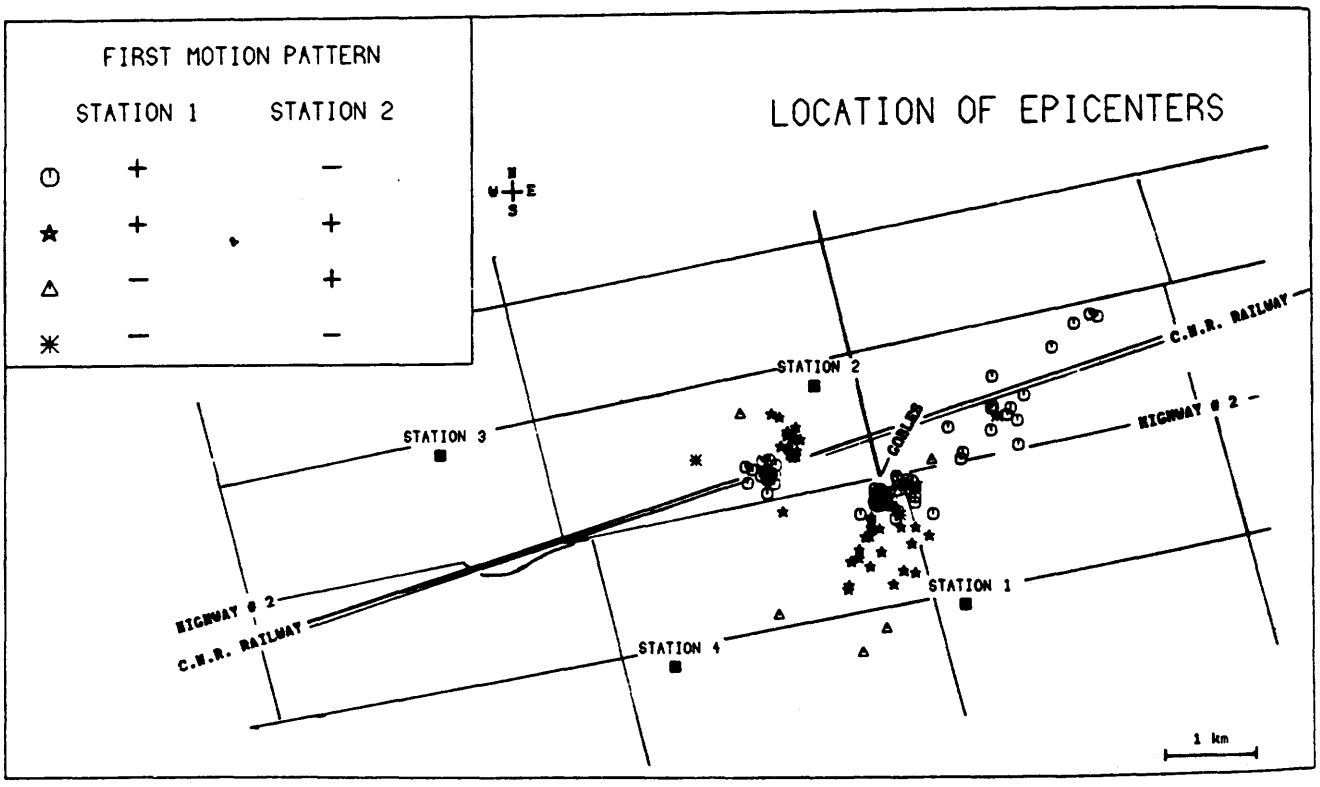

B

Figure A14. Continued.

with secondary recovery operations in southwestern Ontario (Mereu and others, 1986) suggests that a relation may exist between the older historical earthquakes in western New York and the adjacent solution mining operations in production at the time. Solution salt mining operations have been in operation in the northwestern region of the State since the late 19th century (Dunrud and Nevins, 1981). In 1929, a large (M 5.2) earthquake occurred near Attica (fig. A3), that caused significant damage in the epicentral region [VIII on the Modified Mercalli Intensity Scale (MM), Appendix C]. Subsequent earthquakes in 1966 (M 4.6) and 1967 (M 3.8) also generated relatively high intensities for their size (Herrmann, 1978). These high intensities were attributed to the shallow focal depths of the earthquakes (about 2 km, or roughly on the same order as the depth of the active solution salt mining wells). Past investigators have attributed these earthquakes near Attica to tectonic slip along the Clarendon-Linden fault system (fig. A3); however, the shallow focal depths and the proximity to protracted mining operations suggest that these earthquakes also may have been triggered by the adjacent mining operations. Unfortunately, the lack of detailed records of injection activities or direct measurements of the state of stress in the epicentral region make any definitive correlation between these older historical earthquakes and mining operations difficult.

Northeastern Ohio

The association of solution mining with the occurrence of small earthquakes in western New York State (Fletcher and Sykes, 1977) and the extensive salt mining operations in northeastern Ohio (Clifford, 1973) suggested the possibility that some of the earthquake activity in Ohio also may be related to solution salt mining (fig. A17). Solution mining for salt began in northeastern Ohio in 1889 (Clifford, 1973; Dunrud and Nevins, 1981) and continues to the present, although several previously active operations have been closed down. The target horizon for the mining operations is the Silurian Salina Formation at a depth of 600 to 900 m, depending on the distance from Lake Erie. On the basis of their spatial proximity and temporal association, it could be argued that several earthquakes in the northeastern region of the State are related to active solution salt mining operations. In particular, earthquakes in 1898, 1906, and 1907 (Stover and others, 1979), which were located within the Cleveland metropolitan area, as well as earthquakes in 1932 and 1940, which were about 50 km south of Cleveland, are possible examples. However, in view of the large number of earthquakes reported before the initiation of solution mining and the apparent occurrence of at least some earthquakes in northeastern Ohio beyond the range of the expected influence of mining operations, it seems reasonably clear that at least some of the earthquakes are

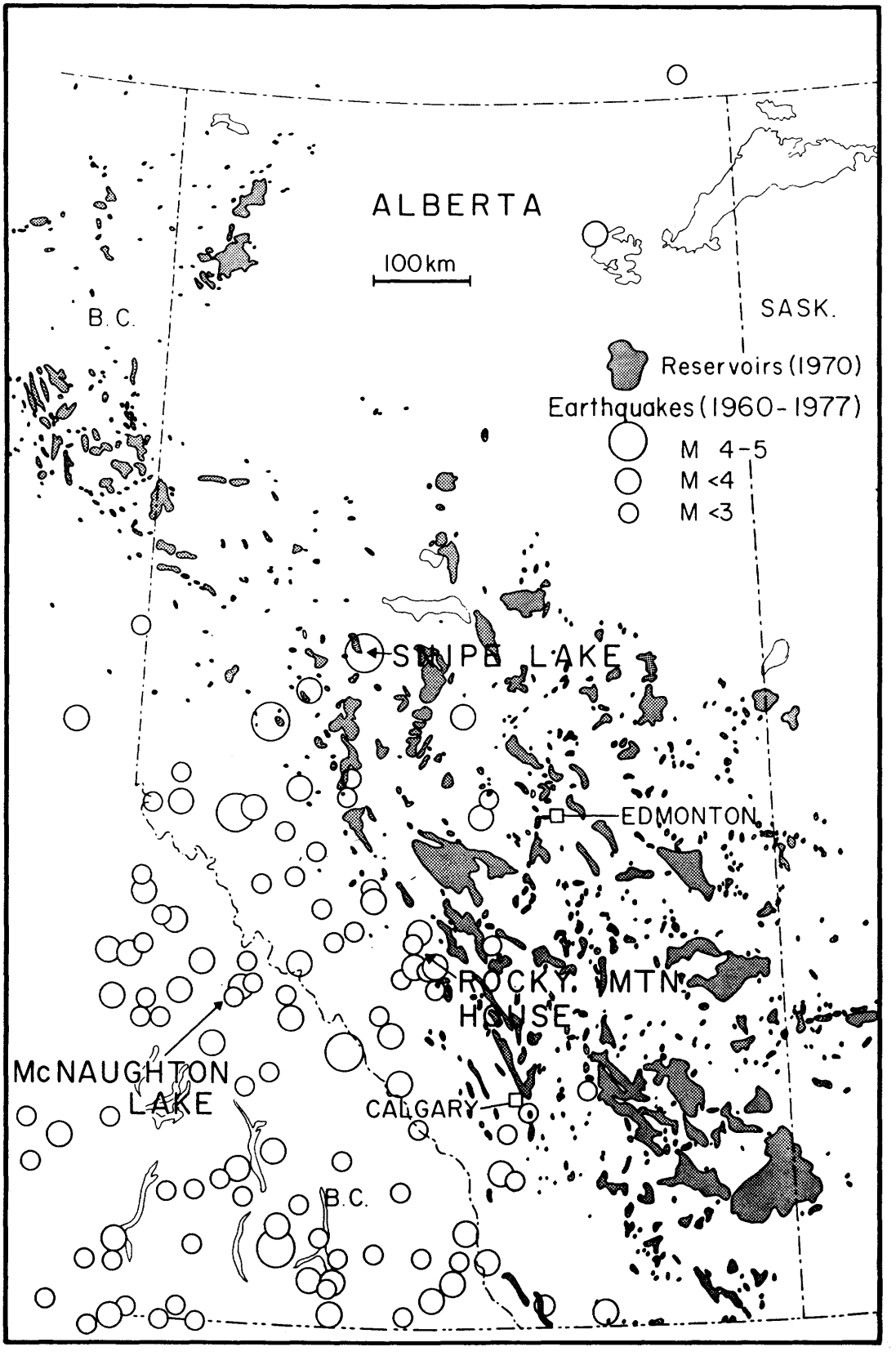

Figure A15. Earthquakes in Alberta, Canada (1960–77), and locations of active oil and gas reservoirs (shaded areas). Reprinted from Wetmiller (1986) and published with permission.

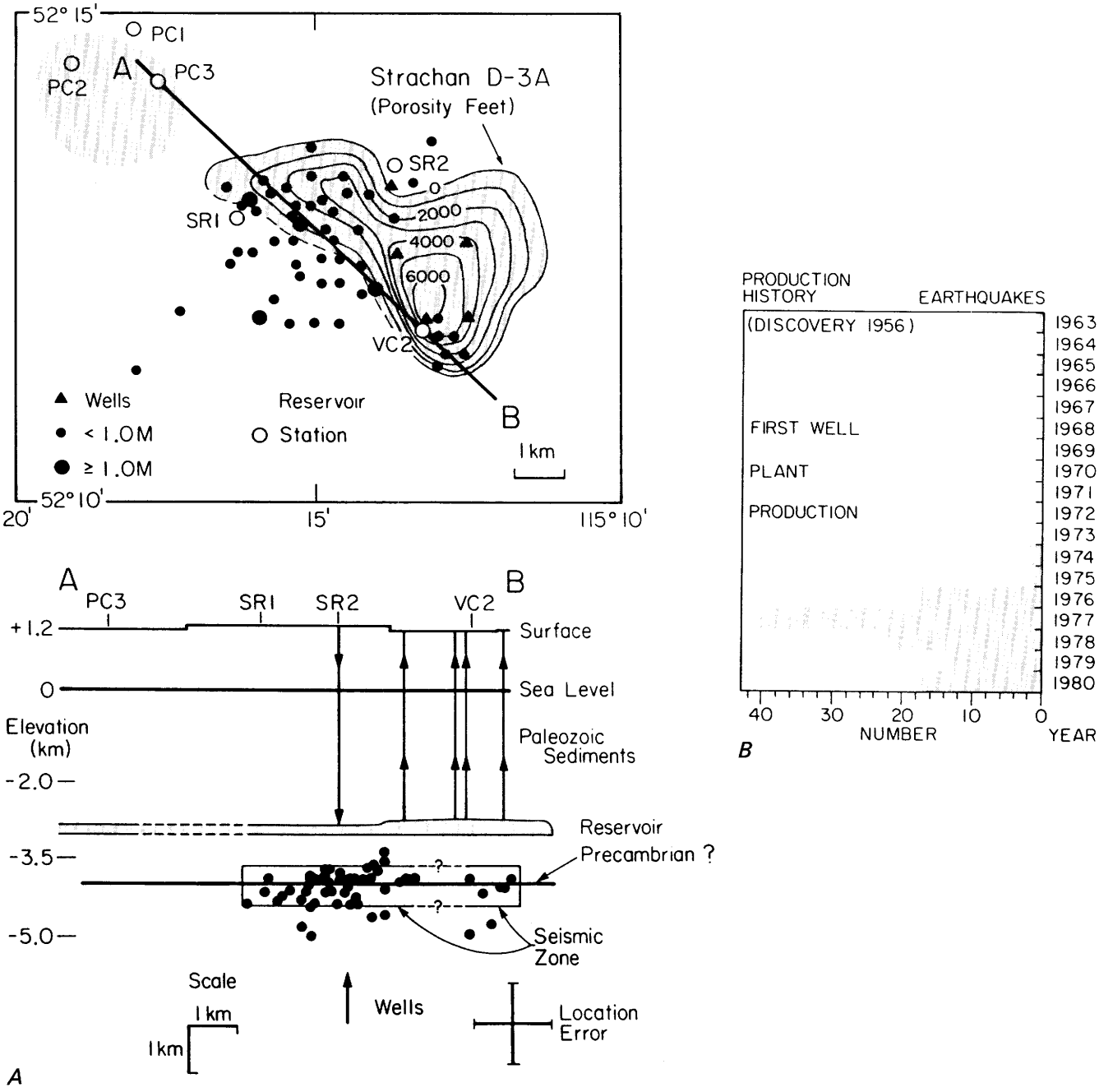

Figure A16. Locations of microearthquakes, production history, and earthquake activity, Strachan D-3A reservoir and gas field, western Alberta, Canada. *A*, Detail of the distribution in area and cross section of the microearthquakes (solid circles) located by the 1980 field survey within the reservoir and main production wells (solid triangles). *B*, Production history and annual earthquake activity at the field. Reprinted from Wetmiller (1986) and published with permission.

natural and that solution mining is not a necessary condition for the occurrence of earthquake activity.

Recent Seismicity and Injection Operations in Northeastern Ohio

On January 31, 1986, at 11:46 EST, an earthquake of magnitude 5.0 occurred about 40 km east of Cleveland, Ohio, and about 17 km south of the Perry Nuclear Powerplant (fig. A18). Within hours, a dense network of portable stations was installed to monitor possible aftershock activity (Wesson and Nicholson, 1986). As of April 15, only 13 aftershocks were detected, 6 of which occurred within the first 8 d. At the time of the mainshock, three deep injection wells for the disposal of hazardous and nonhazardous waste were operating within 15 km of the epicentral region and,

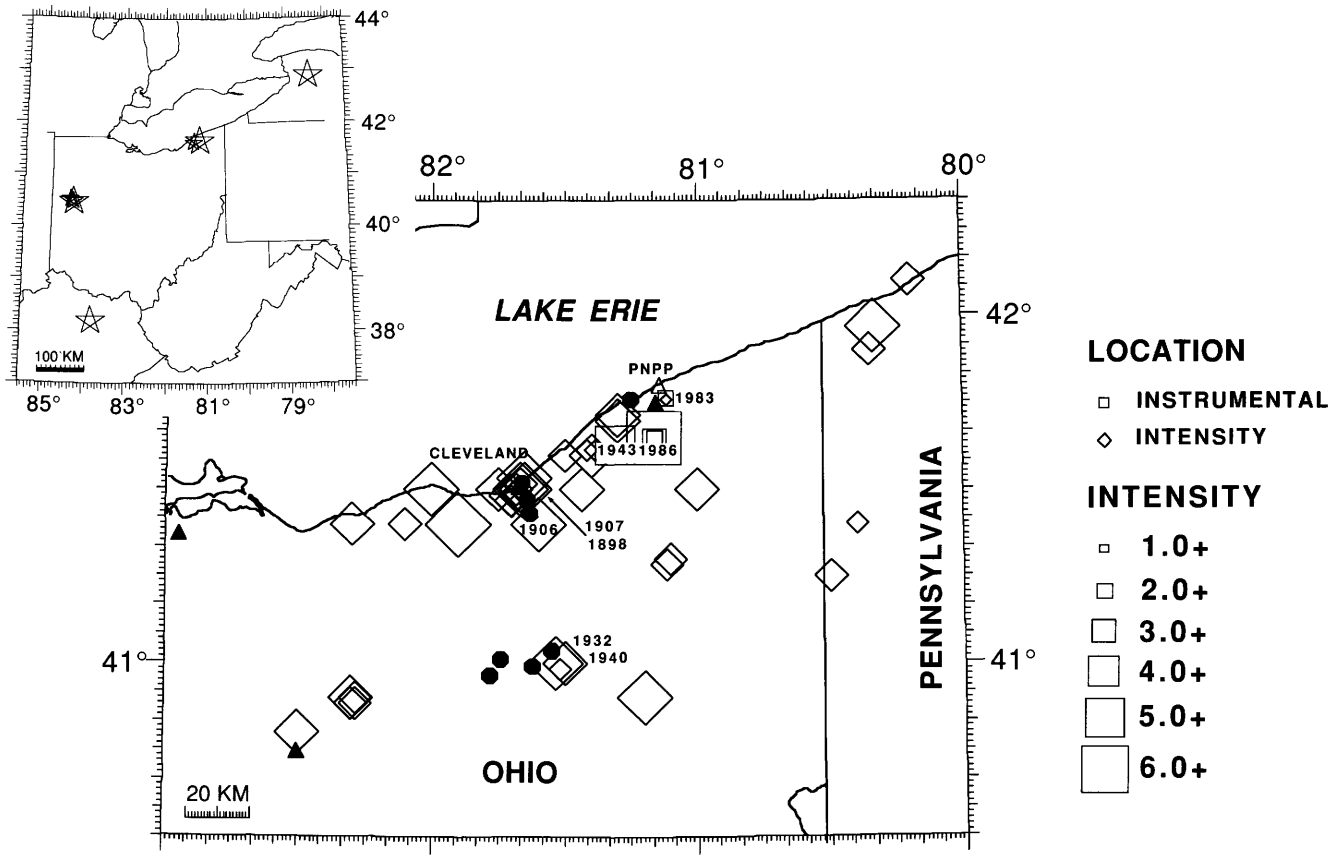

Figure A17. Locations of the Perry Nuclear Powerplant, the January 31, 1986, earthquake, and the significant historical seismicity and dates of occurrence, northeastern Ohio. Most of the seismicity precedes initiation of injection activities. PNPP, powerplant; large square, January 31 earthquake; solid octagons, sites of solution salt mining, typically in operation from 1900 to 1940; solid triangles, deep waste injection wells drilled from 1968 to 1971; diamonds, poorly located earthquakes, typically based on felt reports; squares, instrumentally located earthquakes; and stars, recent regional $M \geq 4.5$ earthquakes (from Nicholson and others, 1988).

since 1975, have been responsible for the injection of nearly 1.2 billion L of fluid at a nominal depth of 1.8 km. Injection pressures at typical injection rates of 320 L/min reached a maximum of 112 bars THP.

Although the distance between the major injection wells and the January 31 earthquake (12 km) is greater than the corresponding distances in either the Denver or the Dale earthquakes, the total volume of fluid injected and the injection pressures involved are proportionately greater. Estimates of stress inferred from commercial hydrofracturing measurements suggest that the state of stress in northeastern Ohio is close to the theoretical threshold for failure along favorably oriented preexisting fractures, as determined by the Mohr-Coulomb failure criterion (fig. 5). The maximum horizontal compressive stress is greater than the vertical stress of 460 bars, the minimum horizontal stress is about 300 bars, and, before injection, the initial formation pore pressure was measured at about 200 bars (Wesson and Nicholson, 1986). This implies that, at a nominal injection pressure of 110 bars, the zone immediately surrounding the well bottom would be in a critical stress state for favorably oriented fractures that have cohesive strengths of as much as 40 bars and a coefficient of friction (μ) of 0.6 (fig. 5). Calculations of the pressure effect in the epicentral region based on modeling the fluid flow away from the wells and comparison with the history of pressure increase at the wells with time and continued pumping suggest that a radial flow model (instead of the narrow confined aquifer implicated in the Denver case) is the most appropriate. This model implies that, as a result of fluid injection since 1975, the expected fluid pressure increase in the epicentral region of the 1986 earthquakes would have been only a few bars. Since 1983, however, several small earthquakes have occurred at shallow depths and within less than 5 km from the wells (fig. A18)—where the calculated pressure increase as a result of fluid injection is about 15 bars or greater (Nicholson and others, 1988).

The increased depth and distance from the wells to the 1986 mainshock epicenter and its aftershocks, the lack of large numbers of small earthquakes typical of many induced sequences, the history of small to moderate earthquakes in the region before the initiation of injection, and

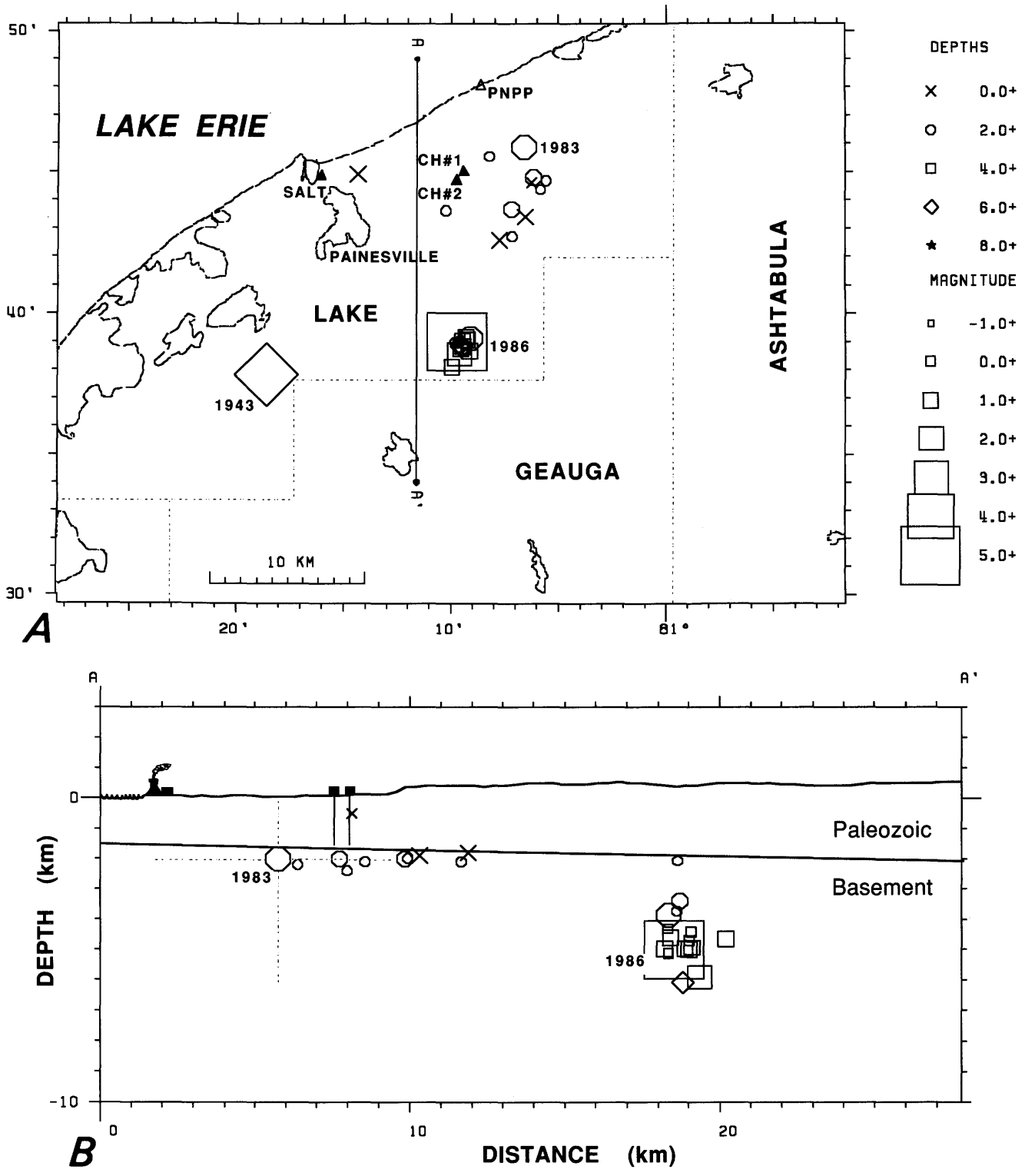

Figure A18. Deep injection wells and earthquake epicenters, Lake County, Ohio. *A*, Location of deep injection wells and earthquake epicenters through early 1987. Large uncertainties in location are associated with the 1943 and the 1983 earthquake epicenters. Solid triangles, injection wells; CH#1 and CH#2, deep waste-disposal wells; SALT, Painesville brine well; PNPP, Perry Nuclear Powerplant. *B*, Vertical cross section, no exaggeration, along the line *A–A'* shown in *A* (from Nicholson and others, 1988).

the attenuation of the pressure field with distance from the injection wells all argue for a "natural" origin for the January 31 earthquake. In contrast, the proximity to failure conditions at the bottom of the wells and the spatial association of at least a few small events suggest that triggering by well activities can not be precluded.

Ashtabula, Ohio

Confirmation that deep well fluid injection in northeastern Ohio has the potential for triggering earthquake activity was demonstrated dramatically on July 13, 1987. A M 3.6 earthquake occurred near Lake Erie, just east of Ashtabula and about 40 km northeast of the location of the January 31, 1986, earthquake (fig. A19). Except for one earthquake in 1857, no other earthquakes were known to have occurred within 30 km of Ashtabula. In the weeks following the mainshock, an unusually large number of aftershocks (more than 70 events) were generated (Armbruster and others, 1987). All the well located earthquakes were clustered in a narrow east-west-striking vertical plane about 1.5 km long that extended from about 1.6 to 3.2 km in depth (fig. A20; Armbruster and others, 1987; Seeber and others, 1988). The earthquakes occurred less than 1 km from the bottom of a hazardous-waste-disposal well that had been in operation only since July 1986. The injection well is about 1.8 km deep and operates at a nearly uniform flow rate of 114 L/min and at an injection pressure of about 100 bars THP (Ernie Rotering, Ohio EPA, written commun., 1987). Between July 1986 and June 1987, well operations were responsible for nearly 62 million L of hazardous fluid waste being injected into the basal sandstone layer (the Mount Simon Formation). The proximity to the active injection well and the temporal correlation of the seismicity with the initiation of well activities (about a year earlier) strongly suggests that the Ashtabula earthquakes of July 1987 were induced (Seeber and others, 1988).

Los Angeles Basin, California

The massive withdrawal of oil from one of the largest fields in the Los Angeles Basin, the Wilmington oil field (fig. A21), resulted in significant subsidence within the city limits of Long Beach. Up to 8.8 m of surface subsidence was observed over an elliptically shaped area between 1928 and 1970 (Mayuga, 1970). This rapid subsidence, which reached a maximum rate of 71 centimeters per year in 1951 9 mo after peak oil production (fig. A22), resulted in several damaging earthquakes, specifically in the years 1947, 1949, 1951, 1954, 1955, and 1961. In all cases, the earthquakes were unusually shallow (approximately 500 m deep) and generated high intensities for their size. The largest earthquake occurred on November 17, 1949, and caused nearly 200 wells to go off production, many of them permanently (Richter, 1958). Damage was estimated to be in excess of $9 million. The area affected equaled over 5.7 square kilometers (km^2) and involved measured displacements of 20 centimeters. This would correspond to an earthquake that had a moment magnitude of 4.7 and is consistent with a magnitude of 5.1 estimated from the

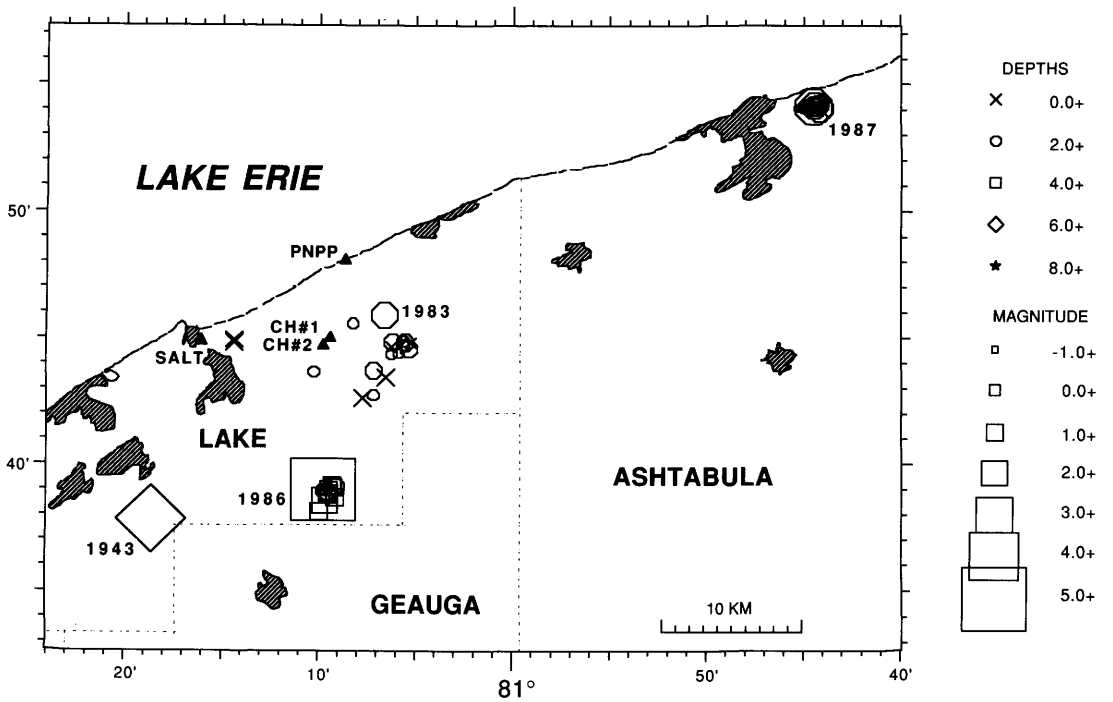

Figure A19. Location of the 1987 induced earthquake sequence in northeastern Ohio near Ashtabula relative to the 1986 earthquakes in Lake County.

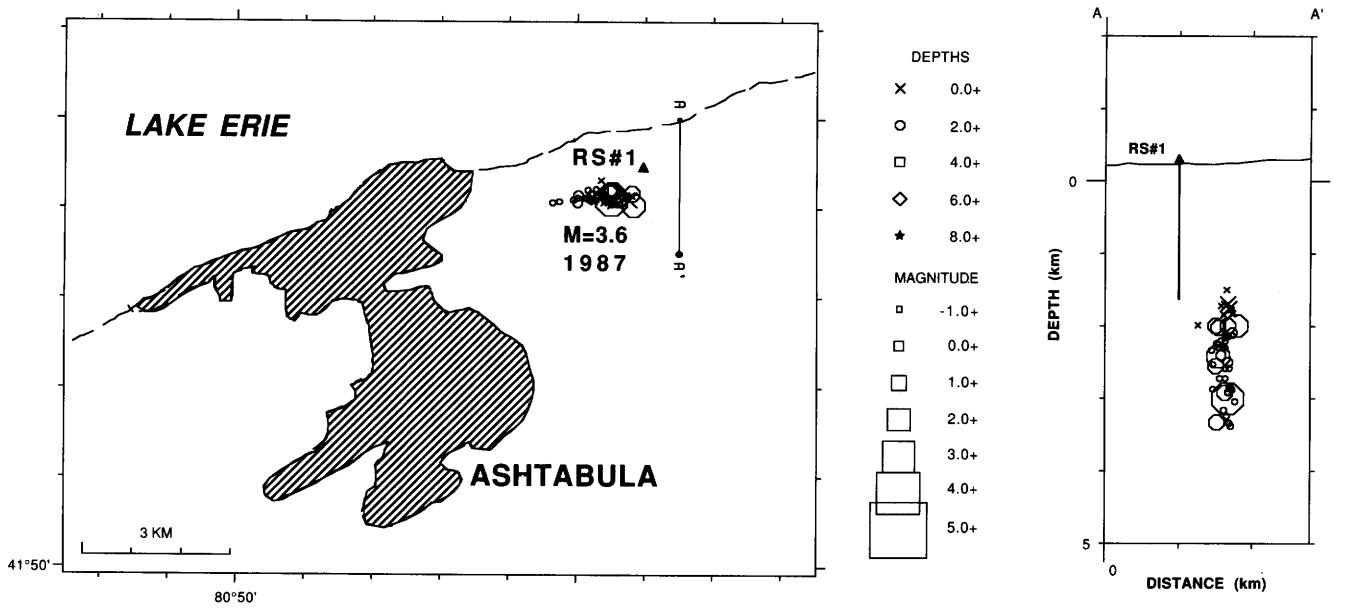

Figure A20. The 1987 Ashtabula, Ohio, earthquake hypocenters relative to the location of a nearby active, high-pressure, waste-disposal injection well (triangle, RS#1). Earthquake data provided courtesy of John Armbruster (Lamont-Doherty Geological Observatory, written commun., 1987).

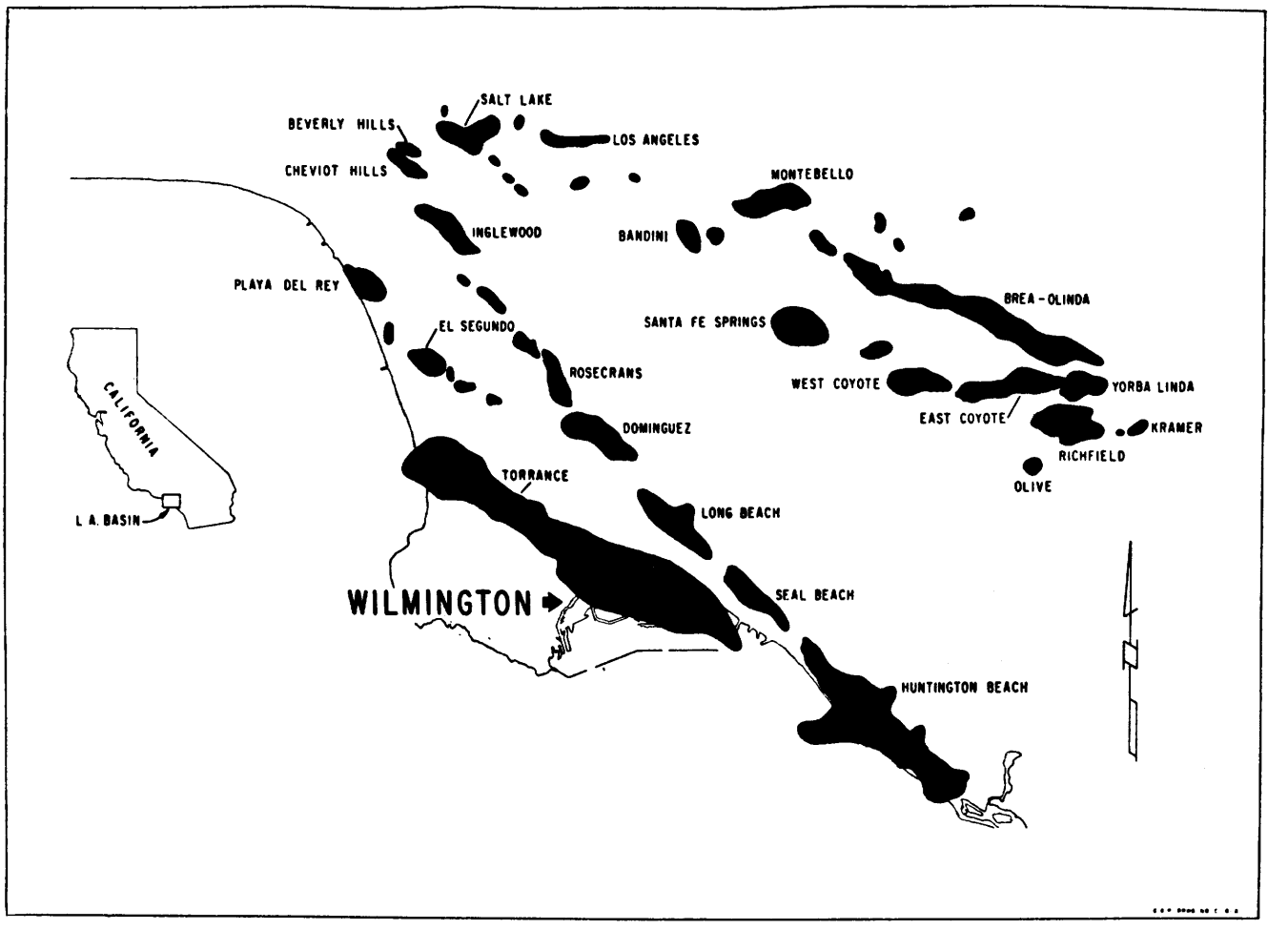

Figure A21. Distribution of the oil fields (shaded areas) in the Los Angeles Basin, Calif. (from Mayuga, 1970).

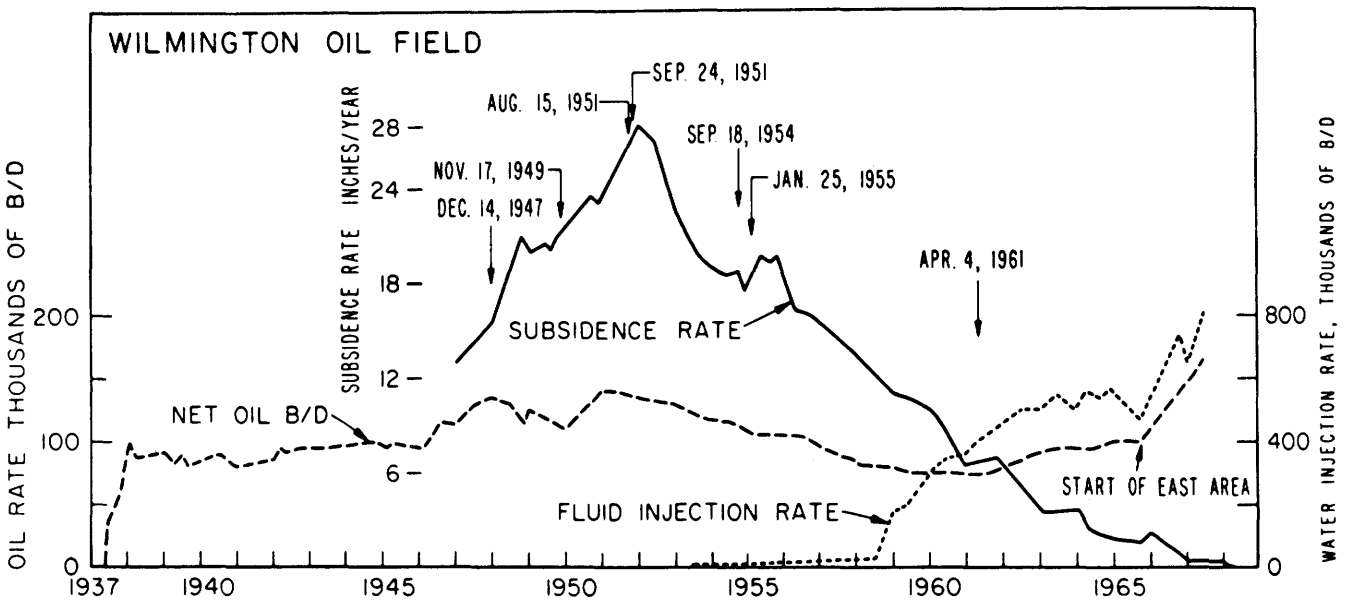

Figure A22. Subsidence rate in the center of the Wilmington oil field, California, compared with oil production and water injection rates. Arrows, major damaging earthquakes. Reprinted from Kovach (1974) and published with permission.

unusually well developed surface waves generated by the event (Kovach, 1974).

Water flooding of the field and adjacent areas was initiated in 1954 in an attempt to halt subsidence and to enhance the secondary recovery of oil. Teng and others (1973) reported on the seismic activity associated with 14 oil fields operating within the Los Angeles Basin where water-flooding operations were taking place. As of 1970, total fluid injection was 250,000 million L at depths that ranged from 910 to 1,520 m.

Although much of the seismicity in the area is natural and occurs predominantly at depths as deep as 16 km along the Newport-Inglewood Fault (Hauksson, 1987), seismic activity during 1971 appeared to correlate, at least in part, with injection volumes from nearby wells (fig. A23; Teng and others, 1973). However, many of the earthquakes detected were small ($M<3.2$) and occurred at depths of 5 km or more, which made it difficult to distinguish them from the natural background seismicity. Subsequent injection operations have stabilized to the point where fluid injection nearly equals fluid withdrawal and little, if any, seismic activity can be directly attributable to injection well operations (Egill Hauksson, University of Southern California, oral commun., 1986).

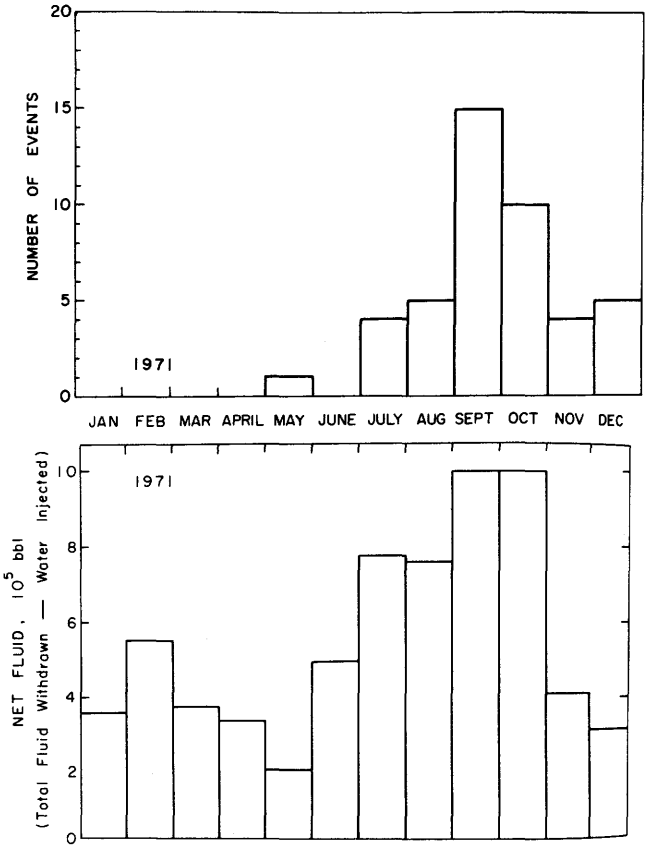

Figure A23. Seismicity and volumes of fluid injected along the Newport-Inglewood Fault, Los Angeles County, Calif., in 1971. Reprinted from Teng and others (1973) and published with permission.

Northern Texas Panhandle and East Texas

In 1984, a small network of monitoring stations was operated under contract to the Office of Nuclear Waste Isolation, U.S. Department of Energy, in the Palo Duro Basin of the northern Texas Panhandle (Stone and Webster

Engineering, written commun., 1985). Between April 27 and October 5, 1984, 34 small earthquakes were detected near the Mansfield station in eastern Oldham County (Davis, 1985). The largest of these events occurred on May 21 and had a local magnitude of 3.1 (pl. 1). Before this episode of seismicity, only one other earthquake was known to have occurred in this part of Texas—a M 3.4 event on April 3, 1983 (Davis, 1985). Several small oil fields had been discovered recently in eastern Oldham County and were producing at the time both earthquakes occurred. In particular, the Lambert No. 1 field, located about 7 km from the Mansfield station, began injection of water for secondary recovery in September 1979 at an average rate of 39,750 liters per day. Definitive correlation of the seismicity with oil field operations, however, was not possible because of the poor earthquake location capability of the wide-aperture network.

In East Texas, a sequence of four earthquakes occurred near Gladewater on March 19, 1957. The largest of these events had an estimated magnitude of 4.3 and generated a felt area of 47,000 km^2 (Nuttli and Herrmann, 1978). Little else is known about this sequence; however, Docekal (1970) recognized that the earthquake epicenters corresponded to an area of active oil production located in East Texas on the western flank of the Sabine Uplift and speculated on whether the earthquakes may have been induced. Water flooding to enhance production had been in effect in at least one field since 1942 at injection pressures of greater than 100 bars (Texas Railroad Commission, 1971). More recently, commercial stimulation of the Cotton Valley tight gas sands, which also are located in East Texas, triggered microearthquake activity at a depth of 2.6 to 3.7 km (Lacy, 1985).

Oklahoma

On October 30, 1956, a M 4.2 to 4.7 earthquake occurred near Catoosa, about 20 km east of Tulsa in northeastern Oklahoma (fig. A24; Nuttli and Herrmann, 1978). This event generated a relatively high maximum intensity (MM VII) for its size and felt area, which suggested a shallow focal depth (Nuttli and Zollweg, 1974). The maximum intensity reported for this event was based on damage to the Coshow No. 2 oil and gas well, which was active at the time of the earthquake (Brazee and Cloud, 1958). The well was forced to shut down because apparent displacements in the producing formation, as a result of the earthquake, disrupted the wellbore. Producing wells within the Catoosa District gas field were operational by 1941, and water flooding to enhance secondary recovery was conducted at one time, but details of the operation are not available (Robert McCoy, Oklahoma Corporation Commission, oral commun., 1987). In March 1960, two smaller earthquakes were felt in the same general area (fig. A24; Luza and others, 1978) shortly after an industrial-waste-disposal well became operational in January (Johnson and others, 1980). Since then, however, no significant seismic activity has been detected in the region, even though gas-production and waste-disposal operations have continued and sensitive seismic monitoring equipment has been operating in nearby Tulsa since 1961 (Luza and Lawson, 1983).

In Carter and Love Counties, southern Oklahoma, 400 earthquakes were detected from May 1, 1977, to December 31, 1978 (Luza and Lawson, 1980). Most of these events were too small to locate (fig. A24); however, of the few that were, nearly all occurred in areas of active oil and gas production, and all occurred at relatively shallow focal depths. On June 23, 1978, commercial stimulation of a 3,050-m-deep well near Wilson triggered 70 earthquakes in 6.2 hours (hr) (Luza and Lawson, 1980).

A similar situation occurred in May 1979, when a well located about 1 km from the Wilson monitoring station (fig. A24) was stimulated over a 4-d period in a massive hydraulic fracturing program. Three different formations were eventually hydrofractured on three separate occasions at average depths of 3.7, 3.4, and 3.0 km (J.E. Lawson, Jr., Oklahoma Geophysical Observatory, written commun., 1987). Maximum injection pressures reached 277 bars THP, and the instantaneous shut-in pressure (ISIP) at the greatest depth was measured to be 186 bars THP. The well was fractured from the bottom up. The first fracturing episode was followed about 20 hr later by about 50 earthquakes over the next 4 hr; the second fracture (at a depth of 3.4 km) was followed immediately by about 40 earthquakes in the subsequent 2 hr; and no increase in activity was noticed following the third fracture (J.E. Lawson, Jr., Oklahoma Geophysical Observatory, written commun., 1987). The largest earthquake in any of the sequences had a magnitude of 1.9; two of the earthquakes were felt. The largest total volume of fluid injected during any one procedure amounted to 5.7×10^4 L at an average injection rate of 230 L/min.

Oil has been produced in this same area since 1953. Earthquakes in the southern portion of the State have been detected since 1974, and earthquakes in Love County have been detected ever since a local monitoring station was installed in 1977 (fig. A24; Luza and others, 1978). Secondary recovery operations in Love County began in May 1965 (Tim Baker, Oklahoma Corporation Commission, oral commun., 1987). It must be noted, however, that similar commercial hydrofracturing operations in other nearby wells did not trigger noticeable increases in seismic activity, as did the massive hydraulic fracturing program in 1978 and 1979.

Whether additional earthquakes that have occurred in Oklahoma (fig. A24) are associated with oil and gas production is difficult to assess. Over 3,100 oil and gas fields exist within the State (most of which are still active), and nearly every felt or located earthquake has been found

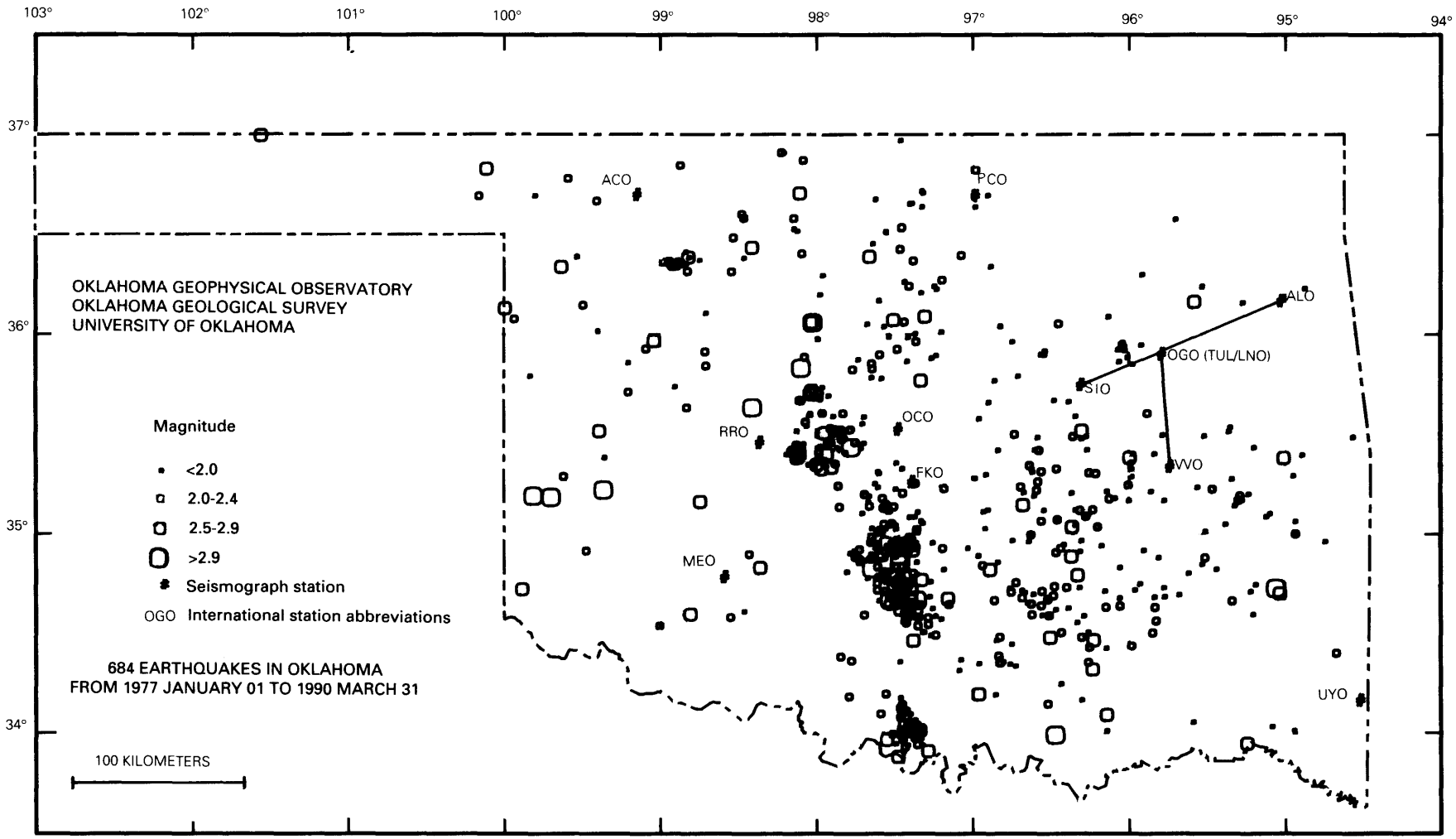

Figure A24. Earthquake epicenters in Oklahoma (684) from January 1, 1977, to March 31, 1990) (J.E. Lawson, Jr., Oklahoma Geophysical Observatory, written commun., 1990).

to occur in close proximity to at least one of them. The converse, however, is not true. Since the early 1900's, oil and gas production has been active in large areas of Oklahoma that have yet to show any detectable signs of seismic activity. Furthermore, many of the regions without earthquakes are actively water flooding to enhance secondary recovery, while many of the seismically active areas are not. Some of these later cases, where seismicity is occurring in areas without fluid injection, may be related to subsidence from massive oil and gas withdrawal, as in the cases of the Flashing gas field in southern Texas or the War-Wink oil and gas field in West Texas. A possible example is a series of nine earthquakes that occurred between October 12 and 18, 1968. All were concentrated in the vicinity of the East Durant gas field, Bryant County (fig. A24), which had been in production since 1958. The largest earthquake in the series was a magnitude 3.5 and generated a maximum intensity of MM VI at the epicenter (Luza and others, 1978).

Gulf Coast Region—Louisiana and Mississippi

In 1978, a magnitude 3.5 earthquake was felt strongly in Melvin, Ala. (pl. 1). Portable monitoring equipment was installed shortly after the earthquake, but only one small aftershock was detected. On the basis of the hypocenter determined for this one event, both earthquakes appeared to be at a focal depth of about 1 km and within 1 to 2 km of the Hunt oil field, which is located just across the State border in Mississippi (J.E. Zollweg, U.S. Geological Survey, oral commun., 1978, 1987). Four earthquakes of similar magnitudes (3.0–3.6) had been detected in the same area since 1976. Although no injection procedures were apparently in operation at the time of the 1978 earthquake, water flooding to enhance extraction had occurred previously.

A similar situation was noted in 1983, when a M 3.8 earthquake was detected in southwestern Louisiana near Lake Charles (pl. 1). Oil and gas operations had been active in the region for several decades, as well as injection activities from a nearby waste-disposal well, but lack of station coverage precluded accurate determination of the earthquake's location and focal depth and so made any direct correlation with particular well operations unresolvable. However, a small microearthquake network, which was installed in 1980 to monitor potential seismicity associated with a geothermal energy project located farther south, has continued to detect a low level of seismic activity in the Lake Charles region, presumably associated with the 1983 earthquake (Stevenson, 1985).

APPENDIX B—SUMMARY OF RESERVOIR-INDUCED SEISMICITY

The phenomenon of seismicity induced by the impoundment of reservoirs is more widespread and better documented than that of injection-induced seismicity; however, the mechanism of reservoir-induced seismicity is more complicated and not as well understood (Gupta and Rastogi, 1976; Simpson, 1986a). Reservoir-induced earthquakes were first described in association with the filling of Lake Mead, Nev. (Carder, 1945), but it was not until the late 1960's, when earthquakes larger than M 5.5 occurred at four major reservoirs (Hsinfengkiang, China, Kremasta, Greece, Lake Kariba, Rhodesia, and Koyna Reservoir, India), that sufficient concern was raised to warrant investigation of the mechanism controlling reservoir-induced seismicity. The largest of the earthquakes believed to have been induced by the impoundment of a reservoir occurred at Koyna Reservoir in 1967 and had a magnitude of 6.5. It caused over 200 deaths, 1,500 injuries, and considerable damage to the nearby town and the dam. Thus, the hazard associated with reservoir-induced seismicity is significant.

Unlike injection operations that only affect pore pressure, the presence of a large reservoir modifies the environment in several ways. First, the large mass of the reservoir represents a large increase in the imposed load, which increases the *in situ* elastic stresses. The load of water also affects the pore pressure directly (by the infiltration of the reservoir water and subsequent raising of the water table) and indirectly (through the closure of water-saturated pores and fractures in the rock beneath the reservoir load). This coupling between the elastic and the fluid effects in the rock, as well as the poorly understood response of inhomogeneities in material and hydrologic properties of the rock to changes in stress induced by the reservoir load, make modeling the impact of reservoirs much more difficult than for cases of fluid injection (Simpson, 1986a). Nevertheless, there are enough similarities between injection- and reservoir-induced earthquakes that they both provide a number of constraints on the mechanism of triggered seismicity.

Although the magnitude of the net pore pressure change produced by reservoir impoundment is often considerably less than at many fluid injection sites, the larger physical dimensions of the reservoirs allows their influence to extend over much broader areas. There are, however, a number of cases of reservoir-induced seismicity in which the load effect from the reservoir is believed to be minimal. These cases include some of the largest earthquakes associated with reservoir impoundment and are usually characterized by a large distance between the earthquake and the reservoir, as well as a long time interval between impoundment and the earthquake occurrence; for example, 1975 M_s 5.7 Oroville, Calif., and 1981 m_b 5.3 Aswan, Egypt.

If these cases do indeed represent seismicity induced by the reservoir, then the triggering mechanism is believed to be similar in many respects to that of injection-induced seismicity. In these cases, the mainshocks occurred along major mapped surface faults that intersected the reservoir. Thus, increased fluid pressure as a result of impoundment may have been able to migrate out along the fault zones, which reduced effective stress levels and thereby enhanced the probability for failure in an earthquake. Because the changes in pore pressure as a result of impoundment are believed to be relatively small at the increased distances involved in these cases, this suggests that the states of stress in those areas were already near critical levels for failure prior to impoundment (Simpson, 1986a).

A particularly good example of reservoir-induced seismicity occurred at the Nurek Reservoir, Tadjikistan, Soviet Central Asia (fig. B1; Simpson and Negmatullaev, 1981). In this case, the water height and the rate of change in water height proved to be critical parameters (fig. B2). At Nurek and at several other similar sites of reservoir-induced seismicity, changes in water height of only a few meters, which correspond to pressure changes of less than 1 bar, have triggered swarms of small earthquakes (fig. B2). This observation suggests that seismicity can be triggered on faults that otherwise remain stable, even at stress levels extremely close to failure (Leith and Simpson, 1986). In many cases of reservoir-induced seismicity, an accurate assessment of the magnitude of the critical stress change necessary for failure is difficult to determine because major heterogeneities in elastic and hydrologic properties of the rock may tend to concentrate or amplify changes in pore pressure caused by compaction and the redistribution of pore fluids in response to changes in water level (Simpson, 1986b). In the case of fluid injection, however, the total mass of the fluid involved is relatively small, and so the need to consider the coupled interaction among applied load, elastic stresses, and pore pressure is generally absent.

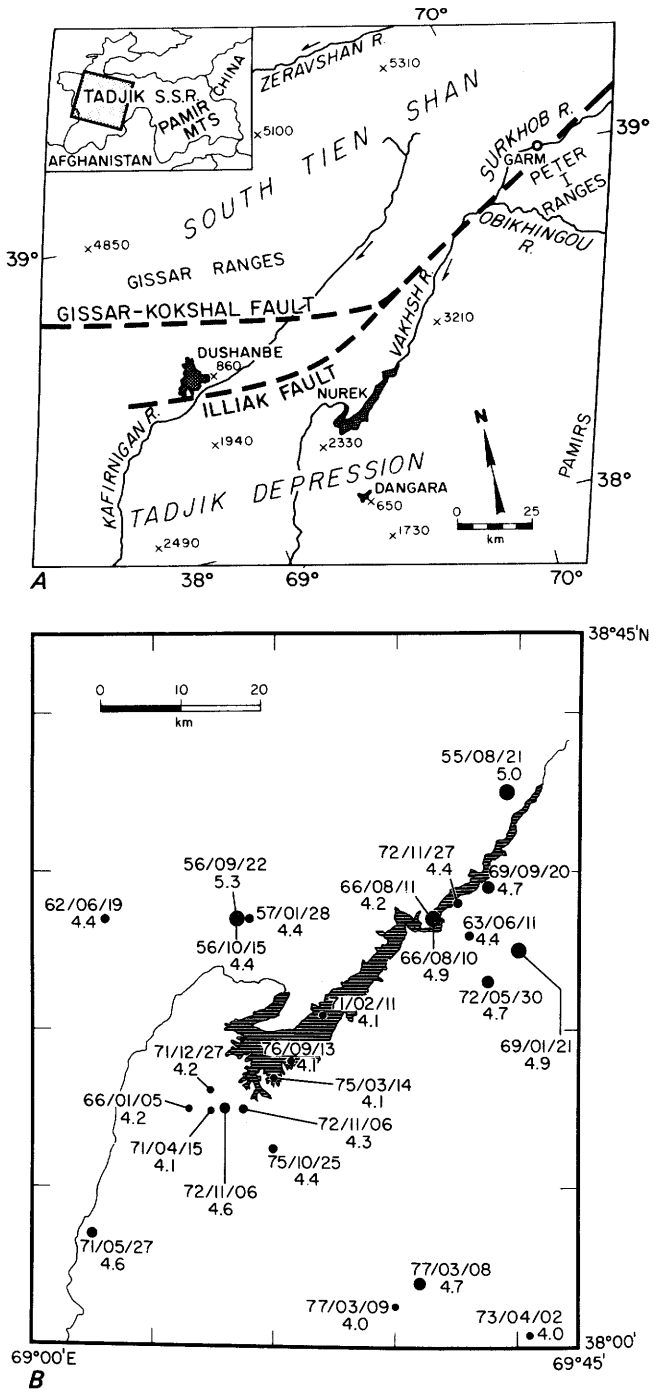

Figure B1. Location and historical seismicity, Nurek Reservoir, Tadjikistan, Soviet Central Asia. *A*, Location map of the reservoir. *B*, Historical seismicity in the vicinity of the dam. Reprinted from Simpson and Negmatullaev (1981) and published with permission.

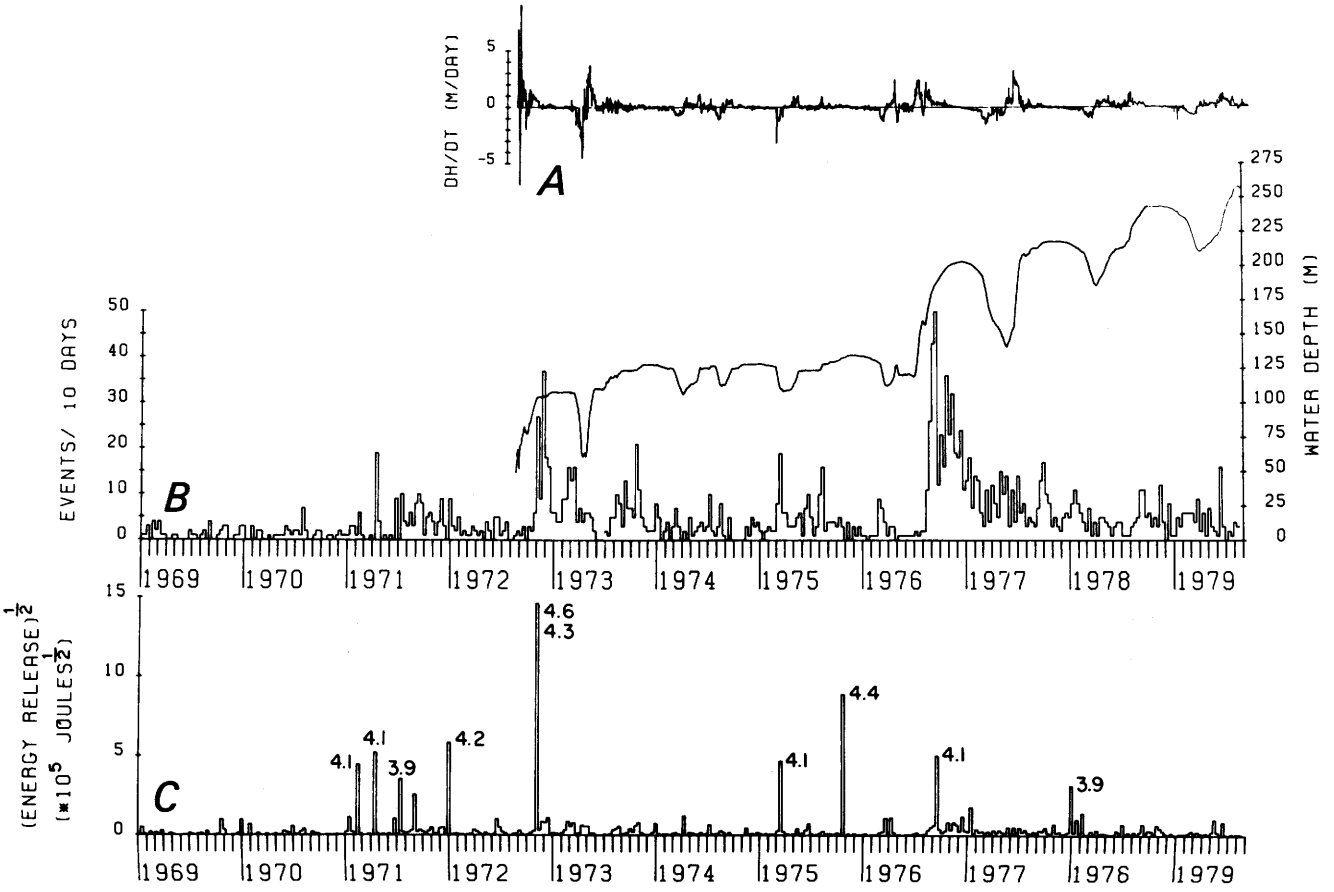

Figure B2. Temporal variations in seismicity, seismic energy release, water height, and daily changes in water level (DH/DT), Nurek Reservoir, Tadjikistan, Soviet Central Asia. Reprinted from Simpson and Negmatullaev (1981) and published with permission.

APPENDIX C—MODIFIED MERCALLI INTENSITY SCALE

This scale measures the intensity of ground shaking as determined from observations of the effects of an earthquake on people, structures, and the Earth's surface. This scale assigns to an earthquake event a Roman numeral from I to XII.

I Not felt by people, except rarely under especially favorable circumstances.

II Felt indoors only by persons at rest, especially on upper floors. Some hanging objects may swing.

III Felt indoors by several. Hanging objects may swing slightly. Vibration like passing of light trucks. Duration estimated. May not be recognized as an earthquake.

IV Felt indoors by many, outdoors by few. Hanging objects swing. Vibration like passing of heavy trucks or sensation of a jolt like a heavy ball striking the walls. Standing automobiles rock. Windows, dishes, doors rattle. Wooden walls and frames may creak.

V Felt indoors and outdoors by nearly everyone; direction estimated. Sleepers awakened. Liquids disturbed, some spilled. Small unstable objects displaced or upset; some dishes and glassware broken. Doors swing; shutters, pictures move. Pendulum clocks stop, start, change rate. Swaying of tall trees and poles sometimes noticed.

VI Felt by all. Damage slight. Many frightened and run outdoors. Persons walk unsteadily. Windows, dishes, glassware broken. Knickknacks and books fall off shelves; pictures off walls. Furniture moved or overturned. Weak plaster and masonry cracked.

VII Difficult to stand. Damage negligible in buildings of good design and construction; slight to moderate in well-built buildings; considerable in badly designed or poorly built buildings. Noticed by drivers of automobiles. Hanging objects quiver. Furniture broken. Weak chimneys broken. Damage to masonry; fall of plaster, loose bricks, stones, tiles, and unbraced parapets. Small slides and caving in along sand or gravel banks. Large bells ring.

VIII People frightened. Damage slight in specially designed structures; considerable in ordinary substantial buildings, partial collapse; great in poorly built structures. Steering of automobiles affected. Damage to or partial collapse of some masonry and stucco. Failure of some chimneys, factory stacks, monuments, towers, elevated tanks. Frame houses moved on foundations if not bolted down; loose panel walls thrown out. Decayed pilings broken off. Branches broken from trees. Changes in flow or temperature of springs and wells. Cracks in wet ground and on steep slopes.

IX General panic. Damage considerable in specially designed structures; great in substantial buildings, with some collapse. General damage to foundations; frame structures, if not bolted, shifted off foundations and thrown out of plumb. Serious damage to reservoirs. Underground pipes broken. Conspicuous crack in ground; liquefaction.

X Most masonry and frame structures destroyed with their foundations. Some well-built wooden structures and bridges destroyed. Serious damage to dams, dikes, embankments. Landslides on river banks and steep slopes considerable. Water splashed onto banks of canals, rivers, lakes. Sand and mud shifted horizontally on beaches and flat land. Rails bent slightly.

XI Few, if any, masonry structures remain standing. Bridges destroyed. Broad fissures in ground; earth slumps and landslides widespread. Underground pipelines completely out of service. Rails bent greatly.

XII Damage nearly total. Waves seen on ground surfaces. Large rock masses displaced. Lines of sight and level distorted. Objects thrown upward into the air.

APPENDIX D—GLOSSARY

[Terms set in bold type are defined elsewhere in the glossary. Sources: Ziony (1985), Bates and Jackson (1987), and Nance (1989)]

Acceleration. The time rate of change of velocity of a reference point during an **earthquake**. Commonly expressed in percentage of gravity (g) equal to 980 centimeters per square second.

Active fault. A **fault** that is considered likely to undergo renewed movement within a period of concern to humans. *Also called* capable fault.

Aftershock. An **earthquake** or tremor that follows a larger earthquake or mainshock and originates at or near the **focus** of the larger earthquake. Generally, **major earthquakes** are followed by many aftershocks, which decrease in frequency and magnitude with time. Such a series of tremors may last many days for small earthquakes or many months for large ones.

Amplification. An increase in **seismic** signal **amplitude** as waves propagate through different earth materials.

Amplitude. Zero-to-peak value of any wavelike disturbance; corresponds to half the height of the crest of a wave above the adjacent trough.

Aquifer. A geological subsurface formation containing and transmitting ground water, usually restricted to a body of rock that is sufficiently permeable to yield useful quantities of water to wells or springs.

Aseismic. (1) Not associated with an **earthquake** or earthquake activity. (2) An area that is not subject to earthquakes.

Attenuation. A decrease in **seismic** signal **amplitude** as waves propagate from the seismic source. Attenuation is caused by geometrical spreading of **seismic wave** energy and by the absorption and scattering of seismic energy in different earth materials.

Basement rock. Relatively hard, undifferentiated solid rock that underlies commonly softer sedimentary rock, unconsolidated sediment, alluvium, or soil. *Also called* bedrock.

Body wave. A **seismic wave** that travels through the interior or body of the Earth and is not related or confined to a specific boundary surface. **Primary** and **secondary waves** are examples of body waves.

Bottom-hole pressure. The fluid pressure measured in the bottom of a well. It consists of the wellhead pressure (**top-hole pressure**) plus a term to account for the weight of the column of fluid in the well. The abbreviation is BHP.

Breakdown pressure. The hydraulic pressure needed to **fracture** the intact rock of a borehole wall. The symbol is P_b. *Also called* fracture pressure.

Coefficient of friction. Constant of proportionality for that part of the shear strength of a rock or other intact solid that depends on the **normal stress** applied across the potential shear surface or **fracture**. The symbol is μ.

Cohesion. The **shear** strength of a rock not related to internal friction; that is, dependent on applied **normal stress**. The symbol is τ_0. *Also called* inherent shear strength.

Compressibility. The relative change of volume with pressure on the **aquifer** matrix. Reciprocal of the elastic bulk modulus of the medium. For solids, the symbol is α; for fluids, the symbol is β.

Core-induced fractures. Vertical fractures found in oriented bottom-hole cores caused by the downcutting drill bit. *Also called* petal-centerline fractures.

Creep. Slow, more or less continuous movement that may occur either along faults owing to ongoing **tectonic** deformation or along slopes owing to gravitational forces.

Crust. The outermost major layer of the Earth, ranging from about 9 to 60 km thick worldwide; characterized by **primary-wave** velocities of less than 8 kilometers per second (km/s).

Density. Mass per unit volume. The symbol is ρ.

Deviatoric stress. The difference in magnitude between the maximum (σ_1) and minimum (σ_3) **principal stresses**.

Dip. Inclination of a planar geologic surface (for example, a **fault** or formation) from the horizontal.

Displacement. The difference between the initial position of a reference point and any later position. (1) In seismology, displacement is typically calculated by integrating an accelerogram twice with respect to time and is expressed in centimeters. (2) In geology, displacement is the permanent offset of a geologic or manmade reference point along a fault or landslide.

Dynamic viscosity. A measure of the internal resistance of a fluid to flow. The symbol is η. *Also called* viscosity coefficient or absolute viscosity.

Earthquake. Groups of **elastic waves** propagating in the Earth, generated by a sudden disturbance of the Earth's elastic equilibrium, usually caused by a sudden movement in the Earth's **crust**.

Earthquake hazard. Any physical phenomenon associated with an **earthquake** that may produce adverse effects on human activities.

Effective stress. In the presence of a fluid, **stress** is partly compensated by the buoyancy of the fluid pressure. This reduces the effective magnitude of the stress by an amount equal to the **pore pressure**.

Elastic rebound theory. The theory that movement along a **fault** is the result of an abrupt release of a progressively increasing elastic **strain** between the rock masses on either side of the fault. Such movement (or faulting) returns the rocks to a condition of little or no strain and converts the stored elastic strain energy into

kinetic energy (motion along the fault), heat caused by friction, new fractures, and the generation of **elastic waves**, which radiate outwards from the point of rupture, the **hypocenter**.

Elastic wave. A wave that is propagated by some kind of elastic deformation; that is,a deformation that disappears when the forces causing the deformation are removed. A **seismic wave** is a type of elastic wave.

Epicenter. The point of the Earth's surface vertically above the **hypocenter** or **focus** of an **earthquake** (where a **seismic** rupture initiates).

Fault. A **fracture** or fracture zone along which there has been **displacement** of the sides relative to one another parallel to the fracture plane or planes.

Fault trace. Intersection of a **fault** with the ground surface; also, the line commonly plotted on geologic maps to represent a fault.

Favorably oriented fracture. A **fracture** whose orientation in an existing **stress** field is close to the orientation for maximum **shear stress** resolved across the fracture plane; typically within the range 30° to 45° relative to the maximum **principal stress** direction (σ_1).

Focal depth. The depth of the **hypocenter** or **focus** of an **earthquake**.

Focal mechanism. An analysis to determine the attitude of the causative **fault** and the direction of slip along the fault during an **earthquake** from the radiation pattern of **seismic waves** generated. The analysis most commonly uses the direction of first motion of **primary waves** recorded at numerous **seismograph** stations and yields two possible orthogonal orientations for the fault rupture and the direction of seismogenic slip. From these data, inferences can be made concerning the principal axes of **stress** in the region of the earthquake. *Also called* fault-plane solution.

Focus. The source of a given set of **elastic waves**; the true center of an **earthquake**, within which the **strain** energy is first converted to elastic wave energy. *See also* **Hypocenter**.

Foreshock. A small tremor that precedes a larger **earthquake** or mainshock by seconds to weeks and that originates at or near the **focus** of the larger earthquake.

Fracture. (1) A breakage in the rock strata due to mechanical failure by applied **stress**. (2) Deformation due to momentary loss of **cohesion** or loss of mechanical resistance to differential stress and a release of stored elastic energy.

Fracture-opening pressure. The injection pressure needed to just open a newly created **hydraulic fracture**. The symbol is P_{fo}.

Frequency. (1) Rate of occurrence. (2) Number of cycles occurring in unit time. Hertz, which is the unit of frequency, is equal to the number of cycles per second.

Geophysical survey. The use of one or more techniques of physical measurement to explore Earth properties and processes. For subsurface exploration, this usually involves indirect methods, such as gravity measurements, to infer rock densities, and so forth.

Head. (1) The elevation to which water rises at a given point as a result of reservoir **pore pressure**. (2) Water-level elevation in a well or elevation to which water of a flowing artesian well will rise in a pipe extended high enough to stop the flow.

Hydraulic conductivity. The ease with which water is conducted through an **aquifer** and is defined as the rate of flow of water through a unit cross section under a unit **hydraulic gradient** at the prevailing temperature. The symbol is **K**. *Also called* coefficient of permeability.

Hydraulic fracture. An artificial **fracture** generated in the rock around a well by high pressure fluid injection. *Also called* hydrofracture.

Hydraulic gradient. In an **aquifer**, the rate of change to **total head** per unit distance of flow at a given point and in a given direction.

Hydrostatic pressure. The pressure exerted by the water at any given point in a body of water at rest. For ground water, the hydrostatic pressure is equal to the weight of the water above the reference point or reference horizon, or the product of the fluid **density** (ρ), the **acceleration** of gravity (g), and the fluid depth.

Hypocenter. The point in the Earth where an **earthquake** rupture initiates.

Induced seismicity. Earthquake activity triggered by environmental changes caused by man; usually associated with either the injection or extraction of large amounts of fluid in the ground or the impoundment of a **reservoir**.

Instantaneous shut-in pressure. The fluid pressure recorded in the wellbore after a new **hydraulic fracture** is opened, injection is stopped, and the well is "shut-in" or closed. Under ideal conditions, this is a measure of the minimum **principal stress** (σ_3) acting to close the fracture. The abbreviation is ISIP.

Intensity. A subjective measure of the damage of an **earthquake** at a particular place as determined by its effects on people, structures, and earth materials. Intensity depends not only on the earthquake **magnitude**, but also on the distance from the point of reference to the **epicenter**, the earthquake **focal depth**, the type of faulting, and the local geology. The principal scale used in the United States today is the Modified Mercalli Intensity Scale (Appendix C).

Intrinsic permeability. The characteristic resistance to fluid flow of a porous medium alone, independent of the properties of the fluid. The symbol is k.

Isoseismal. A line connecting points on the Earth's surface at which **earthquake intensity** is the same. It is usually a closed curve around the **epicenter**.

Lithostatic pressure. The vertical pressure at any point at depth in the rock due to the overburden or weight of the overlying rock mass. *See also* **Vertical stress**.

Magnitude. A number that characterizes the size of an **earthquake**, usually based on measurement of the maximum **amplitude** recorded by a **seismograph** for **seismic waves** of a particular **frequency**. Scales most commonly used are (1) **local magnitude** (M_L), (2) **surface-wave magnitude** (M_S), and (3) **body-wave magnitude** (m_b). None of these scales satisfactorily measures the largest possible earthquakes because each relates to only the amplitude of certain frequencies of seismic waves and because the spectrum of radiated seismic energy changes with earthquake size. To compensate, the **moment magnitude** (**M**) scale, based on the concept of seismic moment, was devised and is uniformly applicable to all sizes of earthquakes.

- **Body-wave magnitude.** This scale measures the maximum **amplitude** of waves that pass through the interior—the body—of the Earth and that have a period between 1 and 10 seconds (s). The symbol is m_b.
- **Local magnitude.** This scale is commonly referred to as Richter magnitude. Although only accurately applied to California earthquakes, it is still quite useful today for describing smaller and more moderate earthquakes but not for measuring truly large earthquakes. It provides a good estimate to engineers of the high-frequency **accelerations** generated by an earthquake. The symbol is M_L.
- **Moment magnitude.** This is perhaps the most meaningful scale today for large and great earthquakes, in that it reflects the total energy released. The measurement takes into account the surface area of the **fault** that moved to cause the earthquake, the average **displacement** along the fault plane, and the rigidity of the fault material. Seismic moment (M_o) is the result, and the moment magnitude is simply a scaled logarithm of this value. This scale was developed only in the late 1970's, which is why great earthquakes, such as that in Alaska in 1964, which was originally evaluated as a magnitude M_S 8.5, have been upgraded—Alaska now has an moment magnitude rating of 9.2. The symbol is **M** or M_w.
- **Surface-wave magnitude.** This scale was formulated to describe earthquakes at distant locations. The scale principally measures **surface waves** of 20-s period or a wavelength of approximately 60 km. The symbol is M_S.

Major earthquake. An **earthquake** having a **magnitude** of 6.5 or greater.

Maximum horizontal stress. The maximum component of **principal stress** in the horizontal plane. The symbol is S_H.

Mean stress. The average of the three **principal stresses**.

Microearthquake. A small **earthquake** usually observable only with sensitive instruments. Typically corresponds to an earthquake of **magnitude** 2 or less. *Also called* microseismic event.

Minimum horizontal stress. The minimum component of **principal stress** in the horizontal plane. The symbol is S_h.

Mohr circle. A graphical representation of the state of **stress** at a particular point and at a particular time. The coordinates of each point on the circle are the **shear stress** (τ) and the **normal stress** (σ_n) on a particular plane.

Mohr-Coulomb failure criterion. The condition whereby failure (slip) is expected on a preexisting **fault** whenever the combinations of **shear stress** (τ) and **normal stress** (σ_n) resolved across the fault plane (as defined by the loci of points on the **Mohr circle**) meet or exceed the Coulomb criteria for frictional failure; that is, the shear stress is equal to the inherent fault **cohesion** (τ_o) plus the product of the **coefficient of friction** (μ) and the effective **normal stress** ($\sigma_n - p$). This level of **shear stress** is called the critical stress (τ_{crit}).

Normal fault. A steeply to slightly inclined **fault** in which the block above the fault (the hanging wall) has moved downward relative to the block below (the footwall).

Normal stress. The component of **stress** oriented normal (perpendicular) to a given **fault**, fracture plane or slip surface. The symbol is σ_n.

Permeability. The capacity of a porous rock or soil for transmitting fluid or gas; it is a measure of the relative ease of fluid flow under unequal pressure.

Plate tectonics. A widely excepted theory that considers the Earth's **crust** and upper mantle to be composed of a number of large, rigid plates that move relative to one another. Interaction along plate boundaries is then the major cause of **earthquakes** and volcanic activity.

Pore pressure. Pressure of water in pores of a saturated medium. The symbol is p.

Pore space. Space occupied by voids within the rock matrix capable of holding either fluid or gas.

Porosity. Percentage ratio of void volume to the bulk (total) volume of rock or soil sample. It is a measure of the fluid bearing capacity of the medium. The symbol is n.

Primary wave. A type of elastic **body wave** that propagates by alternating compression and expansion of material in the direction of propagation. It is the fastest of the seismic waves (typically traveling at speeds of 5–6.8 km/s in the crust and 8–8.5 km/s in the upper mantle, just below the crust), and is analogous to a traveling sound wave. The abbreviation is P wave.

Principal stress. A **stress** that is perpendicular to one of three mutually orthogonal planes on which the **shear stress** is zero and in whose direction stresses are purely

compressive; a stress that is normal to a principal plane of stress. The three principal stress are identified as σ_1, maximum or greatest principal stress; σ_2, intermediate principal stress; and σ_3, minimum or least principal stress.

Rake. The direction of **displacement** (slip) resolved across a **fault** plane, measured in degrees from the horizontal.

Reservoir. (1) A recipient for the collection of liquid. In geology, a subsurface rock formation that has sufficient **porosity** and **permeability** to except and retain a large amount of fluid or gas under adequate trap conditions. (2) A manmade body of water impounded behind a dam.

Reverse fault. A moderately inclined fault in which the block above the fault (the hanging wall) has moved upward relative to the block below the fault (the footwall).

Secondary recovery. Production of oil or gas as a result of artificially augmenting the **reservoir** energy, usually by injection of water or other fluid at high pressure. Secondary-recovery techniques are generally applied after substantial reservoir depletion. *See also* **Water flooding**.

Secondary wave. A type of **seismic body wave** that propagates by a shearing motion of material, so that wave motion or oscillation is perpendicular (transverse) to the direction of propagation. It does not travel through liquids or through the outer core of the Earth. Its speed is typically 2.8 to 4 km/s in the crust and 4.3 to 4.5 km/s in the upper mantle, just below the crust. This wave arrives later than the faster **primary wave**. The abbreviation is S wave.

Seismic. Pertaining to an **earthquake** or earth vibration, including those that are artificially produced.

Seismicity. Earthquake activity; the geographical and the historical distribution of earthquakes.

Seismic risk. The probability of social or economic consequences of an **earthquake**.

Seismic wave. An **elastic wave** generated by a sudden impulse, such as an **earthquake** or an explosion.

Seismogram. A record of ground motion or of vibration of a structure caused by an **earthquake** or an explosion; the record produced by a **seismograph**.

Seismograph. An instrument that detects, magnifies, and records ground vibrations, especially **earthquakes**. The resulting record is a **seismogram**.

Separation. In geology, the distance between any two parts of a reference plane (for example, a sedimentary unit or a geomorphic surface) offset by a **fault** measured in any plane. Separation is the amount of apparent fault **displacement** and is nearly always less than the actual slip.

Shear. A mode of failure whereby two adjacent parts of a solid slide past one another parallel to the plane of failure.

Shear stress. The component of **stress** that acts tangential to a plane through any given point in a body. The symbol is τ.

Shear wave. A secondary or transverse **elastic wave**.

Slip rate. The average **displacement** at a point along a **fault** as determined from geodetic measurements from offset manmade structures or from offset geologic features whose age can be estimated. It is measured parallel to the dominant slip direction or estimated from the vertical or the horizontal **separation** of geologic, geodetic, or other markers.

Storativity. The capacity of an **aquifer** to accept (store) or release fluid under a change in applied **pore pressure** (p) and is defined as the amount of fluid in storage released from a column of aquifer with unit cross section under a unit decline in pressure **head**. The symbol is S. *Also called* storage coefficient.

Strain. The amount of any change in dimensions or shape of a body when subjected to deformation under an applied **stress**.

Stress. The force per unit area acting on a surface within a body. Nine values are required to characterize completely the state of stress at a point: three normal components (which are purely compressive) and six shear components, relative to three mutually perpendicular reference axes.

Strike. The orientation of the line of intersection of any plane with the horizontal measured in degrees from true north; the direction or trend taken by a structural surface, such as a **fault** plane, as it intersects the horizontal.

Strike-slip fault. A **fault** in which movement is principally horizontal, parallel to the **strike** of the fault.

Subsidence. Downward settling of the Earth's surface with little or no horizontal motion. May be caused by natural geologic processes (such as sediment compaction or **tectonic** activity) or by human activity (such as mining or withdrawal of ground water or petroleum).

Surface faulting. Displacement that reaches the ground (or sea floor) surface during slip along a **fault**. Commonly accompanying moderate and large **earthquakes** having **focal depths** to 12 km. Surface faulting may also accompany **aseismic tectonic creep** or natural or man-induced **subsidence**.

Surface wave. Seismic wave that propagates along the Earth's surface.

Tectonic. Pertaining to either the forces or the resulting structural features from those forces acting within the Earth; refers to crustal rock-deformation processes that affect relatively large areas.

Tensile strength. The maximum applied **tensile stress** that a body can withstand before failure occurs. The symbol is T_0.

Tensile stress. A **normal stress** that tends to cause separation across the plane on which it acts.

Top-hole pressure. The fluid pressure measured at the wellhead. The abbreviation is THP.

Total head. The sum of the elevation **head**, pressure head, and velocity head of a liquid. For ground water, the velocity-head component is generally negligible.

Transmissivity. The rate at which water is transmitted through a unit width of **aquifer** under a unit **hydraulic gradient**; it is equal to the product of the **hydraulic conductivity** and the thickness of the aquifer. The symbol is T.

Vertical stress. The **stress** at any point at depth in the rock due to the overburden or weight of the overlying rock mass; equal to the product of the average **density** of the overlying column of rock, the **acceleration** of gravity, and the depth. The symbol is S_v. *See also* **Lithostatic pressure**.

Water flooding. A **secondary recovery** technique in which water is injected into a petroleum **reservoir** to force additional oil out of the reservoir rock and into producing wells.

Water table. The upper surface of a body of unconfined ground water at which the water pressure is equal to the atmospheric pressure.

Wellbore breakouts. Deformation of the wellbore wall caused by spalling of weak material induced by compressive **shear** failure. *Also called* borehole elongations.